RETA LILA WESTON INSTITUTE OF NEUROLOGICAL STUDIES

INSTITUTE OF NEUROLOGY

UNIVERSITY COLLEGE LONDON

DEFINING THE GENETIC BASIS OF THREE HEREDITARY NEUROLOGICAL CONDITIONS IN FAMILIES FROM THE INDIAN SUBCONTINENT

Dr Vafa Alakbarzade

PhD Thesis

2016

DEFINING THE GENETIC BASIS OF THREE HEREDITARY NEUROLOGICAL CONDITIONS IN FAMILIES FROM THE INDIAN SUBCONTINENT

Submitted by

Dr Vafa Alakbarzade, MBBS, MRCP (UK), MSc

University College London Student Number: 1028294

to University College London as a thesis for the degree of Doctor of Philosophy, January 2016

I confirm that the work presented in this thesis is my own and information derived from other sources has been indicated in the thesis

(Signature) ……

ACKNOWLEDGEMENTS

Foremost I would like to thank the families who took part in these studies.

I am sincerely grateful to Professor Tom Warner and Professor Andrew Crosby, without whom I would never have had all the wonderful experiences this PhD brought me. They have always supported and encouraged me in whatever scientific endeavours I have followed.

Dr. Barry Chioza and Dr. Sreekantan-Nair Ajith provided invaluable support and advice throughout my PhD; I am hugely appreciative of their guidance and encouragement. None of the work in this thesis would have been possible without guidance of Dr. Barry Chioza.

I would specifically like to appreciate contribution of the team of Prof. David Silver and Dr. Kulkarni Abhijit who provided functional follow up of our genetic findings and Dr. Iype Thomas and Dr. Arshia Ahmad who provided clinical information of the families under investigation. David Newman has shaped out my thesis for which I am deeply grateful for.

I would also like to thank all the members of the Crosby group for their help.

On a personal level I would like to sincerely thank my beloved mother who has always been there for me.

ABSTRACT

Neurogenetic studies have revolutionised our understanding of the genetic and molecular basis of inherited neurological disorders, primarily as a result of the identification of single disease-causing genes. The incidence of such disorders is increased amongst populations with common shared ancestry or a high rate of consanguinity. Hence, the investigation of inherited neurological conditions in genetic isolates provides a robust opportunity to define the molecular pathogenic basis of these conditions.

Neurological and neurodevelopmental disorders present important public health issues in the developing countries in the Indian subcontinent. The global burden of these disorders is worsened by the lack of targeted research funding and relevant in-country research capacity.

This project, undertaken as part of a wider research study investigating inherited disorders in the Indian subcontinent, aimed to define the molecular genetic bases of three extended families with distinct neurological and neurodevelopmental disorders. In the first family with multiple individuals affected by a severe autosomal recessive form of neurodevelopmental delay with microcephaly, genetic studies identified mutation in a gene (*MFSD2A*), not previously associated with inherited disease, which led to a reduction of fatty acid transportation in patients homozygous for the disease-causing mutation. In the second family, genotyping identified a complex chromosomal rearrangement associated with diverse clinical outcomes including Wolf Hirschorn-, 3p deletion-, and 4p duplication syndrome, among ten

chromosomally-imbalanced affected individuals. In the third family, a duplication event on chromosome 15q24 encompassing the *LINGO1* gene was identified as a likely cause of dystonic tremor in affected individuals. Together these molecular discoveries provide fundamentally important biological insight into the pathogenic basis of abnormal brain growth and control of movement with the potential diagnostic and treatment applications.

CONTENTS

LIST OF TABLES

LIST OF FIGURES

ABBREVIATIONS

AA	…….	Amino acid
AD	…….	Autosomal dominant
AGTC-India	…….	Applying Genomic Technologies to address Clinical Challenges in the Indian Subcontinent
AR	…….	Autosomal recessive
BAF	…….	B allele frequency
BBB	…….	Blood brain barrier
Bb	…….	Base pair
BC	…….	Basket cells
CCTMDS	…….	Consensus criteria for tremor of the movement disorders society
CDC	…….	Centres for Disease Control and Prevention
cDNA	…….	Complementary deoxyribonucleic acid
CGH	…….	Comparative genomic hybridization
cM	…….	Centimorgan
CNS	…….	Central nervous system
CNV	…….	Copy Number Variation
CSF	…….	Cerebro-spinal fluid
DbSNP	…….	Single Nucleotide Polymorphism Database
DNTP	…….	Deoxynucleotide
DHA	…….	Docosahexaenoic acid
DSM-5	…….	Diagnostic and Statistical Manual of Mental Disorders
DT	…….	Dystonic tremor
ET	…….	Essential tremor
EVS	…….	Exome Variant Server
ExAC	…….	Exome Aggregation Consortium
FGFR3	…….	Fibroblast growth factor receptor
FISH	…….	Fluorescent *in situ* hybridization
GABA	…….	Gamma-aminobutyric acid
GC	…….	Granular cells
GDD	…….	Global developmental delay
HC	…….	Head circumference
HEK293	…….	Human Embryonic Kidney 293 cells
ID	…….	Intellectual disability
IGV	…….	Integrative genomic viewer

IQ	…….	Intelligence quotient
Kb	…….	Kilobases
LETM1	…….	Leucine zipper/EF-hand-containing transmembrane protein 1
LINGO1	…….	Leucine-rich repeat and Ig domain containing Nogo receptor interacting protein-1
LPC	…….	Lysophosphatidylcholine
Mb	…….	Megobase
MCPH	…….	Autosomal recessive primary microcephaly
MDS	…….	Movement disorders society
Mfsd2a	…….	Major facilitator superfamily domain
MLPA	…….	Multiplex Ligation-dependent Probe Amplification
MS	…….	Multiple sclerosis
NDD	…….	Neurodevelopmental disorders
NGS	…….	Next-generation sequencing
NVU	…….	Neurovascular unit
NYBB	…….	New York Brain Bank
OFC	…….	Occipitofrontal circumference
OMIM	…….	Online Mendelian Inheritance in Man
PC	…….	Purkinje cells
PCR	…….	Polymerase chain reaction
PD	…….	Parkinson’s disease
PR	…….	Pair read
RNA	…….	Ribonucleic acid
ROH	…….	Runs of homozygosity
RT PCR	…….	Reverse transcriptase polymerase chain reaction
SCA12	…….	Spinocerebellar ataxia type 12
SDS	…….	Standard deviation score
SNP	…….	Single nucleotide polymorphisms
SSR	…….	Short sequence repeat
TAWD	…….	Tremor associated with dystonia
TD	…….	Touch-down temperature
WES	…….	Whole exome sequencing
WGS	…….	Whole genome sequencing
WHO	…….	World health organization
WHSC1	…….	Wolf-Hirschhorn syndrome candidate 1 gene
WHSCR-2	…….	Wolf-Hirschhorn syndrome critical region
WT	…….	Wild type

Chapter 1

General Introduction

General Introduction

1.1 Abnormal brain development: embryological aspects, definitions and underlying causes

1.1.1 Structural development of the brain

The complex architecture of brain develops in a sequence of stages which are intricately orchestrated by efficient and effective execution of genome maintenance, DNA replication and ultimately cell division.

The neural tube, the origin of the central nervous system (CNS), is formed from the neural plate, a thickened area of embryonic ectoderm. This process, also called neurulation begins during the early part of the fourth week. The cranial opening of the rostral neuropore of neural tube closes on approximately the 25th day while the caudal pore closes 2 days later. The walls of the neural tube thicken to form the brain and spinal cord, while the lumen of the neural tube forms the ventricular system of the brain filled with cerebrospinal fluid (CSF) (Moore et al., 2011). Even before the neural folds are completely fused, three distinct vesicles are recognizable in the rostral end of the neural tube: forebrain, midbrain, and hindbrain (Figure1-1). During the fifth week, the forebrain (prosencephalon) partially divides into two secondary brain vesicles, the telencephalon and diencephalon (thalamus and hypothalamus) (Moore et al., 2011). The midbrain (mesencephalon) forms the rostral part of the brain stem, whilst the hindbrain (rhombencephalon) forms the caudal proportion of the brain stem, the pons, and the cerebellum (Figure1-1).

Figure 1-1 Developing brain vesicles and ventricular system

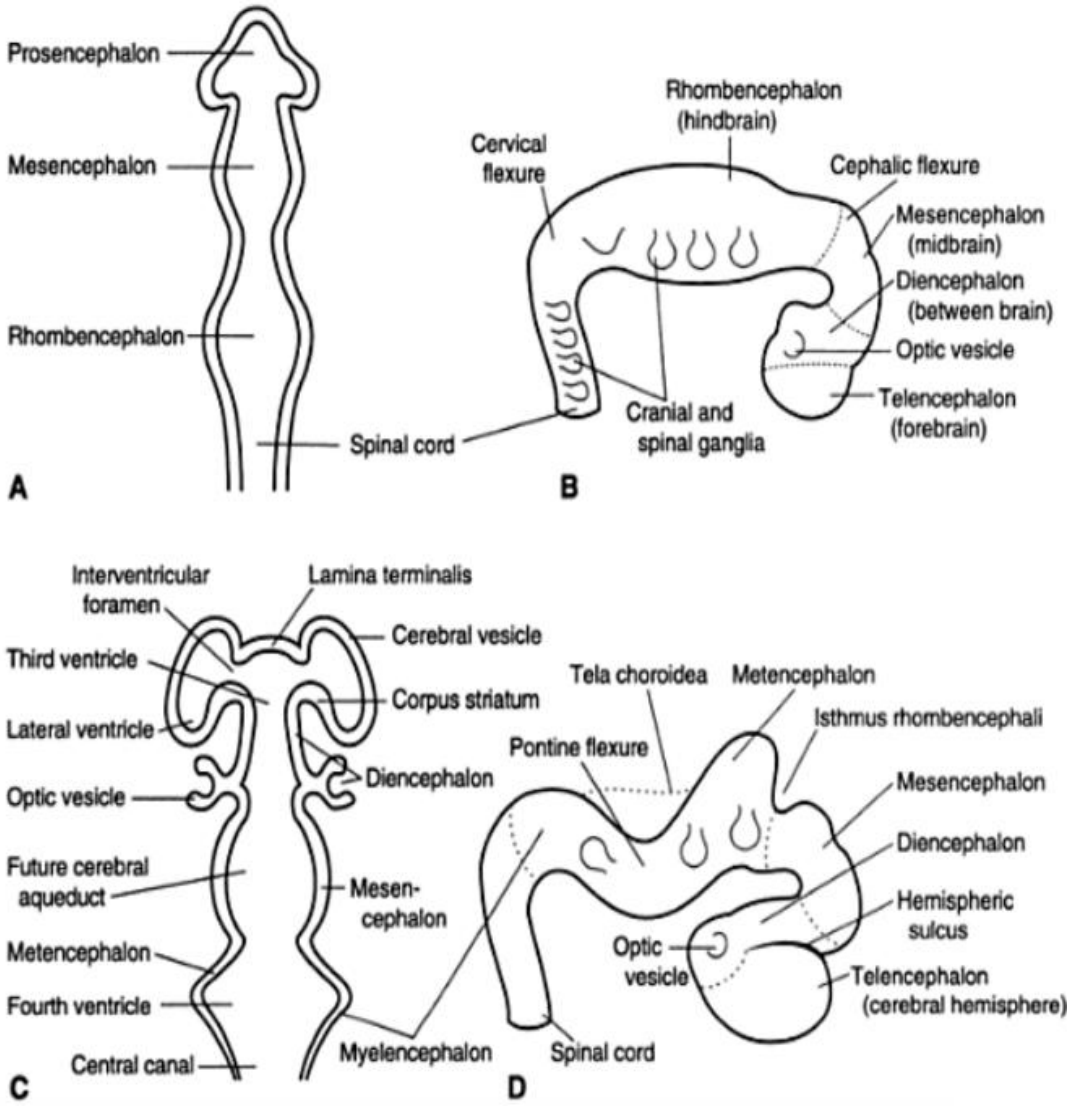

Schematic illustration of the developing brain vesicles and ventricular system. (A and B) Three-brain-vesicle stage of 4-week old embryo; (C and D) Five-brain-vesicle stage of a 6-week-old embryo.

(Dudek and Fix, 1998)

The telencephalon gives rise to the cerebral hemispheres which are covered by grey matter, cerebral cortex. The cerebral cortex is a central region in the mammalian brain that controls complex cognitive behaviors (Kaas, 2013; Geschwind and Rakic, 2013). Convolutions in the cortex or cortical folding enable the brain to grow markedly in volume and to expand in surface area, despite being housed in a confined skull, which is crucial for normal brain function, as patients with microcephaly show a range of cognitive deficits.

Microarchitecture of the cortex has complex laminar layered structure. The growth of the cortex relies on the symmetric self-renewal or proliferation of neural stem cells and neural progenitors. This proliferation stage is then replaced by asymmetric division of neuroprogenitor cells (Alvarez-Buylla and Temple, 1998). Radial glial cells, the key neuroprogenitor cells play a critical role in corticogenesis by providing neuronal migration and contributing to the formation of diverse neuronal and glial lineages via asymmetric division. Conceptually, the cortical development hypothesis postulates that the cortex is assembled from radial progenitor units that consist of proliferative radial glial cells and more differentiated daughter cells, including neurons, which ultimately migrate radially along radial glial cell fibers to form the characteristic six-layered cortical structure, from the inside out (Figure1-2) (Rakic, 2007; Rakic, 2009; Tan and Shi, 2013; Rakic, 1988). Proliferation *versus* neurogenic differentiation of neuroprogenitor cells is dictated by orientation of the mitotic spindles (Figure1-3) (Alcantara and O'Driscoll, 2014). Nearly all neurons in the cerebral cortex complete proliferation by mid-gestation, although glial genesis and brain volume continues to grow until adulthood (Spalding et al., 2005).

Figure 1-2 Cerebral cortex neurogenesis

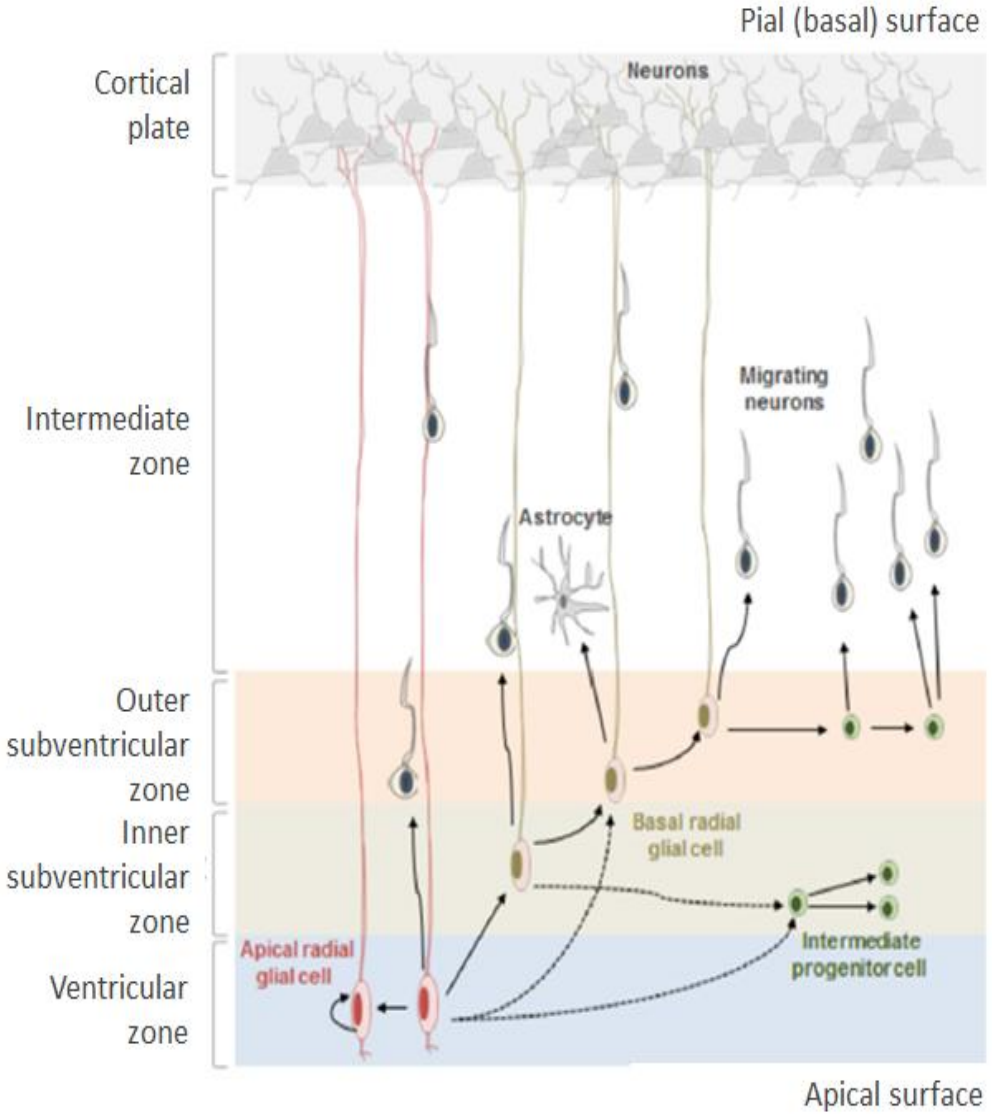

Illustration of cerebral cortex cellular layered development. Radial glial cells (in red), the key neuroprogenitors, lie in the ventricular zone and their radial fibers span the width of the cerebral cortex. These can differentiate into neurons, as well as intermediate progenitors (in dark green) that migrate to the subventricular zone and can further generate more progenitor cells and neurons by repeated asymmetric cell division. Finally, radial glial cells also can give rise to astrocytes and oligodendrocytes at later stages. Ultimately the migrating neurons become the pyramidal cells of the cerebral cortex.

(Alcantara and O'Driscoll, 2014)

Figure 1-3 Proliferative versus neurogenic (differentiating) cell division

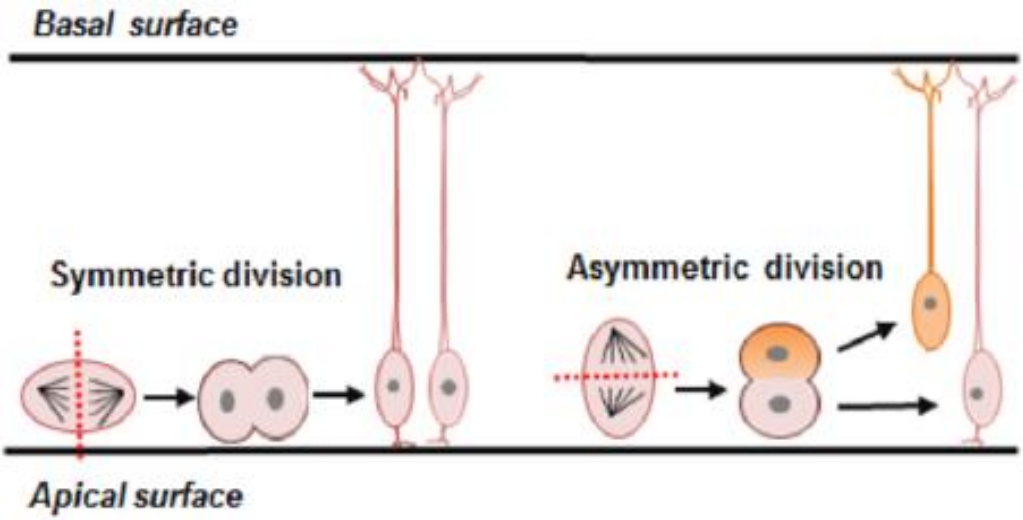

Dotted red line is an orientation of neuroepithelial cells division. Orientation of the mitotic spindle is parallel to the apical surface during symmetric cell division, with the resulting cleavage plan intersecting the apical plasma membrane. A deviation in the orientation of the mitotic spindle results in an asymmetric cell division, with only one of the daughter cells inheriting the apical plasma membrane region (pink cell).

(Alcantara and O'Driscoll, 2014)

In mammals, vascularization of the neuroepithelium occurs via sprouting angiogenesis, and endothelial cells of these blood vessels underlie blood–brain barrier (BBB). The development of the BBB is a complex process that involves brain endothelial cells, neural progenitors, pericytes, astrocytes and different environmental cues (Blanchette and Daneman, 2015). The BBB stringently regulates CNS homeostasis, shields the brain from potential neurotoxins and regulates the delivery of energy metabolites and essential nutrients to the brain. Integrity and transport function of the BBB is especially important during brain development (Moretti et al., 2015; Betsholtz, 2014b; Nguyen et al., 2014b; Ben-Zvi et al., 2014). Transport function of the BBB is controlled by highly specialized substrate-specific transport proteins expressed in brain endothelium (Zlokovic, 2008). Although, the blood-CSF barrier also transports molecules to the brain, delivery takes hours to days compared with the BBB pathway which is almost instantaneous delivery. Thus BBB transporters are crucial during the brain development (Bell et al., 2010; Blinder et al., 2013; Carmeliet and Ruiz de Almodovar, 2013; Zlokovic, 2011). There is increasing experimental and limited clinical data about impact of BBB dysfunction on the developing brain as well as on an abnormal pattern of head growth (Moretti et al., 2015; Betsholtz, 2014b; Nguyen et al., 2014b; Ben-Zvi et al., 2014) (discussed in section 3.1).

The cerebellum resides at the anterior end of the hindbrain and is classically defined by its role in sensory-motor processing. In humans it contains over half of the mature neurons in the adult brain. Compared to cerebral cortex neurogenesis, cerebellar cortical neurogenesis continues after birth into early prenatal life (up to 2 years in humans). The cerebellar cortex is composed of

a monolayer of inhibitory Purkinje cells, sandwiched between a dense layer of excitatory granule cells (GC) and a subpial molecular layer of GC axons and Purkinje cells dendritic trees. GC receive inputs from outside the cerebellum and project to the Purkinje cells, the majority of which then project to a variety of cerebellar nuclei in the white matter. In mammals the medial vestigial and interposed cerebellar nuclei mainly target descending motor systems, while the lateral zone of the cerebellar hemispheres is chiefly linked to the thalamus-cerebral cortex via the dentate nucleus (Butts et al., 2014). Inhibitory interneuron cells, such as basket cells coordinate Purkinje-granule cell circuit further shaping cerebellar communication with the cortex via the thalamus (discussed in section 5.3).

1.1.2 Microcephaly

An abnormal small brain, microencephaly is a neuroimaging or neuropathological diagnosis, while microcephaly which is defined as an abnormal head growth and can be measured (Menkes et al., 2006). As head growth is driven by brain growth, microcephaly usually implies microencephaly with exception of generalised skull growth restriction such as craniosynostosis cases (Leroy and Frias, 2005; Woods, 2004; Director and Columbia, 2005). On the other hand, children with microencephaly may have normal head growth (Menkes et al., 2006).

Microcephaly can be assessed by the measurement of head circumference (HC) or occipito-frontal circumference (OFC). Measurement and appropriate charting of OFC is part of the evaluation of children with neurodevelopmental disorders. A measuring tape encircling the head should include an area 1 to 2 cm above the glabella anteriorly and the most prominent portion of the occiput posteriorly for OFC assessment. The World Health Organization (WHS) growth charts are used to determine head growth in healthy children between 0 to 2 years, whilst the Centers for Disease Control and Prevention (CDC) growth charts are used for children older than two years (Grummer-Strawn et al., 2010). Meanwhile, the mean OFC in certain national or ethnic groups is different from the WHO means (Natale and Rajagopalan, 2014), hence the origin of a child needs to be adjusted accordingly before OFC calculation (http://www.who.int/childgrowth/standards/hc_for_age/en/).

Microcephaly is characterised by a reduced OFC. Some authors define microcephaly as a OFC more than 2 standard deviations (SD) below the

mean for a given age, sex, and gestation, while others more than 3 SD below the mean (Fenichel, 2005; Gartner et al., 1997; Zitelli and Davis, 2007; Ashwal et al., 2009; Rios, 1996; Woods, 2004; Leviton et al., 2002). Qualifying terms such as ‘mild microcephaly’ with SD between 2 and 3 below the mean, and ‘severe microcephaly’ with SD more than 3 SD below the mean has also been suggested (Swaiman et al., 2006).

Children with microcephaly also require neuroimaging assessment. In the majority of symptomatic microcephaly cases structural abnormalities such as white matter periventricular leukomalacia, delayed or disturbed myelination or migrational abnormalities can be identified (Ashwal et al., 2009; Custer et al., 2000; Sugimoto et al., 1993; von der Hagen et al., 2014). Hydrocephaly, infarction and intracranial calcifications are the common findings in acquired microcephaly (Sugimoto et al., 1993).

Microcephaly can be caused by genetic abnormalities, environmental insults, metabolic disorders, or associated with structural brain malformations such as abnormal gyrification, agenesis of corpus callosum, and pituitary abnormalities (Figure1-4) (Stoll, 2001; Menkes et al., 2006; Alcantara and O'Driscoll, 2014).

Environmental insults such as congenital infections, in utero drug or toxin exposure, hypoxic-ischaemic insults, intraventricular hemorrhage or stroke leading to ischaemic damage, severe malnutrition, systemic diseases as well as metabolic diseases as a potential cause of microcephaly must be evaluated in every affected individuals in genetic studies.

Figure 1-4 Causes of microcephaly

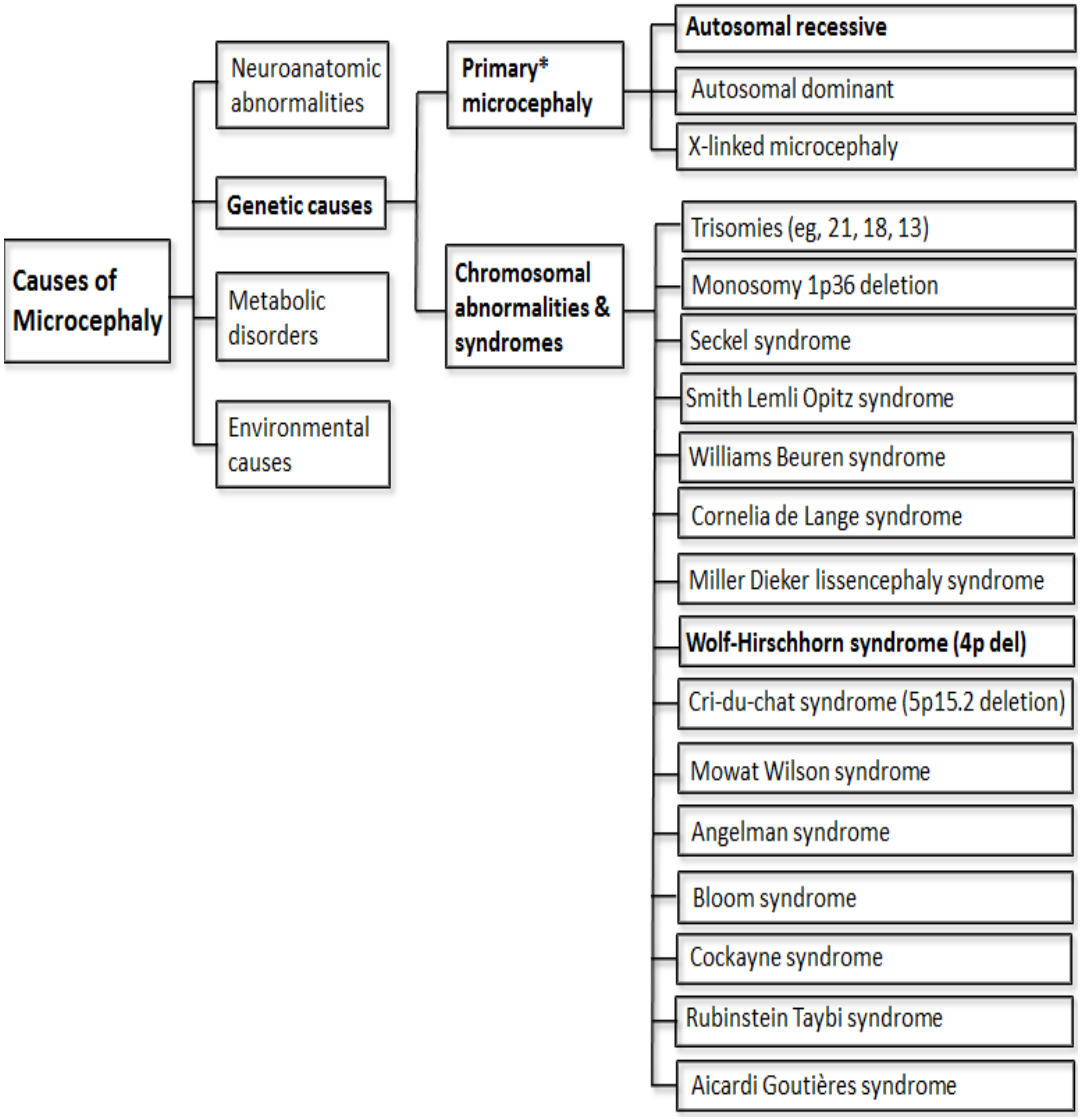

*Primary microcephaly also known as isolated microcephaly, true microcephaly, microcephaly vera. Subsections in bold are further discussed in the Chapter 3 and 4

Congenital microcephaly is defined as microcephaly at birth, while postnatal microcephaly is defined as normal OFC measurement at birth, followed by deceleration in head growth after birth. Genetically, congenital microcephaly may arise via a range of genetic causes including identifiable chromosomal abnormalities and manifest as part of a syndrome such as Wolf-Hirschhorn syndrome, or as a part of a monogenic gene disorders (Figure 1-4). Congenital microcephaly associated with single gene mutation is distinguished as primary microcephaly which is present with relatively normal brain anatomy. Congenital microcephaly associated with chromosomal abnormalities has broader classification as virtually all visible chromosome aberrations alter mental capacity and may cause specific malformations (Director and Columbia, 2005). This is the results of the fact that each chromosome contains numerous genes that participates in brain formation and maintenance of its structure and function.

Autosomal recessive primary microcephaly (MCPH) is a neurodevelopmental disorder that is characterised by a reduction in HC, a thin cortex and a decrease in brain surface area (Woods et al., 2005). Children with MCPH exhibit intellectual disability but show no significant motor control deficits. So far, linkage mapping has identified fifteen genetic loci that are associated with MCPH (Table 1-1) (OMIM search).

Table 1-1 Primary autosomal recessive microcephaly

Locus (gene)	Protein	OMIM	Localization and function
MCPH1	Microcephalin	251200	Centrosome-role in DNA repair and G2-M dynamics
MCPH2 *(WDR62)*	WD-repeat containing protein 62	604317	Mitotic spindle pole formation-scaffold for JNK pathway
MCPH3 (*CDK5RAP2/ CEP215*)	Cyclin dependent kinase 5 regulatory subunit-associated protein 2	604804	Centrosome, spindle and microtubule organizing function
MCPH4*(CASC5)*	Cancer susceptibility candidate 5	604321	Kinetochore [KNM] component-spindle-assembly checkpoint
MCPH5 *(ASPM)*	Abnormal spindle-like, microcephaly associated	608716	Microtubule associated protein-spindle organization
MCPH6 (*CENPJ/CPAP*)	Centromeric protein J	608393 613676	Centriole length control/microtubule function
MCPH7 (*STIL*)	SCL/TAL1 interrupting locus	612703	Spindle organisation/cell cycle progression
MCPH8 (*CEP135*)	Centrosomal protein 135kDa	614673	Spindle organisation/cell cycle progression
MCPH9 (*CEP152*)	Centrosomal protein of 152 kDa	614852 613823	Centrosome-centriole biogenesis and genome stability
MCPH10 (*ZNF335)*	Zinc Finger Protein 335	615095	Interacts with a chromatin-remodeling complex
MCPH11 *(PHC1)*	Polyhomeotic Homolog 1	602978	Increase in DNA damage and defective DNA repair
MCPH12 *(CDK6)*	Cyclin-Dependent Kinase 6	603368	Disorganized mitotic spindles and supernumerary centrosomes
MCPH13 *(CENPE)*	Centromere Protein E, 312kDa	117143	Abnormalities in spindle microtubule organization
MCPH14 *(SASS6)*	Spindle Assembly 6 Homolog	609321	Impairs the centriole-forming function
MCPH15 (*MFSD2A)*	Major Facilitator Superfamily Domain Containing 2A	614397	Docosahexaenoic acid transport impairment

Adapted from Online Mendelian Inheritance in Man (OMIM)

Interestingly, all of the MCPH-associated genes that have been identified until recently encode centrosome-associated proteins (Woods et al., 2005; Mochida and Walsh, 2001; Megraw et al., 2011; Kaindl et al., 2010). Symmetrical division of neuroprogenitor cells results in neuroepithelial cell proliferation, whilst asymmetrical cell division causes neurogenic differentiation (discussed in section 1.1.1). Proper centrosome duplication and positioning are crucial for spindle organization and orientation which in turn controls symmetrical versus asymmetrical divisions, determines the fate of daughter cells and cell cycle progression, and eventually dictates cortical size (Sun and Hevner, 2014). Disruption of centrosome duplication and positioning secondary to mutations encoding centrosome-associated proteins disrupts spindle orientation in neuroprogenitor cells and thereby causes a reduction in the size of the neuroprogenitor pool, which results in a smaller cortex (Sun and Hevner, 2014). In this thesis we present a new mechanism giving rise to autosomal recessive primary microcephaly (MCPH 15) that is not associated with centrosome-associated proteins (Alakbarzade et al., 2015; Guemez-Gamboa et al., 2015) (discussed in section 3.3).

1.2 Neurodevelopmental disorders and congenital malformations: definitions

Neurodevelopmental disorders (NDDs) are a diverse group of childhood onset hereditary neurological disorders. NDDs are the biggest cause of disabled children and young people with the estimated prevalence being around 3–4% of children in England (Emerson, 2012). On the other hand, congenital malformations are estimated as the most common cause of death during the first year of life in developed countries (Mathews et al., 2003; Muhuri et al., 2004; Serenius et al., 2001).

NDD is an umbrella term that includes homogeneous subgroupings of NDDs with shared features (Figure 1-5) (DSM-5). The classification of NDDs developed by Diagnostic and Statistical Manual of Mental Disorders (Fifth Edition) makes it easier for the clinician to specify association of separate NDDs with a known genetic condition (Harris, 2014).

DSM-5 classification replaces the outmoded term ‘mental retardation’ with a group of ‘intellectual disabilities’. Intellectual disability (ID), is defined as a deficit in intellectual and adaptive functioning that presents before 18 years of age (http://aaidd.org/intellectual-disability/definition) (American Psychiatric (Association, 2013). Adaptive deficits, in turn include limitations in at least one of three domains: conceptual, social, and practical, while deficit in intellectual capacity includes limitation in learning, reasoning, and problem solving, abstract thinking, and judgment. The term ID usually is applied to children five years or older, when the severity of impairment is more reliably assessed (American Psychiatric (Association, 2013).

Figure 1-5 DMS-5 classification of neurodevelopmental disorders

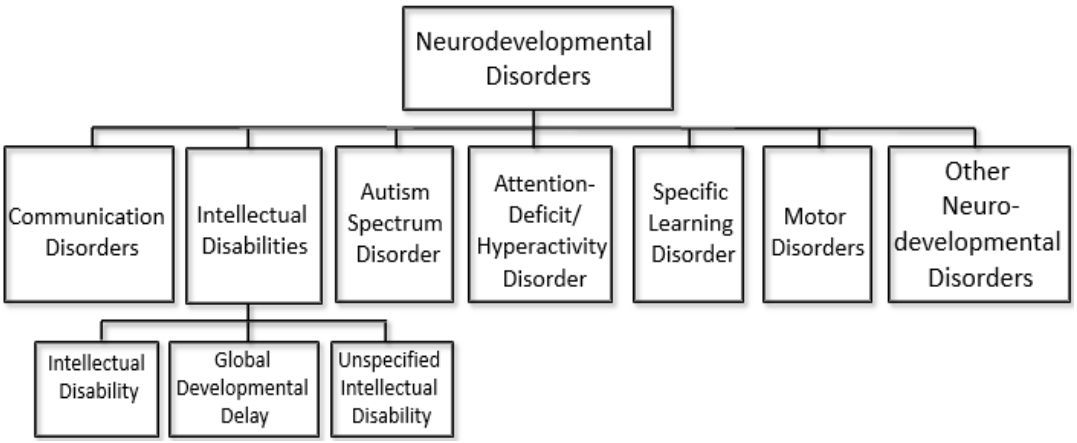

Diagnostic and Statistical Manual of Mental Disorders Fifth Edition

NDD section in DSM-5 classification also defines levels of severity based on adaptive functioning and not intelligence quotient (IQ) scores (Appendix 6.1) (Harris, 2013; Salvador-Carulla et al., 2011). Limitations in intellectual and adaptive functioning must be assessed relative to the child's age, experience, and environment, differences in language, culture, communication, motor, sensory, and behavioral factors (American Psychiatric (Association, 2013). Children with severe ID, a known genetic disorder and those presenting with obvious dysmorphic features and microcephaly tend to come to medical attention at an early age. Clinically, ID may be further categorized as syndromic or non-syndromic ID. Children with 'syndromic ID' present with one or more clinical abnormalities or comorbidities of a known syndrome in addition to ID, whereas those with 'non-syndromic ID' presents with ID alone (Kaufman et al., 2010).

Global developmental delay (GDD), is another sub-branch of 'intellectual disabilities' that describes intellectual and adaptive impairment in children younger than five years of age, based on failure to meet expected developmental milestones in several areas of intellectual functioning (American Psychiatric (Association, 2013). However, not all children with GDD will meet criteria for ID as they grow older.

Language disorders and speech disorders are the two major types of communication disorders. While speech disorders refers to an impairment of the articulation of speech sounds, fluency, and/or voice, the term "language disorder" refers to impaired comprehension and/or use of spoken, written, and/or other symbol systems (American Speech-Language-Hearing

Association (1993)). Developmental language disorder is another term used to describe a variety of developmental disorders, including those associated with cognitive impairment, in which speech and language also are affected; while specific language impairment is a developmental disorder that occurs in the absence of intellectual disability (mental retardation), hearing loss, motor disorder, socio-emotional dysfunction, or frank neurologic deficit (Plante, 1998). Developmental language disorder is the most common developmental disability of childhood, occurring in 5 to 10% of children (Richardson, 1992).

Early clinical and etiologic recognition of NDDs is important as it can provide guidance regarding prognosis, recurrence risk, and possible therapeutic options. Identifying a cause enables focused interventions, treatments, surveillance, and appropriate counseling, with anticipation of possible medical or behavioral complications and a more specific prognosis.

A specific genetic cause can be identified in more than 50% of cases of ID (Rauch et al., 2012; Moeschler, 2008; van Karnebeek et al., 2005). Currently the most valuable tool in routine practice to identify the genetic causes of NDD is chromosomal microarray analysis (Discussed in section 1.4.1.b) (Kaufman et al., 2010; Miller et al., 2010). Chromosomal rearrangements resulting from the loss or gain of chromosomal/DNA material is recognized as a frequent cause of NDD with or without congenital malformations (Discussed in section 1.4.1.a) (Kaufman et al., 2010).

Congenital malformations result from a pathologic process during the embryonic period that leads to the presence of structural anomalies at birth.

These structural anomalies encompass defects of organs or body parts which are not formed, are partially formed, or are formed in an abnormal fashion (Figure 1-6). Since most human body structures are formed between the second and the eighth week of development, they may be affected adversely during this vulnerable period. The majority of malformed embryos fail to implant or die following implantation, while the minority continue to develop and result in infants born with malformations (Director and Columbia, 2005).

Congenital malformations are divided into eight categories based on aetiology: (1) Chromosome unbalanced abnormalities (microscopically visible): (2) Submicroscopic chromosomal abnormalities including microdeletions, imprinting mutations; (3) Known teratogen and prenatal infections; (4) New dominant mutations such as achondroplasia; (5) Familial disorders not included as a new dominant such as tuberous sclerosis, fragile X syndrome; (6) Recognized non familial, non-chromosomal syndromes such as Kabuki syndrome; (7) Isolated anomalies not included in the above anomalies such as gastroschisis, isolated cleft lip; (8) Unrelated anomalies from more than one system with no unifying diagnosis (Wellesley et al., 2005). It is important to consider all above mentioned causes in evaluation of an infant with such anomalies. Complete examination, photographs, radiographs, genetic studies including cytogenic analysis, microarray analysis, fluorescence in-situ hybridization (FISH) test, storage of appropriate samples and sometimes autopsy can assist with detection of underlying cause (Mattos et al., 1987; Director and Columbia, 2005) (discussed in section1.4.1.b).

Figure 1-6 Congenital malformations

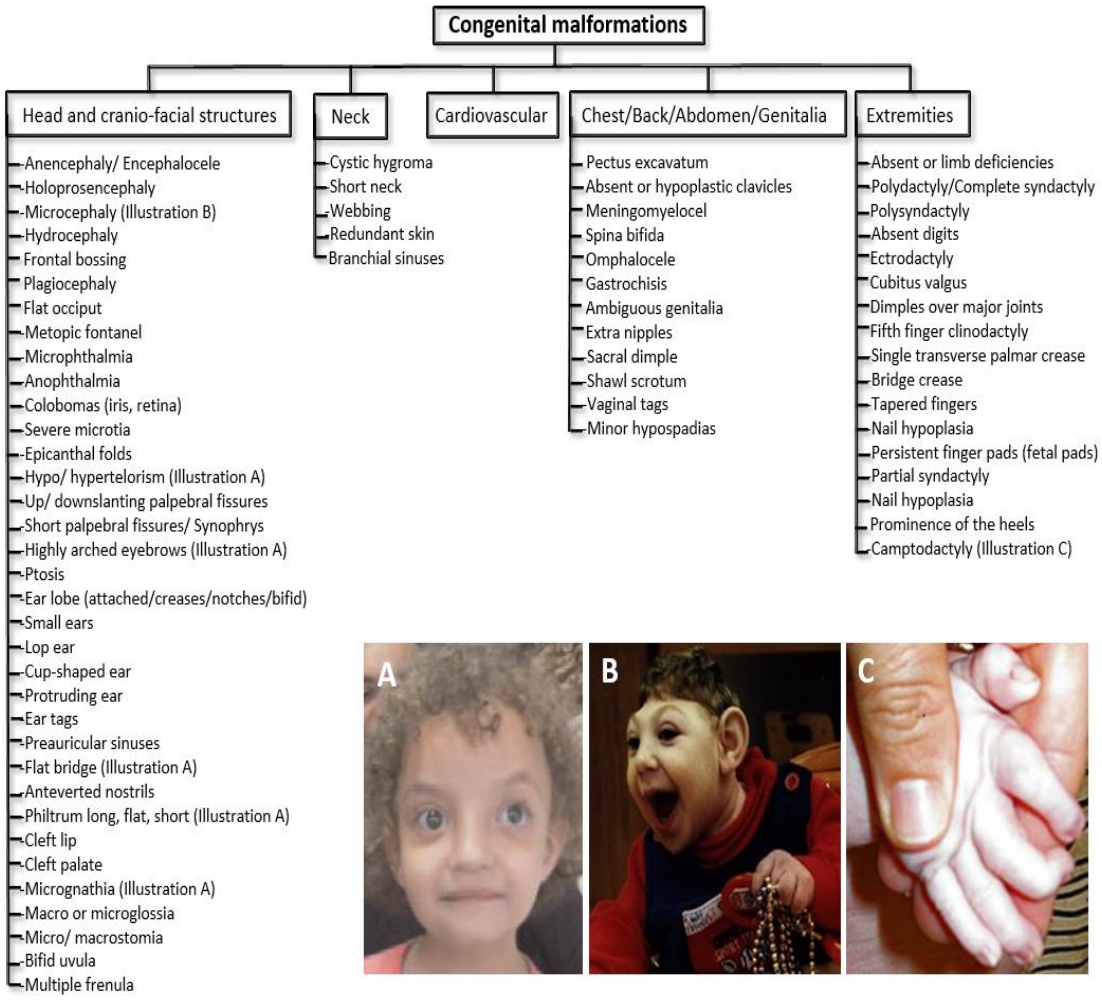

Table of different forms of congenital malformations. Illustration A is an example of the ‘‘Greek warrior helmet’’ appearance of the nose, high forehead, prominent glabella, hypertelorism, highly arched eyebrows, protruding eyes, epicanthal folds, short philtrum, distinct mouth with downturned corners, micrognathia (Battaglia et al., 2008); B Severe microcephaly (Paciorkowski et al., 2013); C Camptodactyly (Thunstrom et al., 2015)

1.3 Dystonic tremor

1.3.1 Definitions, classifications and misdiagnosis

Tremor is defined as a movement disorder characterised by an involuntary rhythmic sinusoidal oscillation of a body part (Deuschl et al., 1998). It is classified on the basis of topographic distribution, relation to rest, posture and action, amplitude of tremor, frequency of tremor and presence of additional symptoms such as parkinsonian signs and neuropathy (Figure 1-7) (Deuschl et al., 1998). The most frequent tremor type is believed to be essential tremor (ET), defined as a bilateral, largely symmetric postural/kinetic tremor involving hands/forearms with possible head tremor in the absence of abnormal posturing (Deuschl et al., 1998; Louis and Ferreira, 2010). ET has a high prevalence as well as a high misdiagnosis rate with the most frequent false diagnosis being dystonic tremor (DT) (Jain et al., 2006; Quinn et al., 2011; Schrag et al., 2000; Louis et al., 2015). There is a lack of agreement among movement disorder specialists as to how to define ET (Jain et al., 2006).

DT is defined as asymmetric postural or kinetic tremor with a greater tendency to vary with different postures or voluntary motor tasks in the same body region affecting dystonia (Quinn et al., 2011; Tinazzi et al., 2013; Defazio et al., 2013). Tremor associated with dystonia (TAWD) is defined as a tremor in the body regions unaffected by dystonia (Deuschl et al., 1998). Since both DT and TAWD share similar demographic and clinical features, it was suggested to summarize both under the term of DT (Quinn et al., 2011).

Figure 1-7 Syndromic classification of tremors

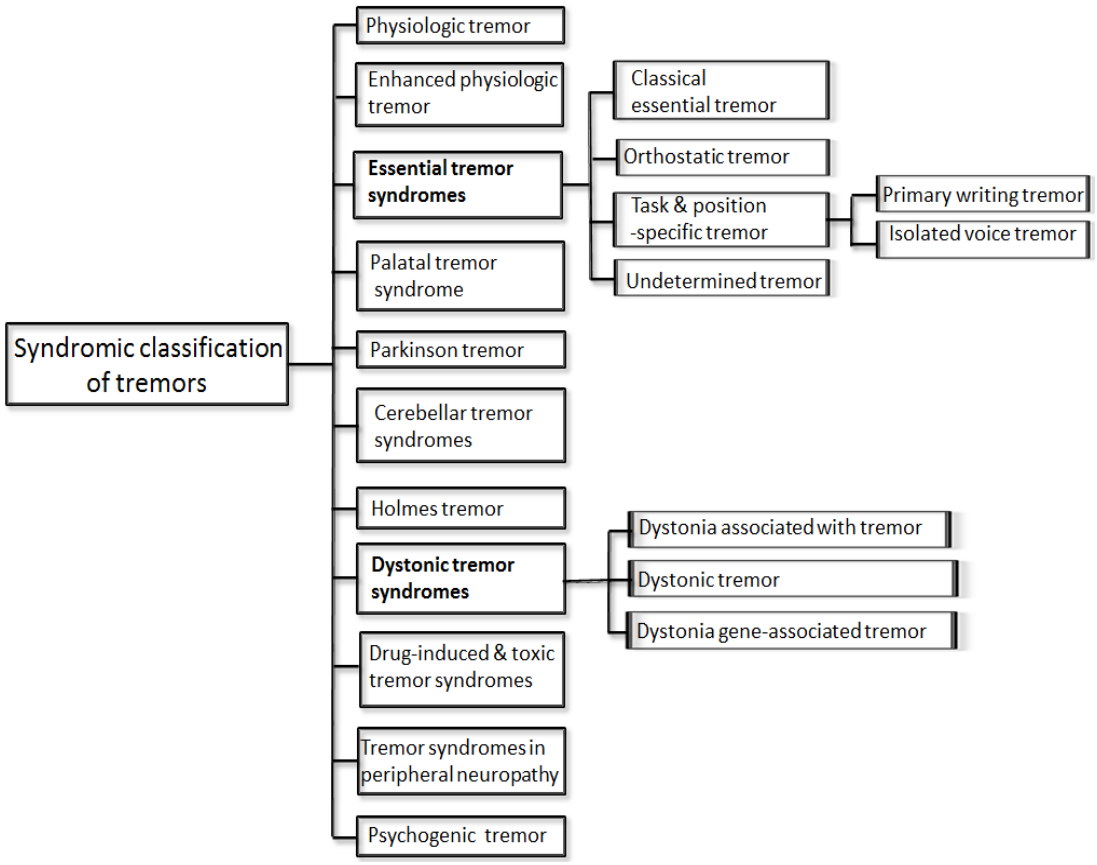

Classification of tremor on the basis of topographic distribution, relation to rest, posture and action, amplitude of tremor, frequency of tremor and presence of additional symptoms such as parkinsonian signs and neuropathy

Adjusted from (Deuschl et al., 1998)

Dystonia is a movement disorder characterised by sustained or intermittent muscle contractions causing abnormal, often repetitive movements, postures, or both (Albanese et al., 2013). Dystonic movements are typically patterned, twisting, and may be tremulous. Dystonia is often initiated or worsened by voluntary movements and associated with overflow muscle activation. The clinical classification of dystonia includes age at onset, body distribution, temporal pattern, coexistence of other movement disorders and other neurological manifestations (Table 1-2) (Balint and Bhatia, 2014). In terms of etiology, dystonias are classified according to whether they are the result of pathological changes or structural damage, have acquired causes or are hereditary. If there is no clearly defined etiology, the dystonia is considered as an idiopathic familial or idiopathic sporadic.

Dystonia may occur in isolation or in combination with myoclonus, parkinsonism or other movement disorders, etc. In ‘isolated dystonia’, dystonia is the only motor feature, with the exception of tremor (Albanese et al., 2013). A spontaneous oscillatory, rhythmical, often inconstant, patterned movement produced by contractions of dystonic muscles may give an impression of ‘tremor’ and often exacerbated by an attempt to maintain primary posture (Albanese, 2003; Lalli and Albanese, 2010).

In most patients with DT, tremor starts at dystonia onset or thereafter, affects women more frequently than men. It is usually a postural and action tremor but can also be seen at rest (Defazio et al., 2015). However, there are dystonias where tremor is the early presenting sign with late onset mild dystonia (Stamelou et al., 2013). More recently it has been highlighted that

dystonia patients can present with an asymmetric arm, head and voice tremor without clear dystonic posturing and these case can be misdiagnosed as ET (Stamelou et al., 2013). Moreover, there is still the lack of consensus about which symptoms can be accepted as dystonia, when considering DT phenomenology. Some consider any asymmetry of posture without clinical relevance to be dystonia, whereas some require more definite evidence of dystonia (Deuschl et al., 1998; Quinn et al., 2011).

Table 1-2 Classification of dystonia according to clinical and etiological features

Axis I: Clinical features	Age at onset	Infancy (birth to 2 years)
		Childhood (3–12 years)
		Adolescence (13–20 years)
		Early adulthood (21–40 years)
		Late adulthood (40 years and older)
	Body distribution	Focal (one isolated body region)
		Segmental (two or more contiguous regions)
		Multifocal (two or more non-contiguous regions)
		Hemi-dystonia (half the body)
		Generalized (trunk plus two other sites)
	Temporal pattern	Disease course (static vs. progressive)
		Short-term variation*
	Associated features	Isolated (may include tremor)
		Combined (other neurological or systemic features)
Axis II: Cause	Nervous system pathology	Degenerative
		Structural (focal lesions, degenerative changes, etc.)
		No degenerative or structural pathology
	Heritability	Inherited**
		Acquired***
	Idiopathic	Sporadic
		Familial

*short term variations include persistent, action-specific, diurnal, paroxysmal subcategories; **inherited causes include autosomal dominant, autosomal recessive, sex-linked, mitochondrial; ***acquired causes include brain damage, drugs/toxins, space occupying lesion, vascular, etc.

(Balint and Bhatia, 2014)

1.3.2 Pathophysiology

Co-contraction of agonist-antagonist muscles, excess of movements with loss of selectivity and overflow in muscle activation are clinical aspects of dystonia that are usually present across the different forms of dystonia. This phenomena is likely to depend on an balance between excitatory and inhibitory circuits because of defective inhibitory mechanisms operating at various levels of CNS (Kanovsky et al., 2015). However, it is still unclear whether DT has similar pathophysiology. The spinal circuitry investigation using the technique of reciprocal inhibition between agonist and antagonist muscles showed reduced descending control over spinal circuitry in dystonic patients with early onset arm tremor (Munchau et al., 2001). Moreover, brainstem excitability studied with the blink reflex technique suggested higher brainstem excitability in patients with DT than in patients with ET (Nistico et al., 2012a; Nistico et al., 2012b). 'Sensory trick' phenomenon in dystonia, also indicates the possibility of influence of peripheral sensory inputs onto motor circuits supported by neurophysiological studies (Hallett, 2011; Kanovsky, 2002; Abbruzzese et al., 2001).

Several models of basal ganglia dysfunction have been proposed to explain dystonia. These models postulate that dystonia results from a failure of the basal ganglia filtering that enables voluntary movements and suppresses competing ones that could interfere with the selected movement, or an imbalance between the direct excitatory and indirect inhibitory output pathways of the basal ganglia (Mink, 2003; DeLong and Wichmann, 2007; Gittis and Kreitzer, 2012).

More recent views have proposed that dystonia involves not only the basal ganglia but also other brain regions and related networks including cerebello-thalamo-cortical network (Neychev et al., 2011; Fiorio et al., 2011; Castrop et al., 2012; Niethammer et al., 2011) Studies in patients with clinically manifesting and non-manifesting DYT1 and DYT6 dystonia using diffusion-based tractography showed reduced connectivity of the cerebellum with the thalamus, suggesting that disruption of cerebellar outflow could be an important factor affecting the occurrence of motor symptoms (Argyelan et al., 2009). Several dystonia animal models have implicated cerebellar dysfunction in dystonia, including the tottering mutant mouse and DYT1 mutant mice with the *torsin1A* gene mutation (Ulug et al., 2011; Neychev et al., 2008). Dystonia might result from cerebellar dysfunction or from abnormal interactions of cerebellar and basal ganglia networks. These networks might interact anatomically at the level of the motor cortex or the striatum, as evidenced by histological tract tracing in animals, animal models of dystonia, and functionally in healthy human volunteers, in whom cortical excitability can be modulated after cerebellar interventions or after cerebellar diseases (Bostan et al., 2010; Neychev et al., 2008; Brighina et al., 2009; Hamada et al., 2012; Popa et al., 2013). The cerebellum might contribute to the deficit in sensorimotor integration recorded in dystonia because it processes proprioceptive information, alters somatosensory thresholds in the cortex, and has a key role in both temporal and spatial discrimination (Tinazzi et al., 2009; Stoessl et al., 2014).

1.3.3 Autosomal dominant dystonic tremors

Hereditary dystonias are inherited in autosomal recessive (AR), autosomal dominant (AD) or X-linked pattern. AD dystonias are clinically heterogeneous, could be isolated with childhood/adolescent-onset (DYT1, DYT6 and DYT13) or adult-onset (DYT7, DYT21, DYT23, DYT24 and DYT 25), and combined with other neurological features, including parkinsonism (DYT5, DYT12, DYT11, DYT15, DYT4, DYT8, DYT20, DYT10, DYT19 and DYT 18) (Table 1-3) (Albanese et al., 2013; Camargo et al., 2015).

All isolated AD dystonias manifest as either focal or generalized dystonia, except DYT7, DYT24 and DYT23. DYT1 dystonia, caused by a single 3 bp (GAG) deletion at chromosome 9 (9q34) has been originally identified in a large family with early-onset generalized dystonia (Ozelius et al., 1997). However, DYT1 phenotypic spectrum typically has the age of onset (before twenty years of age) and limb onset (mainly the legs) (Bressman et al., 2000). Similarly, patients heterozygous to *THAP1* mutation (DYT6) can present either as an adolescent-onset generalized dystonia (with the first appearance in the arms) or late-onset craniocervical dystonia (Xiao et al., 2010; Fuchs et al., 2009; Klein, 2014; Camargo et al., 2014). The phenotype of DYT13 is similar to that of DYT6 dystonia except for the lesser involvement of the larynx and legs in the former (Valente et al., 2001). Blepharospasm, cervical dystonia and upper-limb dystonia is prevalent in the affected individuals heterozygous at the DYT21 locus (2q14.3-21.3) with some cases also presenting as generalized dystonia (Forsgren et al., 1988; Norgren et al., 2011).

Table 1-3 Autosomal dominant dystonias

Locus	Gene	Isolated dystonias
DYT1/9q	*TOR1-A*	Early-onset primary generalized dystonia
DYT6/8p	*THAP1*	Mixed dystonia
DYT13/1p	-	Early-onset primary segmental craniocervical dystonia
DYT7/18p	-	Adult-onset focal dystonia
DYT21/2q	-	Late-onset focal dystonia
DYT23/9q	*CIZ1*	Adult-onset primary cervical dystonia
DYT24/11p	*ANO3*	Craniocervical dystonia
DYT25/18p	*GNAL*	Late-onset primary focal dystonia
Locus	**Gene**	**Combined and paroxysmal dystonias**
DYT5/14q	GCH1	Dopa-responsive dystonia
DYT12/19q	*ATP1A3*	Rapid-onset dystonia parkinsonism
DYT11/7q	-	Myoclonus-dystonia
DYT15/18p	*SGCE*	Myoclonus-dystonia
DYT4/19p	*TUBB4*	Dystonia with whispering dysphonia
DYT8/2q	*MR-1*	Paroxysmal nonkinesigenic dyskinesia 1
DYT20/2q	-	Paroxysmal nonkinesigenic dyskinesia 2
DYT10/16pq	*PRRT2*	Paroxysmal kinesigenic dyskinesia 1
DYT19/16q	-	Paroxysmal kinesigenic dyskinesia 2
DYT18/1p	*SLC2A1/GLUT1*	Exercise-induced paroxysmal dyskinesia

Adapted from (Albanese et al., 2013; Klein, 2014)

The gene locus responsible for DYT7 at chromosome 18p is associated with late-onset craniocervical dystonia, upper-limb dystonia and spasmodic dysphonia without further generalization (Leube et al., 1996). No potentially disease-causing mutations including copy-number variation (CNV) have been detected at DYT7 locus (Cassetta et al., 1999; Winter et al., 2012). Similarly, in adult-onset cervical dystonia an exonic splicing enhancer mutation [c.790A > G (p.S264G)] was identified in exon 7 of the *CIZ1* gene (DYT23) do not progress from the focal form to generalized dystonia (Uitti and Maraganore, 1993; Xiao et al., 2012). Neither gene has been found mutated in any other families leading to suspicion the original reports may be wrong.

Tremor can be a prominent clinical feature in some AD dystonias. Mutations of the *ANO3* gene were identified to cause AD tremulous craniocervical dystonia and have been designated to the dystonia locus 24 (DYT24) (Charlesworth et al., 2012). All affected individuals heterozygous to *ANO3* mutation clinically manifest with tremor, which contrasts DYT24 from the typical DYT6 phenotype (Stamelou et al., 2014). Moreover, in some affected individuals carrying an *ANO3* mutation, tremor can be the sole initial manifestation, without or (later) with very mild dystonic posturing leading to misdiagnosis as ET (Stamelou et al., 2014). Tremor has also been described in DYT6 and DYT1 as the prominant feature (Blanchard et al., 2011; Xiromerisiou et al., 2012; Bressman et al., 2009; Clot et al., 2011; Almasy et al., 1997; Stamelou et al., 2013). Another new cause of dystonic head tremor is isolated familial dystonia that is due to guanine nucleotide binding protein

(G protein), alpha activating activity polypeptide, olfactory type (*GNAL*) gene mutations (DYT25) (Fuchs et al., 2013).

DYT5 and DYT12 are AD dystonia loci associated with parkinsonism. Dopa-responsive dystonia (DYT5) is a rare form of dystonia with cases heterozygous to mutations in the *GCH1* gene (Segawa, 2009). The *GCH1* gene consists of six exons, with various mutations in exons as well as introns causing dopa-responsive dystonia. The typical presentation is dystonia concomitantly with or following parkinsonism with a worsening of symptoms during the day in majority of cases and a dramatic response to levodopa therapy (Segawa, 2009; Kamal et al., 2006; Nutt and Nygaard, 2001). Similarly, rapid-onset dystonia-parkinsonism (*DYT12/ATP1A3*) is extremely rare, with a sudden onset of dystonia/parkinsonism triggered by a psychological stressor (Pittock et al., 2000; Brashear et al., 1997; de Carvalho Aguiar et al., 2004). The dystonia typically affects the limbs and face, and distribution of dystonia and parkinsonism signs shows a clear rostrocaudal gradient with the bulbar symptoms being more severe than the symptoms in the upper limbs and less severe in the lower limbs. (Brashear et al., 1997).

1.4 Basic principles of neurogenetic studies

1.4.1 Analysis of structural chromosome variants

1.4.1.a Structural chromosome variants

The spectrum of human genetic variation ranges from single base pair alterations to chromosomal structural events involving small genomic regions to entire chromosomes. Structural variants (SVs) are an example of chromosomal rearrangements that span more than 50 base pairs (bp) (Abecasis et al., 2010). SVs vary widely in size and there are numerous classes of variation including deletions, translocations, inversions, mobile element transpositions, tandem duplications, novel insertions and CNVs (Table 1-4 and Table 1-8).

SVs may develop either when recombination during meiosis occurs between mispaired homologues or when cellular repair mechanisms incorrectly handle unwanted free chromosomal ends produced by chromosome breakage. If two different chromosomes each sustain a single break, incorrect joining of the broken ends can result in a movement of genetic material between chromosomes, a process called translocation. Exchange between an acentric fragment of chromosomes creates products that are stable in mitosis, while exchange of an acentric fragment for a centric fragment producing unstable products (Strachan and Read, 2010). Structural chromosomal abnormalities are balanced if there is no gain or loss of chromosomal segment, while unbalanced if there is a net gain and loss of genetic material. Balanced abnormalities are less likely to manifest clinically

unless a chromosomal break disturbs coding sequence or affects gene expression.

At least two distinct models have been proposed with respect to associations between disease and SVs. The first involves large variants (typically gains and losses of several hundred kilo base pairs in length) that are individually rare in the population (<1%) but collectively account for a significant fraction of disease, as seen for some neurological and neurocognitive disorders (Sebat et al., 2007; Sharp et al., 2006; de Vries et al., 2005; Stankiewicz and Lupski, 2002). Since some genes are dosage sensitive, either duplication which will increase a gene dosage by 150% or deletions which reduce it by 50% affect phenotypic expression of genes. Consequently, ID is the almost universal consequence of autosomal imbalance, and vice versa, much ID is due to a chromosome abnormality (Gardner et al., 2011).

Imbalanced chromosomal abnormalities can arise de-novo or directly via deletion or duplication, or indirectly by malsegregation of chromosomes during meiosis, in a carrier of a balanced abnormality (Gardner et al., 2011). A parental carrier of a balanced reciprocal translocation can produce gametes that give rise to a phenotypically normal balanced carrier child or to various unbalanced karyotypes that always combine monosomy for part of one of the chromosomes with trisomy for part of the other (Strachan and Read, 2010).

SV discovery and genotyping requires accurate prediction of three features: copy, content and structure. In practice, it is difficult as SVs tend to reside within repetitive DNA, which makes their characterisation more difficult.

Current methods for discovery and then for genotyping includes experimental approaches using microarrays, single-molecule analysis and sequencing-based computational approaches (Alkan et al., 2011).

Table 1-4 Types of chromosomal abnormalities

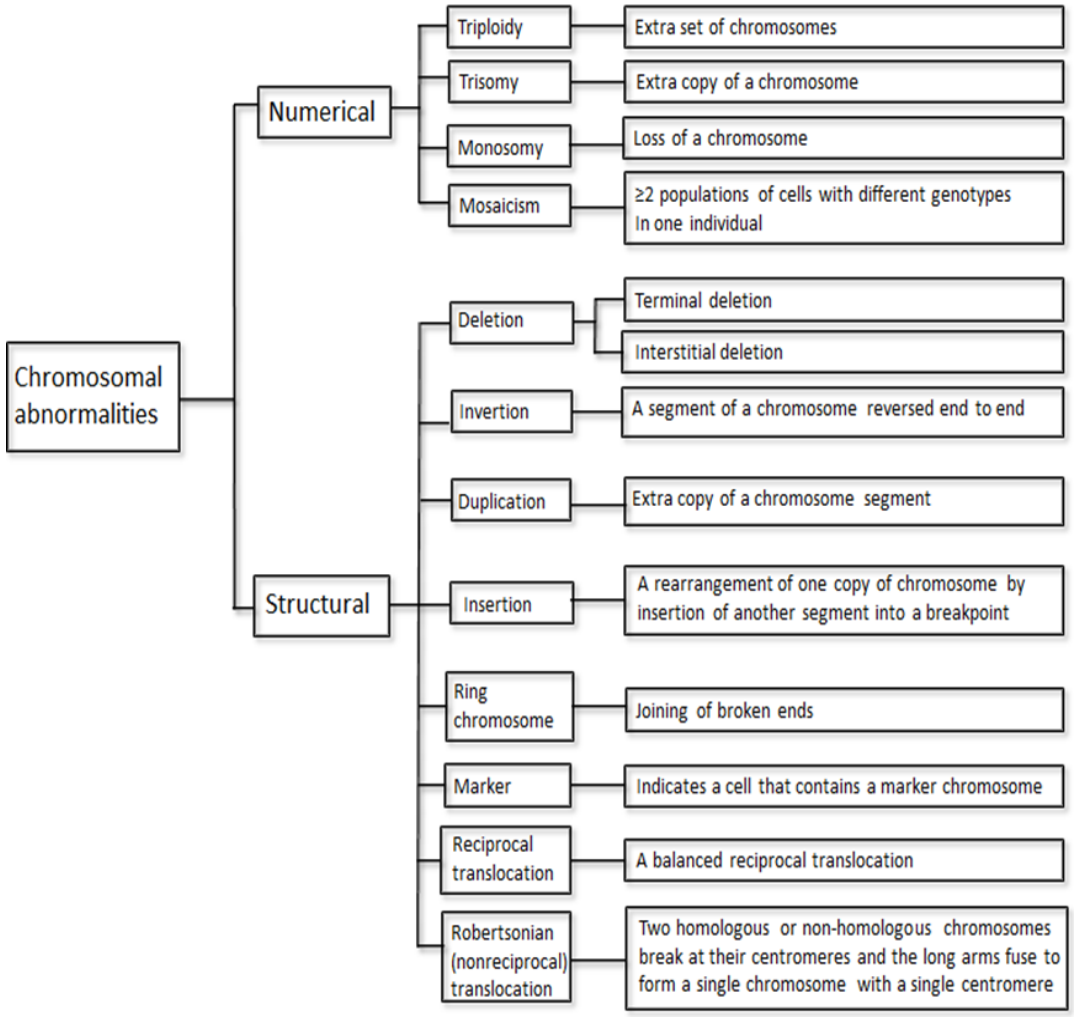

Figure 1-8 Types of structural variation

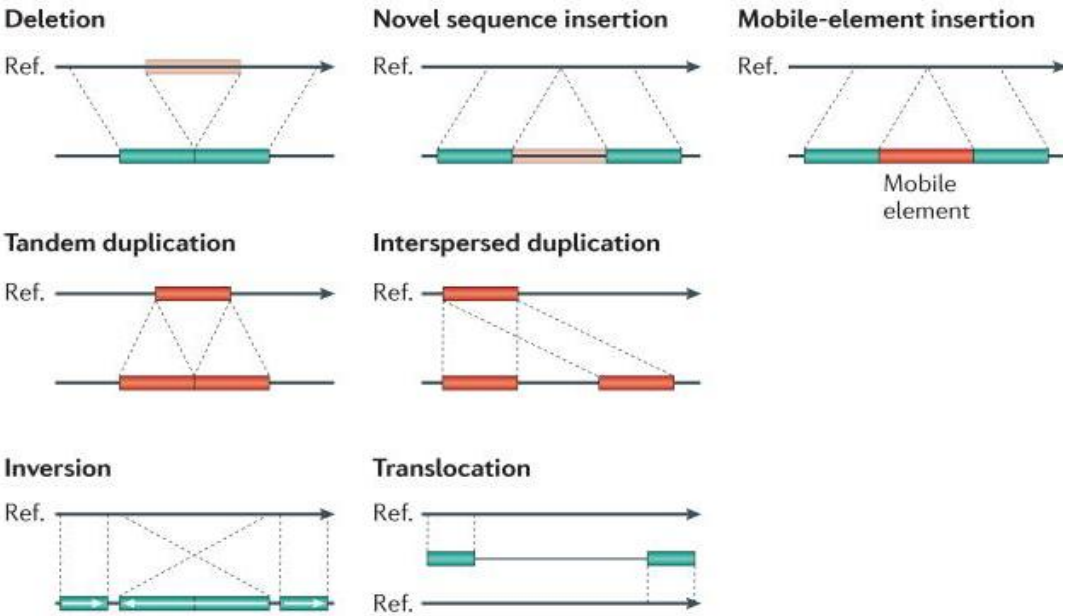

The schematic depicts deletions, novel sequence insertions, mobile-element insertions, tandem and interspersed segmental duplications, inversions and translocations in a test genome (lower line) when compared with the reference genome.

(Alkan et al., 2011)

1.4.1.b Genetic characterisation of structural variation

Hybridization-based technologies such as array comparative genomic hybridization (array CGH) and single nucleotide polymorphism (SNP) microarrays have historically been the chief approaches for the discovery and genotyping of CNVs (Iafrate et al., 2004; Sebat et al., 2004; Locke et al., 2004; Itsara et al., 2009; Snijders et al., 2001; Pinkel et al., 1998). Both array CGH and SNP array platforms are based on the principle of comparative hybridization of tested and reference labelled DNA samples to a set of hybridization targets (typically long oligonucleotide probes). Compared to array CGH, SNP microarray platforms perform hybridization on a single sample per microarray, and use SNP allele-specific probes (McCarroll et al., 2008; Cooper et al., 2008; Peiffer et al., 2006). The number of probes required to detect a single-copy alteration as well as signal-to-noise ratio for each probe varies between platforms. Illumina platform that was used in current study require ten probes to reliably detect a single CNV (Itsara et al., 2009).

Both array CGH and SNP array platforms use the signal ratio, Log2 between a test and reference sample to infer copy number variation (Pinkel et al., 1998; Coe et al., 2007) (Figure 1-9). An increased log2 ratio represents a gain in copy number in the test compared with the reference, while a decrease indicates a loss in copy number. Although signal-to-noise ratio for each probe is lower in SNP microarrays than that of array CGH platforms, SNP arrays also measure B allele frequency (BAF). This metric distinguishes alleles and increases sensitivity of CNV detection. BAF score zero represents the genotype A/A or A/–, whereas 0.5 represents A/B and 1

represents B/B or B/– (Alkan et al., 2011) (Figure 1-9). Different BAF values would occur for AAB and ABB genotypes or more complex genotypes. BAF can only accurately assign copy numbers from 0 to 4 in diploid regions of the genome, as homozygous deletions do not results in BAF clustering (Cooper et al., 2008; Peiffer et al., 2006).

Microarrays platforms are less sensitive in the detection of single-copy gains (3 to 2 copy-number ratio) compared with deletions (1 to 2 copy-number ratio) (Itsara et al., 2009; Cooper et al., 2008; Coe et al., 2007; Craddock et al., 2010). This is particularly difficult when copy number gains encompass only a few probes and SNP arrays may not contain sufficient probe density to use the BAF measurement. Moreover, microarrays platforms are generally unable to resolve breakpoints at the single-base-pair level and identify balanced structural variants requiring additional technologies to detect the accurate boundaries and copy numbers of these events.

FISH is an approach that allows characterisation of chromosomal rearrangements including balanced translocations and detects the origin of the duplicated chromosomal material. FISH analysis is based on the sequence specific hybridization of a fluorescently labeled DNA probe to metaphase preparations from cultured cells where the exact position of the signals can be visualized directly (Kwasny et al., 2012). Complex interchromosomal rearrangements or the origin of the marker could be identified by a 24-color karyotyping technique, multiplex in situ hybridization that enables the simultaneous visualization of all chromosomes in a single hybridization (Anderson, 2010). However, their low throughput and low

resolution limit FISH application to a few individuals and to particularly large structural differences (~500 kilobase (kb) to 5 megobase (Mb)) (Alkan et al., 2011).

Next-generation sequencing technologies (NGS) have been revolutionizing genome research as well as the study of CNVs and SVs on the whole replacing microarrays as the leading platform for the investigation of genomic rearrangement (Tattini et al., 2015). NGS platforms are based on various implementations of cyclic-array sequencing which allow sequencing of millions of short (few hundreds bp) DNA fragments (reads) simultaneously and may process a whole human genome in three days at 500-fold less cost than previous methods (Shendure and Ji, 2008; Shendure et al., 2011; Voelkerding et al., 2009; Metzker, 2010). There are four general types of strategy all of which focus on mapping sequence reads to the reference genome (derived from the 1000 Genomes Project) and subsequently identifying discordant signatures or patterns that are diagnostic of different classes of SV (Medvedev et al., 2009; Mills et al., 2011).

Read-depth NGS approaches assume a random distribution in mapping depth and investigate the divergence from this distribution to highlight duplications and deletions in the sequenced sample (Bailey et al., 2002). Duplicated regions results in higher read depth while deletions show reduced read depth when compared to normal. Split-read NGS approach targets SV breakpoint on the basis of a split sequence-read signature breaking the alignment to the reference. A gap in the read is a marker of a deletion while stretches in the reference reflect insertions (Alkan et al., 2011). Another NGS

method, sequence-assembly approach uses a combination of de novo and local-assembly algorithms to generate sequence that are then compared to a reference genome.

Read-pair (RP) is another NGS method which compares the average insert size between the actual sequenced read-pairs with the expected size based on a reference genome. In paired-end sequencing, the DNA fragments are expected to have a specific distribution around insert size. The discordance between mapped paired-reads whose distances are significantly different from the predetermined average insert size is utilized by pair reads to identify CNVs. In other words, by using the known physical size separation between the paired-end reads from a given fragment (defined by the size of the DNA fragments used for the library prep) anomalous spacing and its orientation (alignment track) can be detected when these reads are mapped back to the reference genome (Lam et al., 2010). Using this approach, a reasonably tight size range of library fragments (~400 bp) can be created using low coverage (around eightfold) genome sequencing. PRs that map too far apart are associated with deletions while those found closer than expected are indicative of insertions (Tattini et al., 2015). Furthermore, orientation inconsistencies can delineate inversions and a specific class of tandem duplications. In tandem duplications a large section of DNA is duplicated and inserted into the genome next to the original sequence (Figure 1-10). The PR sequences become not only duplicated, but also are arranged or aligned opposing as well as in the same direction. PR sequencing approach allows mapping breakpoint region of the SV event in a single base pair level for

further screening a large number of samples at a very low cost per assay by PCR-based techniques.

Conventional polymerase chain reaction (PCR) across sequenced breakpoints, quantitative PCR and multiplex ligation-dependent probe amplification (MLPA) that is based on the quantification of PCR fragments in capillary electrophoresis are approaches that allows a large number of samples to be analyzed at a relatively low cost per sample (Korbel et al., 2007; Weksberg et al., 2005; Schaeffeler et al., 2003; Gomez-Curet et al., 2007; Schouten et al., 2002).

Figure 1-9 CNV detection by array CGH and SNP microarrays

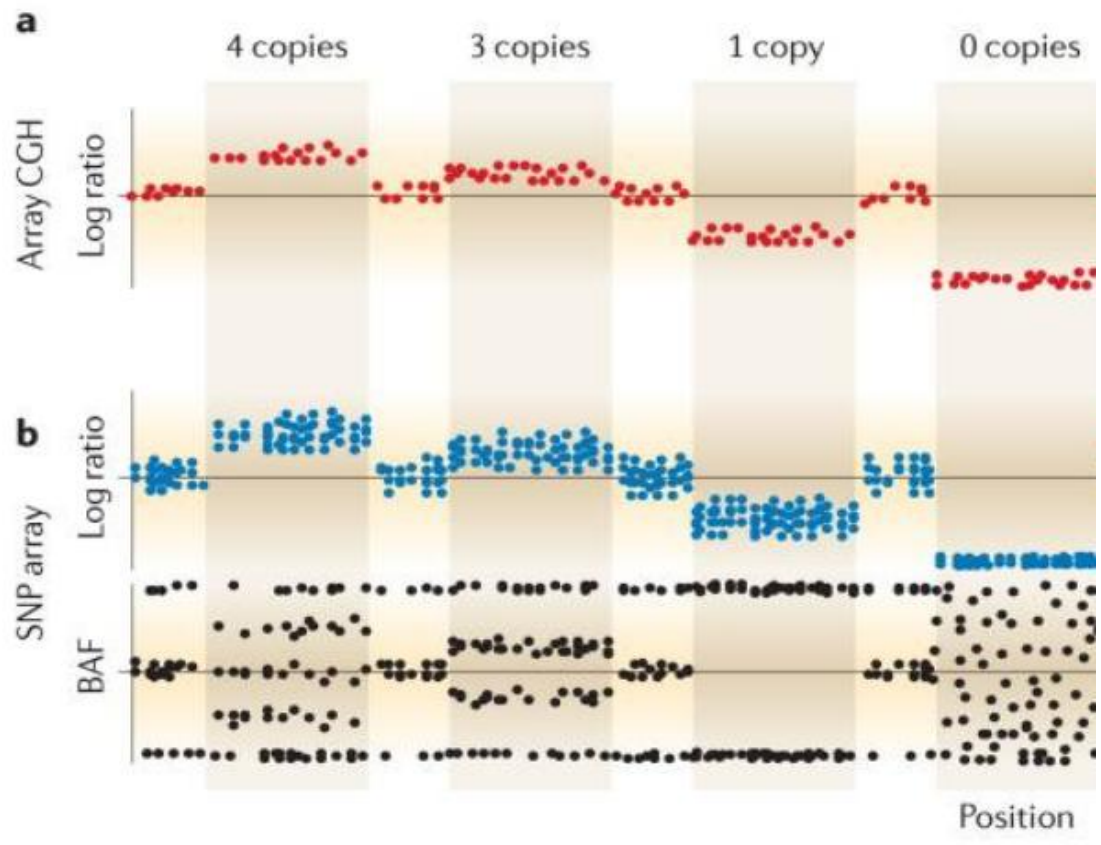

(a) Array CGH $\log_2$ ratio that acts as a proxy for copy number. Dots (blue, red or black) represent single allele. (b) SNP microarray with log2 similar to array CGH log2 is a proxy for copy number. An increased log2 ratio represents a gain in copy number in the test compared with the reference; conversely, a decrease indicates a loss in copy number both. BAF is a B allele frequency that is a metric that enables a more comprehensive assignment of copy number.

(Alkan et al., 2011)

Figure 1-10 Read pair mapping pattern in tandem duplications

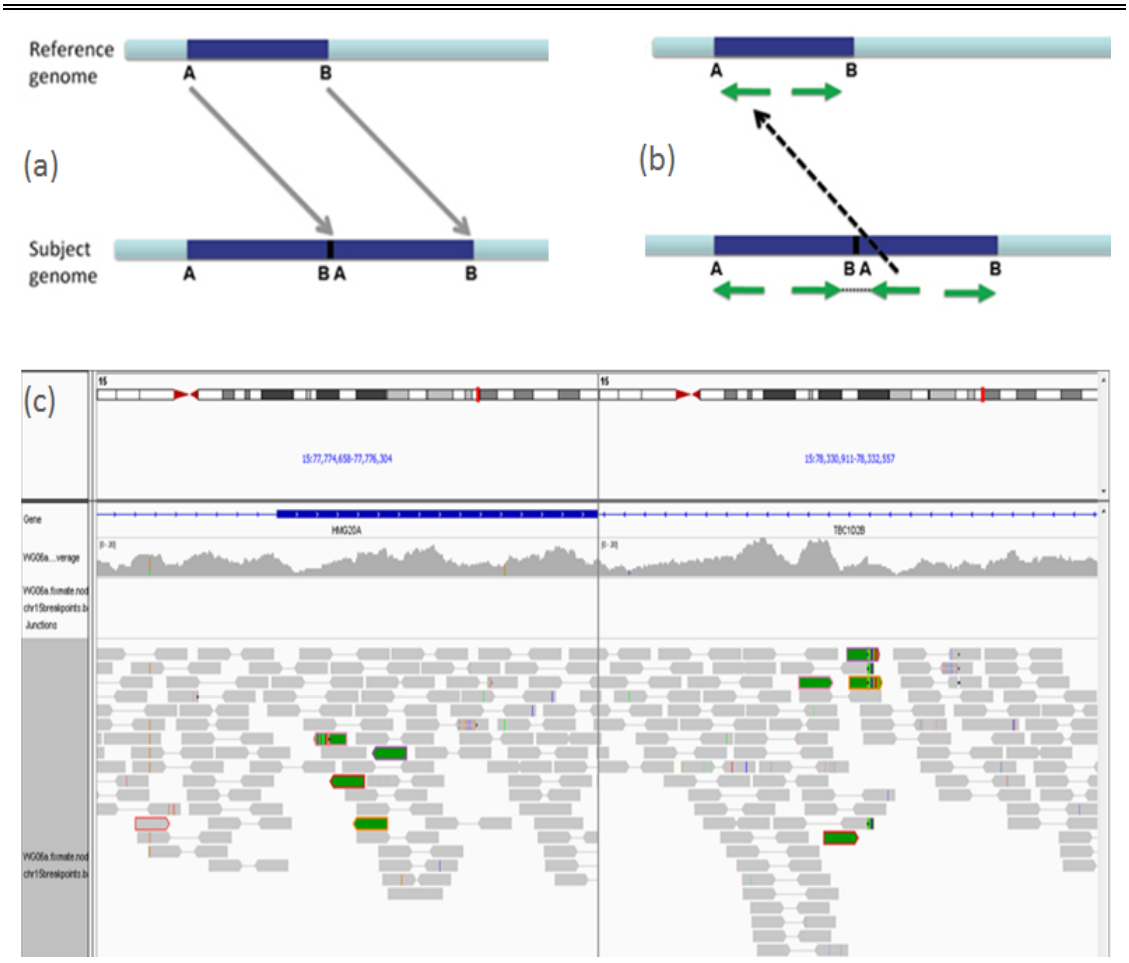

(a) Illustration of the tandem duplication where A stands for 5' end strand and B stands for 3' end. In tandem duplication the DNA fragment is duplicated and aligned in a way that 5' end of duplicated fragment 'A' face 3'end of original or reference fragment 'B'; (b) Illustrated pair read NGS approach where pair-read sequences (green lines) are designed from DNA fragment library. In tandem duplication those pair-reads become arranged in a way that they face each other as well as in opposite direction; (c) Integrative genomic viewer (IGV) display of the tandem rearrangement of case III: 15 from the pedigree Figure 5-3, where coloured lines demonstrate pair reads mapping approximately 550kb away in reverse-forward rather than forward-reverse orientation, suggesting a tandem duplication event.

1.4.2 Systematic elucidation of single gene disorders

1.4.2.a Single gene disorders

Single-gene diseases, also known as Mendelian or monogenic disorders are defined as disorders caused by a mutation in one or both members of a pair of autosomal genes or mutations in single genes on the X or Y chromosomes. The pattern of inheritance of single gene disorders are based on the first (the principle of independent segregation) and second (the principle of independent assortment) laws of inheritance. In AR inheritance, an affected individual inherits both copies of the gene mutation (alleles) from unaffected parents who each carry one copy of the mutated gene. In contrast, one mutated copy of the gene in each cell is sufficient for a person to be affected by an AD disorder.

Compared to single gene disorders where a single gene is both necessary and sufficient to express a disease, complex or multifactorial disorders are likely associated with the effects of multiple genes in combination with lifestyle and environmental factors. Complex disorders often cluster in families' without a clear-cut pattern of inheritance pattern. They usually manifest only later in life, or are relatively mild, while single gene disorders are mostly severe, early-onset conditions, necessitating lifelong care and support. Moreover, as a group, single gene disorders are certainly not rare and it is estimated that around one third of recognizable Mendelian disease traits display phenotypic expression involving the nervous system (Warner and Hammans, 2008).

1.4.2.b Linkage mapping and whole exome sequencing

The initial phase in a map-based genetic study of monogenic disorders is to identify families with the precise phenotypic characteristics of the disease in order to perform errorless linkage analysis. The number of individuals available for study provides the appropriate power in linkage analysis to identify the disease gene location. The next phase involves undertaking linkage analysis to localize the position of the as yet unknown “disease gene” to a small genomic region.

Linkage is the co-segregation of a genetic region (haplotypes) with a disease phenotype within a family. DNA polymorphic markers close to a disease-causing mutation are co-inherited with the disease-causing mutation, unless separated by recombination events (Figure 1-11). The closer the marker to the disease-causing gene, the less likely it will be separated at meiosis. An area of linkage within a family may extend a considerable genetic distance. The basic principle of linkage analysis is the identification of those markers that co-segregate with the disease phenotype. The DNA markers, which constitute part of the normal nucleotide variability of the genome, usually are either single nucleotide polymorphisms (SNP) or short sequence repeats (SSRs). For the linkage analysis studies, the most useful markers are SSRs since they are highly polymorphic. The position, order and distance of markers have been identified throughout the entire genome and used to create linkage maps of all human chromosomes (The International HapMap Project (2003)). These highly polymorphic markers in turn provided the tools to localize the unknown disease related genes to intervals of the genome. Most of the linkage mapping studies uses at least 300 such markers equally

distributed throughout the genome with an average interval of at least 10 centimorgan (cM), or 10% recombination between adjacent markers. Of note, 1 cM which equates to a million base pairs is a unit for the measuring of genetic linkage which corresponds to recombination units in human meiosis.

The success of linkage mapping in a monogenic disease largely depends on the size of the families investigated which correlates with statistical “power” to detect linkage, as well as phenotypic accuracy and genetic heterogeneity of the phenotype. Traditional “parametric” linkage analysis compares the likelihood of the observed transmission of genetic markers in relation to the trait or disease, in the context of a specified model of inheritance. The ability to map a gene depends on the number of recombination events within a pedigree. Thus, large families with many affected individuals, specifically distantly-related individuals who have a high number of meioses and recombination events between them are the most useful for linkage mapping (Duncan et al., 2014). Diseases with late onset of clinical features or with incomplete penetrance however may be harder to investigate by linkage due to possible incorrect attribution of disease status among family members.

Thus linkage mapping is beneficial in that it evaluates DNA sample quality, elucidates whether specified familial relationships are correct, allows the detection of mis-specification of affection status and locus heterogeneity, aids the selection of an individual (or individuals) to undergo whole-genome sequencing (WGS), and facilitates the mapping of the disease locus to a

region (or regions) of the genome, thus reducing the number of variants that need to be followed up (Ott et al., 2015).

The genetic regions identified by linkage studies may harbor many hundreds of genes, and fine mapping with next-generation sequencing (NGS) filtering approaches usually is necessary to identify the exact causative gene. Since the majority of pathogenic mutations are in exons or the flanking intronic regions, the approach of NGS with the use of exome enrichment has been implicated to detect single disease-causing mutations (Figure 1-12) (Ng et al., 2010; Ng et al., 2009). The advantage of this method, also called whole exome sequencing (WES), is that coding DNA represents less than 2% of the entire genome and consequently this degree of enrichment can significantly boost the depth of coverage for a given run at a lower cost.

The major limitation of WES is that heterozygous variants and CNVs are much more challenging to call by WES compared to a homozygous variant. Hence, focusing on exomic variants that are homozygous represents a major enrichment step in the quest to identify the causal variant in the setting of AR. When linkage mapping highlights a single critical locus, considering only variants within that locus offers a helpful lead (Alkuraya, 2012). Further allele frequency and mutation analysis (which has relative significance) search stratifies variants for further manual sequencing and co-segregation analysis.

Figure 1-11 Linkage mapping

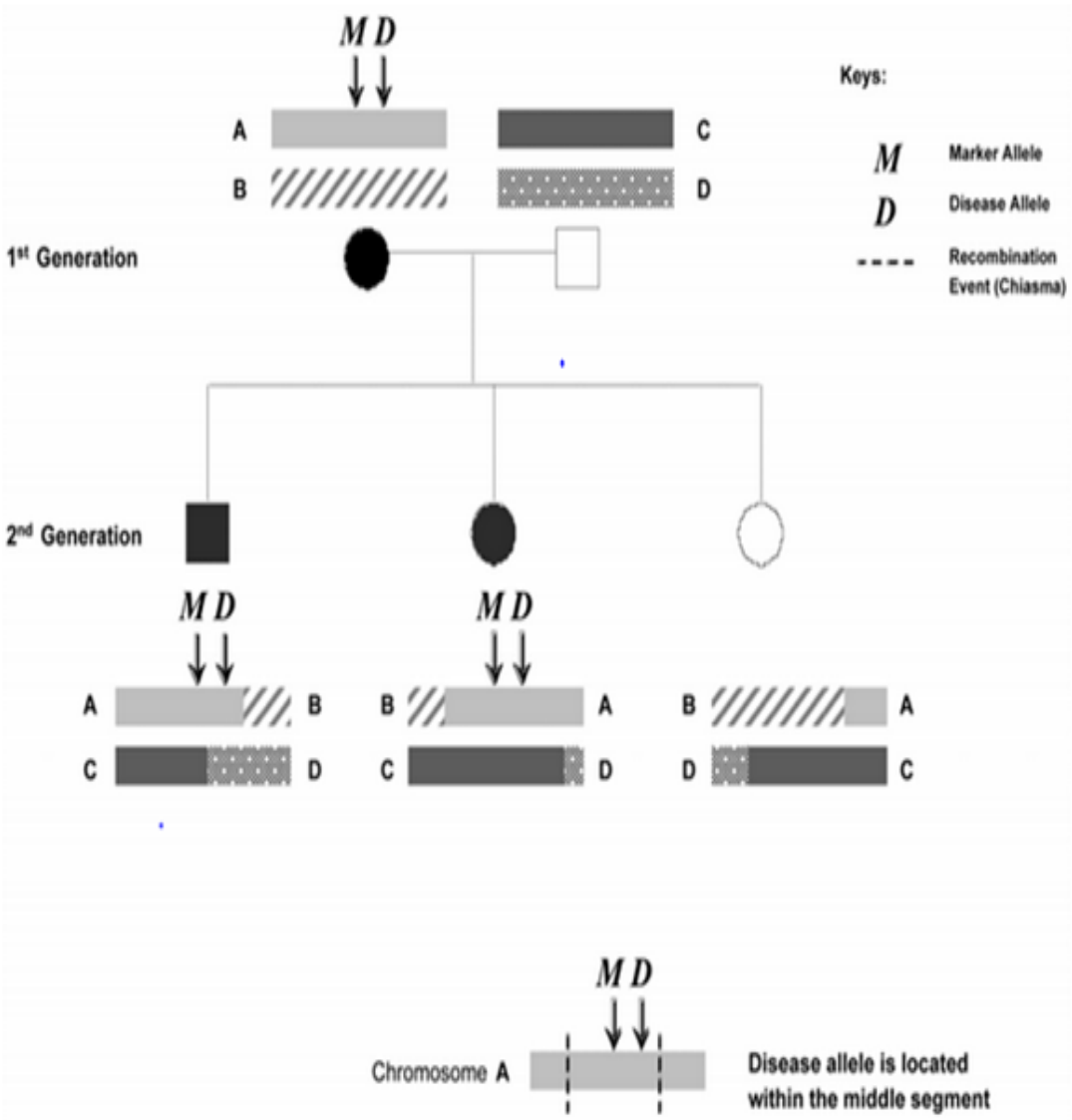

Illustration of the linkage mapping with evidence of a disease-causing allele (D) obtained by coinheritance with a marker allele (M) in a pedigree with AD inheritance pattern. Transmitted recombined haplotypes help to reduce the target region to search for the disease-causing gene.

(Collins, 2007)

Figure 1-12 Whole exome sequencing

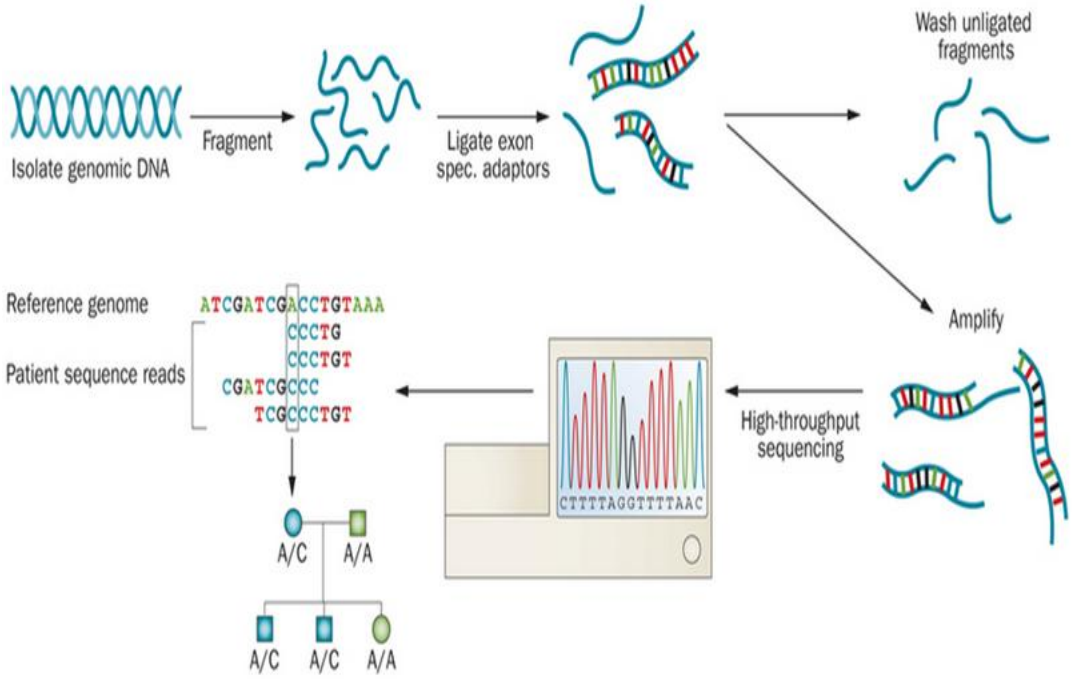

First genomic DNA is isolated from a patient and fragmented; then DNA-based exon-specific adaptors ligate to the coding sequences in the DNA; unligated fragments, which represent the noncoding DNA are removed and the exon–adaptor combinations amplified to increase copy number; the amplified fragments are sequenced using high-throughput sequencing techniques; at the final stage multiple sequence reads from a patient are compared with a reference genome sequence from which a pedigree of variant inheritance can be determined.

(de Bruin and Dauber, 2015)

1.5 Applying Genomic Technologies to address Clinical Challenges in the Indian subcontinent study

1.5.1 Indian subpopulations and founder mutations

The geographical and political boundaries of the Indian subcontinent include India, Pakistan, Bangladesh, Sri Lanka, Nepal, Bhutan and other small islands of the Indian Ocean. The subcontinent has been the seat of some of the oldest civilizations of the world with the earliest historically documented remains dating back to as early as 70,000 years. The majority of South Indian populations originates from East Asia more than 55,000–80,000 years before present (YBP) and share a common ancestor with east-Africans (Majumder, 2010; Tamang et al., 2012) (Figure 1-13). Further population movements from central Asia to India 6,000 YBP originated Indus valley civilization, ancestral of Dravidian race (McElreavey and Quintana-Murci, 2002) (Quintana-Murci et al., 2001; Nehru, 2004; Kumar, 2012). The most recent population expansion from central Eurasia into India gave rise to Aryans or Indo-Europeans (Quintana-Murci et al., 2001). Similarly, the population of Jalbai from Khyber Pakhtunkhwa province, Pakistan is Muslims and Pakhtuns (Pathans) which originates from Indo-European race (Nichols, 2008; Qamar et al., 2002). The Dravidian race was widespread throughout India before the arrival of the Indo-Aryans further segregating to the south of India (Kanthimathi et al., 2008). Evidence from population genetics studies dating back to over 30–100 generations in Indo-European and Dravidian-speaking groups suggests that endogamy prevents founder events from being erased by gene flow (Reich et al., 2009).

AR disease-causing alleles are introduced at a rate proportionate to the human mutation rate of 1.2 in 108 per nucleotide per generation, therefore it is predicted that unaffected individuals carry a number of pathogenic recessive alleles in the heterozygous state (Kong et al., 2012). If a population traces its origin to a few founders, then these alleles will assume a high frequency such that any two individuals taken at random from the reproductive pool may be more likely to be carriers. For example, analysis of 20 Indian spinocerebellar ataxia type 12 (SCA12) families and ethnically matched normal unrelated individuals revealed a specific haplotype to be significantly associated with the SCA12 phenotype, clearly indicating the presence of a common founder mutation for SCA12 in the Indian population (Bahl et al., 2005).

The ‘founder effect’ phenomenon as well as a high rate of consanguinity increases prevalence of AR disorders in population isolates. It has been estimated that the frequency of founder mutations and the burden of heritable genetic disorders has increased in select Indian subpopulations and communities not only due to the shared common recent ancestry, but also a long cultural and religious tradition of intracommunal and intracaste endogamy (Bittles, 2007; Krishnamoorthy and Audinarayana, 2001). More than 50 million individuals in India are affected with single-gene disorders (Singh et al., 2010). Likewise, the prevalence of consanguineous marriages has increased in Khyber Pakhtunkhwa province, Pakistan correlating with the raise of AR inherited disorders (Sthanadar et al., 2015).

Figure 1-13 Major migrations of modern humans in south-west Asia

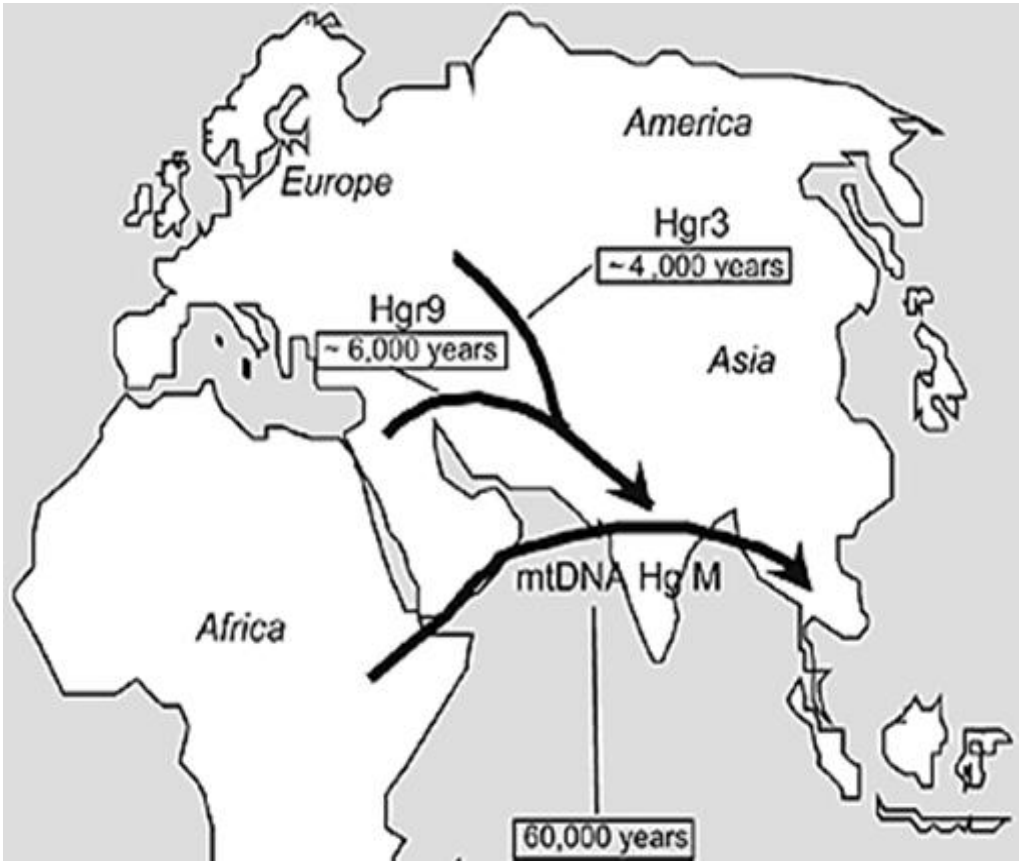

The bottom arrow indicates the migration of the South Indian populations to East Asia more than 60,000 years ago from east-Africa. This was detected by mtDNA (human mitochondrial deoxyribonucleic acid) co-segregation analysis. Top arrows show further population movements from central Asia to India 4.000-6,000 years before present detected by Y chromosome haplotypes (Hgr3/Hgr6). Both Y chromosome and mtDNA avoid recombination and hence are used for the tracing of population origins.

(McElreavey and Quintana-Murci, 2002)

1.5.2 'Applying Genomic Technologies to address Clinical Challenges in the Indian Subcontinent' (AGTC-India)

The WHO has highlighted the need for early diagnosis, prevention, and management of genetic disorders in developing countries and released detailed guidelines (Christianson and Modell, 2004). However, a lack of widespread awareness about genetic disorders in the general population in the developing countries, and the scarcity of specialized medical professionals and affordable genetic tests, increase challenges to practice those guidelines to reduce disease burden (Ankala et al., 2015). In vast countries such as India and Pakistan, where the disease burden is tremendous and resources are limited, low-cost diagnostic tests that target specific common mutations or founder mutations in select communities or subpopulations hold significance (Ankala et al., 2015). Hence, genetic studies aimed at identifying and cataloguing founder mutations are expected to further the development of low-cost and targeted assays with further educational as well as clinical applications and significance.

'Applying Genomic Technologies to address Clinical Challenges in the Indian Subcontinent' (AGTC-India) is a research project that entails a clinical and genomic investigation of inherited neurological conditions occurring within families from the Indian subcontinent. The aim of the project is to identify common as well as founder mutations in the population isolates of Indian subcontinent in order to develop carrier and prenatal screening tools. Apart from the scientific benefits, an investigation of inherited neurological conditions in Indian subcontinent could provide educational, diagnostic as well as therapeutic benefits. Making definite molecular diagnosis could

enable early intervention and clinical care by providing appropriate educational and prognostic guidance to family practitioners and affected families. Furthermore, the identification of known genes in the families with a non-specific clinical presentation could guide the regional physician on which proven-beneficial therapeutics to apply. The direct benefits for the families would be the insight into their disease and available future treatment options.

The studies described in this thesis are based around the investigation of three extended families with multiple individuals affected by distinct neurological conditions defined as part of the AGTC-India study.

1.6 Aims

The overarching aim of this study, undertaken as part of the AGTC-India project, is to clinically characterise and define the molecular basis of three neurological as well as neurodevelopmental disorders. The specific goals of my PhD project includes:

1 To characterise the clinical phenotypes of affected individuals from three extended multigenerational families with neurodevelopmental disorders and dystonic tremor by either interviewing and examining affected and unaffected individuals, or evaluating clinical data of affected individuals collected by other clinicians.

2 To undertake detailed genetic studies, including autozygosity mapping, linkage studies, mutation screening, and next generation sequencing to identify underlying molecular causes in these families.

3 To investigate the function of genes identified in order to provide novel information regarding a disease mechanism in order to aid the design of possible future treatment strategies.

4 To translate genetic findings into clinical benefit by providing knowledge for the development of new genetic screening tools for patients.

2

CHAPTER TWO

MATERIALS AND METHODS

MATERIALS AND METHODS

2.1 Subjects and samples

AGTC-India project studies have been reviewed and approved in an external peer review by the senior investigators from Banaras Hindu University, Varanasi, UP; Medical College, Trivandrum, Kerala, Institute of Biomedical and Genetic Engineering, Islamabad, Pakistan, and the University of Exeter. Study registration numbers are Banaras Hindu University/Medical College of Trivandrum, EC/847; EC, ECR/526/INSt/UP2014 and the University of Exeter, CA023 (consent form in Appendix 6.2).

All three presented families were visited in rural villages of India and Pakistan by a group of investigators and clinicians including Dr. Vafa Alakbarzade, Dr. Thomas Iype, Dr. Christos Proukakis, Dr. Ajith Sreekantan-Nair, Dr. Arshia Q Ahmad, Professor Michael A Patton and regional field workers. Additionally, all clinical data and videos obtained from the family with hereditary tremor were assessed by Professor Tom Warner and Professor Elan D. Louis (Chief, Division of Movement Disorders, Departments of Neurology and Chronic Disease Epidemiology, Yale School of Medicine and Yale School of Public Health, US). Dr. Arshia Q Ahmad (Department of Physical Medicine and Rehabilitation, Indiana University–Purdue University Indianapolis) and Dr. Abdul Hameed (Institute of Biomedical and Genetic Engineering, Islamabad, Pakistan) and Dr. Thomas Iype (Medical College Hospital, Trivandrum, Kerala) provided information about the study to subjects or their guardians in local language. A

developmental history, systemic and neurological examination for the purposes of the research study was obtained for all individuals recruited and photographic as well as video records of pertinent examination findings were taken with informed written consent of subjects or next of kin of minors. Additional clinical records (including results of any investigations) and educational reports were requested using the hospital records. Specifics of examinations are described in each chapter separately.

Blood or buccal samples were obtained from affected children, parents and unaffected family members with informed consent in accordance with all local and international ethical standards and protocols.

Twelve brain samples were obtained from the New York Brain Bank (NYBB) for the study of the family with hereditary tremor which was approved by the Human Investigation Committee, Yale University, US (to Elan Louis; HIC Protocol #: 1411014944).

2.2 Molecular methods

2.2.1 RNA and DNA extraction

RNA was extracted from the PAXgene blood samples obtained from family members of the affected individuals using PAXgene Blood RNA Kit. DNA was extracted from the blood samples obtained from family members of affected and unaffected individuals using ReliaPrep™ Blood gDNA Miniprep. Both protocols can be replicated from the PAXgene Blood RNA Kit Handbook and ReliaPrep™ Blood gDNA Miniprep manual. DNA was also extracted from the post-mortem brain samples from two patients with essential tremor and three patients with Alzheimer's disease and seven age matching controls. Samples were transported from NYBB, kept in -80^{0}C. DNA was extracted using the MagAttract HMW DNA kit (links provided in Appendix 6.3).

2.2.2 Reverse transcriptase PCR reaction

Reverse transcriptase PCR (RT-PCR) is a method for indirectly amplifying RNA by initially making a complementary DNA (cDNA) copy. The amplified cDNA can subsequently be sequenced and the RNA sequence inferred. Prior to starting the procedure the bench top, pipettes and racks were all cleaned with 70% ethanol and subsequently RNaseZap (Ambion) to remove any traces of RNase. Filter tip pipette tips were used for all RNA work. RNA was extracted from whole blood as previously described and stored on ice until required.

RT-PCR primers were designed to target exonic sequences that are separated by at least one intron. Primers were designed using Primer 3, program settings were changed so that the primers would melt at approximately 70^{o}C temperature, with length at least 22 nucleotides (25-30 preferred) and G-C content of 45-60%. Primers were diluted and a mix made with a final concentration of 25μM for each primer.

The SuperScript® VILO™ cDNA Synthesis Kit was used for RT-PCR. The 10X SuperScript® Enzyme Mix includes SuperScript® III RT, RNaseOUT™ Recombinant Ribonuclease Inhibitor, and a proprietary helper protein, while The 5X VILO™ Reaction Mix includes random primers, MgCl2, and dNTPs in a buffer formulation that has been optimized for qRT-PCR. 1ng-1μg of patient RNA was added to each subsequent reaction and the total volume was made up to 20μl with RNase free water. A negative control was added, where water replaced RNA to control for contamination. The final product was incubated at 25° for 10 minutes, 42° for an hour, 85° for 5 minutes and 4°. To determine successful cDNA amplification cDNA concentration was measured and the size of the products was checked by electrophoresis on a 2.5% agarose gel for 90mins with the appropriate DNA ladder.

2.2.3 Quantitative real-time PCR

The expression level of Lingo1 was assessed by quantitative real-time PCR. TaqMan custom probes were designed via www.thermofisher.com/taqman link using the transcript of Lingo1. Reaction mixes included 50 μL 2× TaqMan universal master mix (no AMPerase) (Life technologies, Foster City, USA), 40 μL dH2O and 10 μL cDNA template. 100 μL reaction mix was then

pipetted into the chamber of a TaqMan Low Density Array (TLDA) card, and centrifuged twice for 2 min at 1500 rpm to ensure distribution of solution to each of the TLDA micro-wells. PCR amplifications were performed on the ABI 7900HT platform (Life technologies, Foster City, USA). Cycling conditions were 50 °C for 2 min, 94.5 °C for 10 min followed by 40 cycles of 97 °C for 30 s and 57.9 °C for 1 min. Crossing point (Ct; the cycle at which the signal becomes visible above the fluorescent background) was measured in triplicate for each sample. This measure is directly proportional to the abundance of the test transcript. Gene expression levels was supposed to be calculated by the comparative CT technique (Pfaffl, 2001) relative to three endogenous controls (*GAPDH*, *B2M* and *GUSE*) to yield a change in Ct (ΔCt) value. The endogenous controls were chosen on the basis of empirical data demonstrating transcript stability in response to PFOA or PFOS dosage using the GeNORM function of the StatMiner analysis software (Integromics, UK). Ratios for the relative expression of each test gene have to be then calculated from the equation $2^{-\Delta\Delta CT}$, where ΔΔCt represents the ΔCt of each gene normalized back to the median value for that gene over the entire population for comparison.

2.2.4 Genotyping, linkage & CNV analysis

Assistance for genotyping and analysis was provided by Dr. Barry Chioza. SNP genotyping was carried out for affected and unaffected individuals from all three presented pedigrees and for DNA extracted from the brain samples. The assay requires 200ng of DNA per sample at a concentration of 50ng/µl. SNP genotyping was performed over a three day experiments using Illumina

CytoSNP-12v2.1 330K arrays following the Infinium® HD Assay Ultra manual protocol (link provided in Appendix 6.3).

The Illumina GenomeStudio Integrated Informatics Platform was used to extract, visualize and analyze the genotyping data. The data was then imported into Microsoft Excel for analysis using Excel macro, looking for notable regions of homozygosity (typically >1Mb) and to compare genotyping data across samples and patient cohorts. Quantitative trait linkage analysis was performed using Lander–Green algorithm, MERLIN software for the family with dystonic tremor under a model of AD inheritance with full penetrance (Abecasis et al., 2002) (Link for tutorial in Appendix 6.3). Multipoint linkage analysis was performed with SimWalk2 under a model of AR inheritance with full penetrance, using a disease allele frequency estimated at 0.0001 for the family with neurodevelopmental delay and microcephaly (Sobel et al., 2001).

The genotyping data of affected and unaffected cases from the family with hereditary tremor was also imported to KaryoStudio software that scans 330K Illumina data for intensity changes resulting from changes in copy number. It detects aberrations that are >75kb, displays information about the region including chromosome on which it is found, start and stop position of the region, length, value (copy number), confidence score, CNV index, cytobands, number of markers and genes. The detected region also is displayed in the chromosome browser that represents data in the form of B allele frequency, Log R ratio (intensity information) and smoother Log R ratio. KaryoStudio allows to cross check detected regions against a list of known

regions as well as several different external sources (UCSC, OMIM, Ensemble etc.).

2.2.5 Whole exome sequencing data analysis

Whole-exome sequencing (WES) of samples from the two affected from the family with hereditary tremor and neurodevelopmental delay with microcephaly was performed by the Otogenetics Corporation using the SureSelect Human All Exon V4 (Agilent Technologies) exome enrichment kit on an Illumina HiSeq 2000. Exome sequencing produced 31,783,299 mapped reads, corresponding to 93% of the targeted sequences being covered sufficiently for variant calling (>10× coverage; mean depth of 45×).

WES data were imported into Microsoft Excel for analysis. Filtering of the data were assumed taking into account the mode of inheritance (AD in the hereditary tremor pedigree and AR in the family with neurodevelopmental delay with microcephaly) and damage prediction of the variants identified. The filtered variants were further checked for the allele frequency in public databases (dbSNP, EVS and ExAC) and in WES data of South Indian origin individuals (regional controls) from previous studies conducted by Professor Andrew Crosby's group to exclude common variants. After all filtering applied, the identified variants were manually checked for the type of mutation and impact using the PolyPhen2, SIFT, PROVEAN and MutationTaster software tools. Overall, priority was given to novel putatively functional variants (after PubMed literature search for each variant).

2.2.6 Primer design

The sequences for the gene of interest were obtained from the Ensemble Genome Browser or UCSC browser (GRCh37 assembly, Feb 2009). Oligonucleotide primers were designed flanking the region of interest (typically 200-400bp) using either Primer3 software version 0.4.0 or Primer3plus (for cDNA primers). Primers were designed following the criteria below: (1) Primer sizes were 20-24 bases in length; (2) Melting temperatures were kept as similar as possible (+/- 2-4^{0}C) for both the left and right primers to maintain PCR efficiency (ideally between 59-62^{0}C); (3) Where possible the guanine – cytosine base content was kept between 40-60%; (4) Primers with inter or intra-primer efficiency extending for more than 3 bases were avoided, to prevent the formation of secondary structures and primer dimers; (5) The primer sequences selected were specific and a 100% match to the region to be amplified; (6) In silico PCR analysis and Blast searches were performed using the UCSC Genome Bioinformatics website. Primers arrive as a solid dried pellet which is diluted to a 100pMol/ul stock solution and stored at -20^{0}C. The stock dilution is further diluted to a 10pMol/µl working solution for the use in PCR.

2.2.7 Polymerase chain reaction (PCR)

PCR is an in vitro method of cloning DNA that allows exponential amplification of specific lengths of DNA from only minute amounts of starting material. PCR was used to amplify DNA with candidate gene primers for sequencing. Primers were purchased from Sigma-Aldrich and prepared from dry oligonucleotides to make up a working concentration of 10pmol/µl. For

each PCR, a master mix consisting of forward and reverse primers, a mix buffer (PCRBIO) that consists of MgCl2 and 5mMol dNTPs, Taq DNA polymerase (PCRBIO) and distilled water, was first set up according to the number of PCR reactions required. 9.2 µl of master mix was then aliquoted into individual 0.2 ml Eppendorf tubes, after which 0.8 µl of DNA was added into sample and control tubes, and 0.8 µl of ddH2O into the negative control tube (Table 2-1). One control and one negative control reaction was set up for each PCR reaction, to confirm absence of contamination.

2.2.1 Cycling conditions for PCR

Each PCR reaction underwent a series of cycles of three stages: denaturation, primer annealing, and DNA synthesis (extension). Programs were tailored for touchdown PCR, where annealing temperatures were lowered by 2^0C for each subsequent program. Temperatures for denaturation and extension were set at 95^0C and 72^0C respectively for all PCR reactions. Touch-down temperature (TD), which is the final annealing temperature, was obtained from the gradient PCR of each primer pairs.

Each PCR reaction was divided into three programs. The first two programs consisted of two cycles of denaturation, annealing and extension each, and the third program with 45 cycles. Each stage of the cycle (i.e. segment) was held at 30 seconds (Table 2-2).

Table 2-1 Standard PCR reaction mixture for one tube

Reagents	Volume (µl)
Forward primer (5pM/µl) (Sigma-Aldrich)	0.8
Reverse primer (5pM/µl) (Sigma-Aldrich)	0.8
5xPCRBIO Buffer (PCR Biosystems)	2.0
PCRBIO Taq Polymerase (5u/µl) (PCR Biosystems)	0.1
ddH2O	5.5
DNA	0.8
Total Volume	10 µl

Table 2-2 Cycling conditions for PCR

Steps	Segment	Temperature (^{0}C)	No. of Cycles	Time for each segment
1	Denaturation Annealing Extension	95 TD+4 72	2	30
2	Denaturation Annealing Extension	95 TD+2 72	2	30
3	Denaturation Annealing Extension	95 TD 72	45	30

2.2.2 Agarose gel electrophoresis

1.8 to 2 g of agarose powder (depending on the size of PCR product) was added to 100 ml of 1X TAE in a glass bottle to make a 1.8 or 2% agarose gel. This mixture was heated in a microwave oven at high heat until a clear solution was obtained. Contents were carefully swirled about every half minute to prevent any settling of the gel in the glass bottle. The heated mixture was cooled under running tap water. 5.5 µl of ethidium bromide was added to the mixture before it was poured out to set. Combs were placed across the gel to form the loading wells and this was left to set horizontally for 30 minutes.

The solidified gel then was put into the 1XTAE buffer filled tank. After which, the gel was loaded with PCR products that were pre-mixed with non-denaturing gel-loading dye (40% Ficol, 0.2% xylene cyanol, and 0.2% bromophenol blue). 2 µl of PCR product was mixed with 2.0 µl of gel-loading dye, and 4 µl of this mixture was then loaded into each well. A 1 kilo base (kb) ladder was also loaded together alongside the PCR products to allow estimation of the PCR product size. A voltage of 100 V was applied across the tank with 1XTAE buffer with PCR filled gel for 30 minutes. PCR products were later visualized under ultra-violet light, and photographed.

2.2.3 PCR purification

Prior to sequencing it was necessary to remove unincorporated primers and dNTP that usually remain in the reaction mixture. This was done using EXOSAP which contains exonuclease 1 (EXO) and shrimp alkaline phosphatase (SAP). The exonuclease-1 releases dNTPs from the

unincorporated leftover primers while shrimp alkaline phosphatase catalyzes the release of 5'- and 3'-phosphate groups from extra nucleotides. For the clean-up reaction, 2 µl of ExoSAP was added to 5 µl of PCR product. The samples were then incubated at 37^0C for 30 minutes. 37^0C was the optimal temperature for the enzyme activity. Subsequently, samples were exposed to 95^0C for 5 minutes to deactivate the enzyme.

2.2.4 DNA sequencing and analysis

Purified PCR product underwent a sequencing reaction in order to attach to them a fluorescently labelled di-deoxynucleotides (ddNTPs) which is read by the sequencer machine. This is used to screen the candidate gene in the relevant affected individuals. 2µl of purified PCR products were added to each 8µl reaction mixture set up for forward and reverse primer sequencing amplification (Table 2-3). Amplification is carried out by both forward and reverse primers for confirmation of any sequence change.

Each of the 10µl reaction mixture was placed into a thermo-cycler and conditions for sequencing PCR were set up as follow: Denaturation of 96^0C for 30 seconds, then annealing of 50^0C for 15 seconds and elongation for 60^0C for four minute. This was programmed for 25 cycles (Table 2-4). Amplified products were purified using the BIGDYE® X TerminatorTM Purification Kit (ABI, Applied Biosystems) according to the manufacturer's instructions (Link to protocol in Appendix 6.3). Samples were then placed in the automated sequencer. Sequencing reactions were analysed using 3130xL Genetic Analyzer (Applied Biosystems®). Sequencing files obtained from the 3130xL Genetic Analyzer (Applied Biosystems®) were then

analyzed visually as a chromatogram using either Finch TV 1.4.0 (www.geospiza.com) (for targeted variant screening) or CLC sequence viewer (for a gene screening) (http://www.clcbio.com/products/clc-sequence-viewer/).

For CLC sequence viewer analysis studied sequences were compared to the wild type (WT) DNA sequence, which was available from the online Ensemble database, using alignment trees created in CLC Free Workbench sequence viewer.

2.2.5 Co-segregation analysis

Co-segregation analysis involved screening the entire family for the candidate variants and investigating whether the affected individuals were homozygous mutants and parents and unaffected siblings were carriers for the same variant in the family with the neurodevelopmental delay with microcephaly. Moreover, at least 100 ethnically matched controls were sequenced for the variants which co-segregated completely in the family to confirm that they were not the common variants in the ethnic community/group.

Table 2-3 Sequencing reaction constituents and their volumes

Reagents	Volume (µl)
Big Dye Buffer (Applied Biosystems)	2.0
Primer (forward or reverse) (5pM/µl) (Sigma-Aldrich)	1.0
Big Dye (Applied Biosystems)	0.5
Purified PCR product	2.0
ddH2O	4.5
Total Volume	10

Table 2-4 Conditions for sequencing reaction

Segment	Temperature (0C)	Time	No. of cycles
Denaturation	95	30 seconds	
Annealing	50	15 seconds	25
Extension	60	4 minutes	

2.2.6 Genomic library preparation

Assistance for genomic library preparation was provided by Dr. Richard Caswell. Aim of paired-end whole genome sequencing is to map rearrangement breakpoints to the exact nucleotide. The genotyping data of III: 15 case from the hereditary tremor pedigree was used for genomic library preparation (Genomic library and Agilent SureSelect sample preparation stages detailed in Appendix 6.4).

2.2.7 MFSD2A p.Ser339Leu mutation analysis

Dr. Debra Q Y Quek and Dr. Long N Nguyen from Duke–National University of Singapore, performed the immunoblotting and immunofluorescence microscopy, transport study and targeted mass spectrometry analysis. Detailed description of antibodies, plasmids, cell culture used and Recombinant PNGase F treatment of the protein; protein turnover assays as well as protein extraction; Western blotting and immunohistochemical microscopy; transport assay and lipidomic analysis of plasma samples are detailed in Appendix 6.6, 6.7, 6.8, 6.9 and 6.9.

3

CHAPTER THREE

A PARTIALLY INACTIVATING MUTATION IN THE SODIUM-DEPENDENT LYSOPHOSPHATIDYLCHOLINE TRANSPORTER *MFSD2A* CAUSES A NON-LETHAL MICROCEPHALY SYNDROME

A PARTIALLY INACTIVATING MUTATION IN THE SODIUM-DEPENDENT LYSOPHOSPHATIDYLCHOLINE TRANSPORTER *MFSD2A* CAUSES A NON-LETHAL MICROCEPHALY SYNDROME

3.1 Introduction

Blood vessels in the brain are highly dynamic multicellular structures capable of integrating and responding to both systemic and neural cues. This is realised via an intimate connection between neuronal circuits and their associated blood vessels, that collectively form a functional 'neurovascular unit' (NVU) (Moskowitz et al., 2010; Zlokovic, 2011; Iadecola, 2013) (Figure 3-1). Proper signal transduction in NVU is essential for effective cortical and subcortical information processing of motor functions as well as the higher integrative brain functions associated with cognition, memory, and learning (Zhao and Zlokovic, 2014). Disruption of NVU interrelationship leads to a loss of cerebrovascular integrity evidenced by animal studies (Armulik et al., 2010; Daneman et al., 2010; Bell et al., 2010; Bell et al., 2012).

The NVU comprises vascular cells such as endothelial cells and pericytes at the capillary level and vascular smooth muscle cells at the arterial, glial and neuronal levels (Figure 3-1). Brain vessel endothelial cells form a continuous, highly specialized biological membrane around blood vessels underlying the BBB.

Figure 3-1 Neurovascular unit and blood brain barrier structures

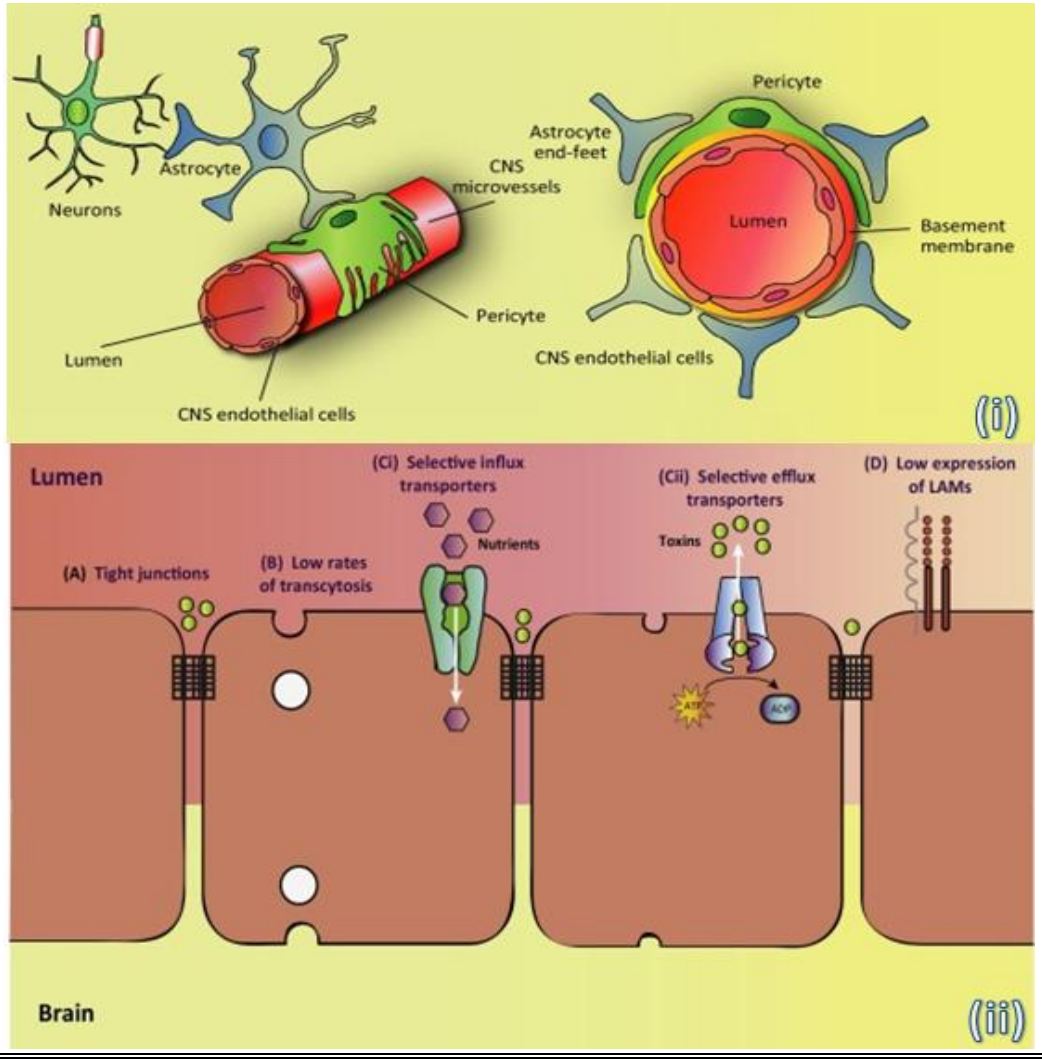

(i) Neurovascular Unit cellular structures and endothelial cells underlying BBB is illustrated. (ii) Molecular properties of brain endothelial cells are illustrated; (A) Specialized tight junction complexes between endothelial cells prevent paracellular flux. (B) CNS endothelial cells have low rates of transcytosis, limiting transcellular flux. CNS endothelial cells mediate (Ci) the selective uptake of nutrients and molecules from the blood using selective influx transporters and (Cii) efflux of toxins against their concentration gradient with ATP-dependent selective efflux transporters. (D) The low expression of leukocyte adhesion molecules (LAMs) contributes to the low level of immune surveillance in the CNS.
(Moskowitz et al., 2010)

The BBB partitions the brain from circulating blood and functions to shield the brain from potential neurotoxins, maintain the homeostatic environment in the CNS for proper neuronal function, and importantly regulate the delivery of energy metabolites and essential nutrients to the brain (Andreone et al., 2015) (Figure 3-1).

The major facilitator super family domain containing 2a (MFSD2A) is one of the proteins enriched in CNS endothelial cells (Ben-Zvi et al., 2014; Nguyen et al., 2014b). Mfsd2a is expressed specifically in the CNS vasculature and not in the choroid plexus (a structure that lacks a BBB), peri/astrocytes and neurons (Ben-Zvi et al., 2014). Moreover it has been shown that at mice embryonic day 15.5 (E13.5) the levels of MFSD2A transcripts are higher by about 80-fold in the BBB endothelium compared to lung (non-BBB) endothelium (Ben-Zvi et al., 2014). MFSD2A has putative dual physiological functions: maintain BBB integrity and transport of omega-3 fatty acids across the CNS endothelium (Zhao and Zlokovic, 2014; Betsholtz, 2014a)(Ben-Zvi et al., 2014; Nguyen et al., 2014b) (Figure 3-2). Genetic deletion to generate transgenic *Mfsd2a*$^{-/-}$ mice leads to BBB defects in the developing CNS, independent of angiogenesis (Ben-Zvi et al., 2014). BBB breakdown in *Mfsd2a*$^{-/-}$ mice has been related to an uninhibited bulk flow transcytosis of plasma across the endothelium. Similar findings have previously been observed in pericytes-deficient *Pdgfb*$^{ret/ret}$ mice (Armulik et al., 2010; Bell et al., 2010). Further micro-array data analysis showed direct correlation between the reduction of *MFSD2A* gene expression and the degree of pericytes coverage (Ben-Zvi et al., 2014).

Figure 3-2 Transporter function of MFSD2A in the BBB

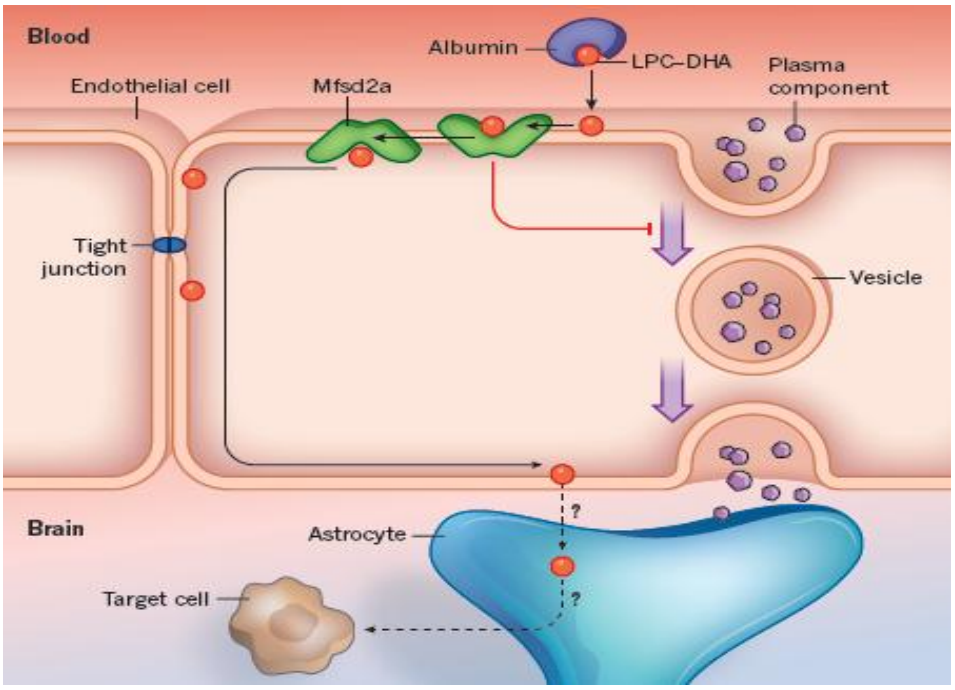

Lysophosphatidylcholine–docosahexaenoic acid (LPC–DHA) bound to the protein albumin during transport in the blood. When it reaches the BBB, LPC–DHA detaches from albumin and is adsorbed to the outer lipid leaflet of the cell membrane of endothelial cells. Mfsd2a binds LPC–DHA and transfers it to the inner lipid leaflet, potentially allowing it to bypass the tight junctions between endothelial cells and reach the brain-facing side of the cell. The targets of DHA in the brain are unknown, as is the method by which it passes through the 'end-feet' structures of astrocyte cells. Mfsd2a suppresses transcytosis in endothelial cells, a transport mechanism by which components of the blood plasma, including proteins, are transferred across the cell in vesicles

(Betsholtz, 2014b)

The brain is the organ with the highest enrichment in lipids like cholesterol, glycosphingolipids, and membrane lipid, phosphatidylglucoside, which function as dynamic platform for signal transduction, protein processing, and membrane turnover (Aureli et al., 2015). Essential events involved in the development and in the maintenance of the functional integrity of the brain depend on the lipid homeostasis (Kidd, 2007; Horrocks and Yeo, 1999; Mozaffarian and Wu, 2011; Connor, 2000; Breckenridge et al., 1972; Innis, 2007; Salem et al., 2001). It has been shown that docosahexaenoic acid (DHA), an essential omega-3 fatty acid accumulates in brain tissue at a rapid rate during the third trimester in association with active periods of neurogenesis, neuroblast migration, and differentiation, synaptogenesis, and gray matter expansion (Carver et al., 2001; Connor et al., 1990). However, DHA cannot be synthesized *de novo* in brain and must be imported from plasma across BBB via secondary transporters (Figure 3-2).

MFSD2A is a plasma membrane protein that belongs to the major facilitator superfamily of secondary transporters, which have 12 membrane-spanning domains (Ethayathulla et al., 2014). It is the major transporter mediating brain uptake of docosahexaenoic acid (DHA) and lysophosphatidylcholines (LPCs) with long-chain fatty acids such as oleate and palmitate (Nguyen et al., 2014b). DHA and long-chain fatty acids are transported across BBB in the form of a sodium-dependent LPC (Nguyen et al., 2014a).

Animal studies of Mfsd2a deficiency showed increased postnatal mortality of *Mfsd2a*-knockout mice early in life, reduced brain size and weight, coupled with motor dysfunction and microcephaly in comparison with wild-type

littermates (Berger et al., 2012). Cerebellum of knockout mice exhibited a significant loss of Purkinje cells and decrease in neuronal cell density in the hippocampus (Nguyen et al., 2014a) (Figure 3-3). Furthermore, behavioral tests of the knockout mice showed severe deficits in learning, memory and severe anxiety which was previously related to omega-3 fatty-acid deficiency (Lafourcade et al., 2011; Carrie et al., 2000; Nguyen et al., 2014a). Moreover, a mass spectrometry study of the brain tissue of *Mfsd2a*-knockout mice showed a marked reduction of the DHA levels (by 58.8%) compared to wild-type mice relating the presenting phenotype to the DHA deficiency (Nguyen et al., 2014a).

Figure 3-3 Neuronal deficits in *Mfsd2a*-knockout mice

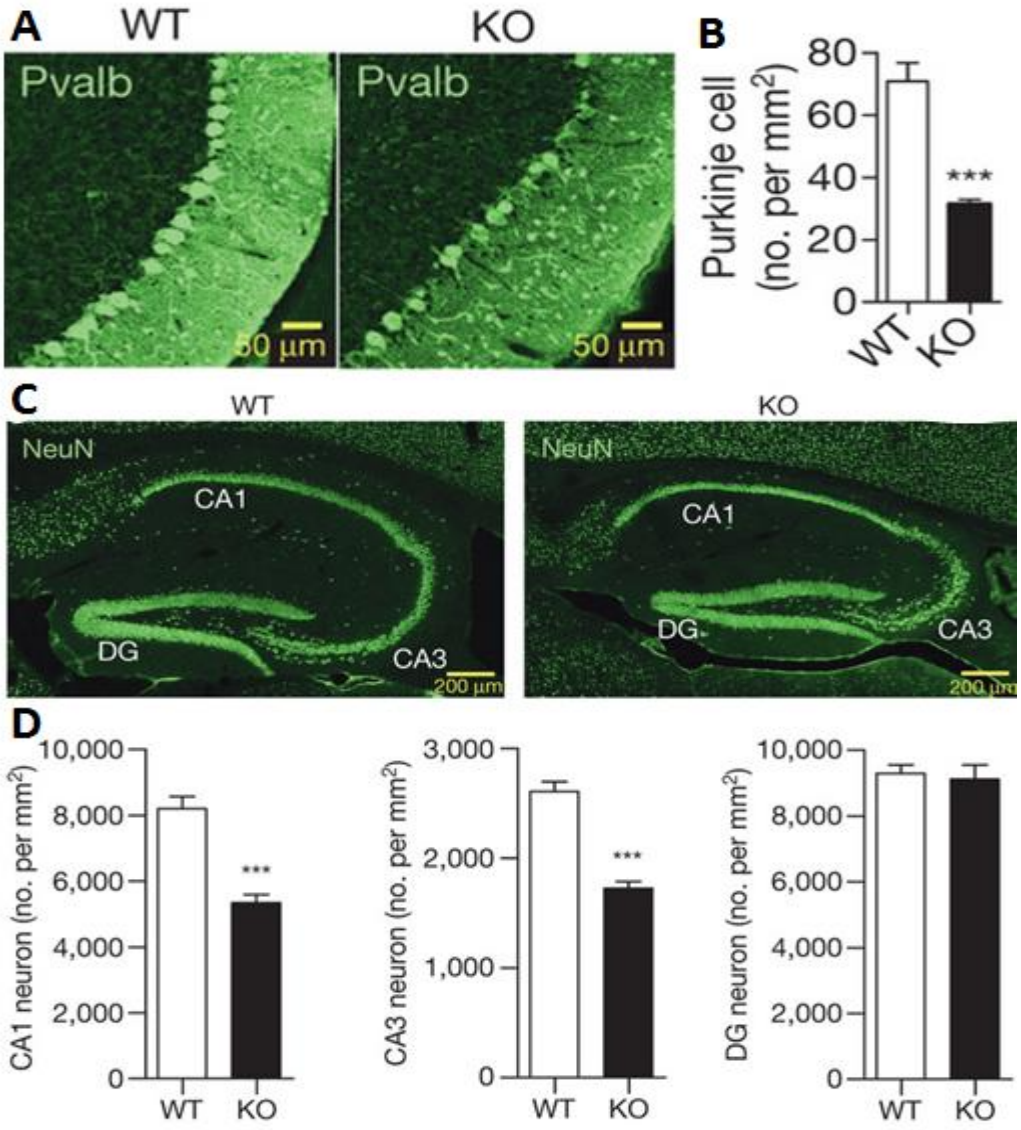

A, Loss of Purkinje cells detected by parvalbumin (Pvalb) staining in cerebellum of knockout (KO) mice. B, Quantification of Purkinje cells in the cerebellum of wild-type (WT) and knockout mice. C, NeuN staining in hippocampus of sagittal brain sections of 8-week-old wild-type and knockout mice indicates decreased mature neurons in specific hippocampal regions of knockout mice. D, Quantification of neuron numbers in CA1, CA3 and dentate gyrus (DG) regions from mice examined in f above. ***$P < 0.001$. Data are expressed as mean ± s.e.m.

(Nguyen et al., 2014a)

3.2 Results

3.2.1 Clinical features

We investigated an extensive Pakistani pedigree with multiple individuals affected by neurodevelopmental delay with microcephaly inherited in an AR pattern (Figure 3-4). The family is resident in a small remote village called Jalbai in Khyber Pakhtunkhwa (KPK) province of Pakistan. Overall, four affected family members, II: 3, III: 2, III: 3 and III: 4 from the pedigree were available for clinical evaluation by the research team. History taking and examination of those affected were performed by Dr. Arshia Q Ahmad, a neurologist (Department of Physical Medicine and Rehabilitation, Indiana University–Purdue University Indianapolis). Interviewing and examination of affected individuals III: 6, III: 7, III: 8, III: 9, III: 10 and III: 15 were performed by a local general practitioner. The collected data including photos and videotapes of examination were further evaluated by Dr. Vafa Alakbarzade and Prof Michael A Patton (a medical geneticist from Institute of Biomedical and Clinical Science, University of Exeter Medical School).

Figure 3-4 Pedigree of a family with non-lethal microcephaly syndrome

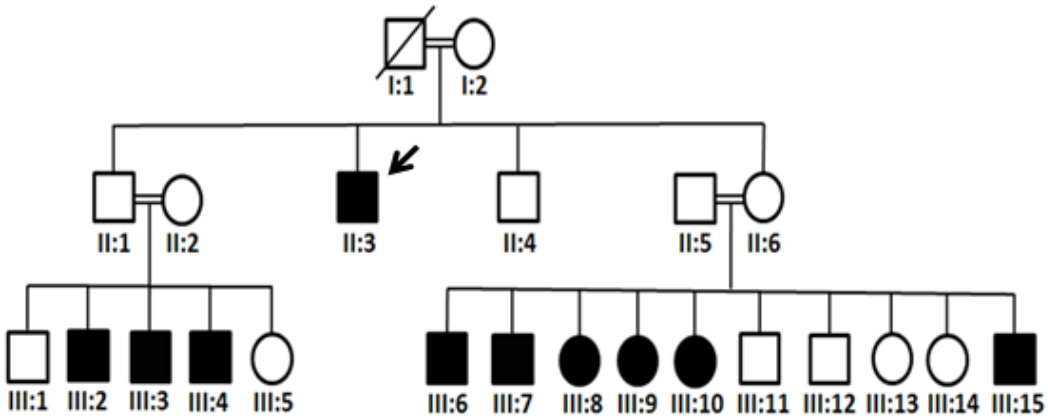

Proband, II: 3 is indicated with an arrow.

Figure 3-5 Photos of affected individuals

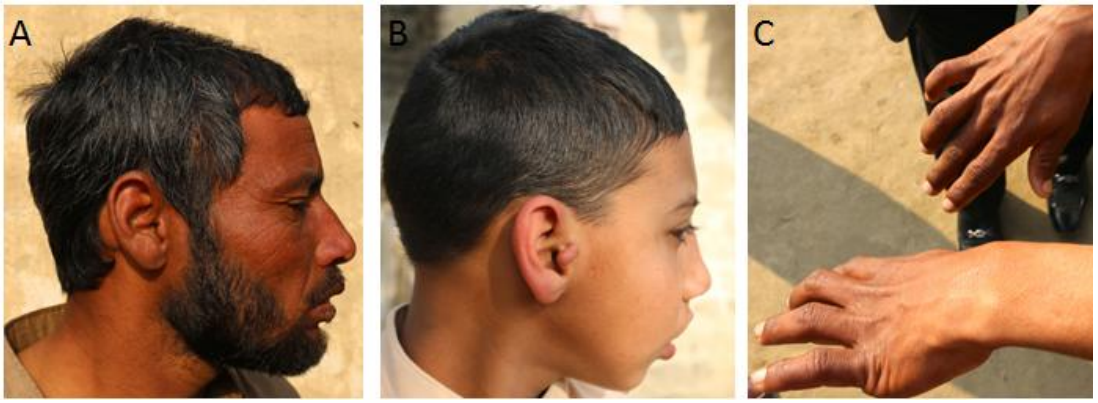

(A) Profile photo of proband II: 3, cranio-facial dysmorphic features include microcephaly, low anterior hairline, up slanting palpebral fissures, micrognathia, dolicocephaly and camptodactyly (C). (B) Profile photo of III: 2 cranio-facial dysmorphic features include microcephaly, trigonocephaly, low anterior hairline, a large ear tag in front of his right tragus, up slanting palpebral fissures, micrognathia, retrognathia

Birth history of affected individuals is limited. The proband II: 3, the eldest affected from the second generation presented with significant delay of developmental milestones with severe learning disability, absent speech and microcephaly. However motor and social milestones were less severely impaired. The patient was able to follow the interviewer, maintain eye contact and carry out simple commands, showed appropriate social response by smiling and engaging. He is relatively independent in keeping personal hygiene, and can undertake simple manual work. Bowel and bladder function was not impaired. Morphological assessment revealed low anterior hairline, up slanting palpebral fissures, micrognathia, short philtrum, hypodontia, dolicocephaly and camptodactyly (Figure 3-5). Neurological examination showed intact vision up to finger counting, intact hearing, drooling without dysphagia, choking, and no fasciculation on the tongue, difficulty carrying out multiple step commands (possible limb apraxia), gait apraxia, and partial flexion contractures at knees and elbows, spasticity, hyperreflexia and upgoing plantar response. Fundoscopy did not identify any abnormality and MRI brain scan revealed a reduction of cerebral white matter volume, particularly around the lateral ventricles, causing scalloping of the ventricular walls (Figure 3-6).

III: 2, III: 3 and III: 4, affected from the third generation had more pronounced delay of developmental milestones with severe learning disability and microcephaly. They had difficulty carrying out commands, poor eye contact, inability of independent feeding and required help with personal hygiene. III: 2 had absent speech, while III: 3 and III: 4 speech disorders were limited to verbalization of sounds. Cranio-facial dysmorphic features of those affected

includes trigonocephaly, low anterior hairline, a large ear tag in front of the right tragus, low set ears, up slanting palpebral fissures, micrognathia as well as retrognathia, short philtrum and hypodontia (Figure 3-5). Neurological examination revealed drooling but no swallowing difficulty and no signs of upper motor neuron involvement.

From clinical data presented by a local general practitioner, affected individuals III: 6, III: 7, III: 8, III: 9, III: 10 and III: 15 all presented with significant pre- and postnatal growth delay (including microcephaly), severe learning disability absent to limited speech, cranio-facial dysmorphic features and variable degree of upper motor neuron involvement on neurological examination.

In summary, affected individuals from the family encompass a wide age range (seven to thirty years of age) and clinical assessment display neurological, cognitive as well as dysmorphic features in common. All affected individuals presented with severe limitation in adaptive and intellectual functioning (according to classification given by DSM-5) (classification of severity of intellectual disability in appendix 6.1), significant delay in language, social developmental milestones and microcephaly. Common neurological abnormal findings include upper motor signs and apraxia. Dysmorphic features common for majority of affected individuals were up slanting palpebral fissures, micrognathia, short philtrum, hypodontia and microcephaly. Although no follow-up assessment of affected individuals is available, more significant spastic muscle tone in arms and legs with exaggerated reflexes, apraxic gait disturbance, and marked drooling in the

oldest affected individual compared to younger individuals indicate that the condition may be progressive in respect to neurological impairment. However younger affected individuals had relatively severe delay in cognitive and social development. There appears to be no increased mortality amongst affected individuals studied.

Figure 3-6 MRI scans of affected individuals

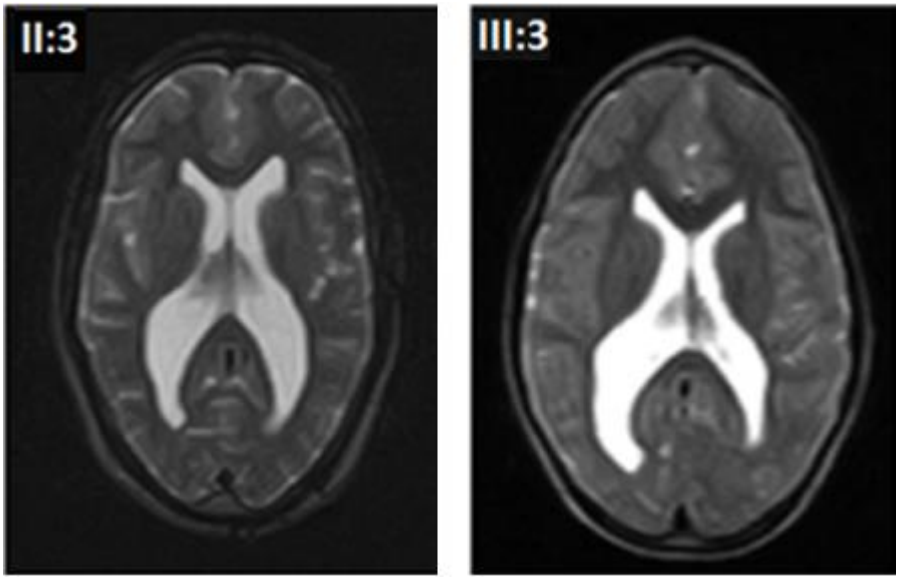

MRI contrast brain scan of II: 3 and III: 3. Axial T2-weighted scans at the level of the lateral ventricle showed a reduction of cerebral white matter volume, particularly around the lateral ventricles, causing scalloping of the ventricular walls. Myelination appeared complete, no evidence of acquired injury, and cortical thickness, and folding was normal. III: 3 had also trigonocephaly.

Images were assessed by Prof Tom Warner and Dr. Phil Rich (Department of Neuroradiology, St. George's Hospital)

3.2.2 330K SNP analysis

In order to map the chromosomal location of the disease gene, 330.000 SNP Illumina microarray scan was undertaken using DNA from the nine affected cases including II: 3, III: 2, III: 3, III: 4, III: 6, III: 7, III: 8, III: 9 and III: 10 assuming that a founder mutation was responsible for this condition. A single homozygous region common to affected family members was identified on chromosome 1, demarcated by SNP markers rs3767088 to rs1033729 (chr1: 37417161-57316268) position (Figure 3-7). The size of the region was 19.8Mb containing a total of 395 genes. The function of each gene was investigated using PubMed database and OMIM ID. Two genes, *MRT12* (OMIM 611090) and *SNIP1* (OMIM 610541) mapping to the region had previously been associated with neurodevelopmental delay.

Figure 3-7 Homozygosity map of affected family members

(i)

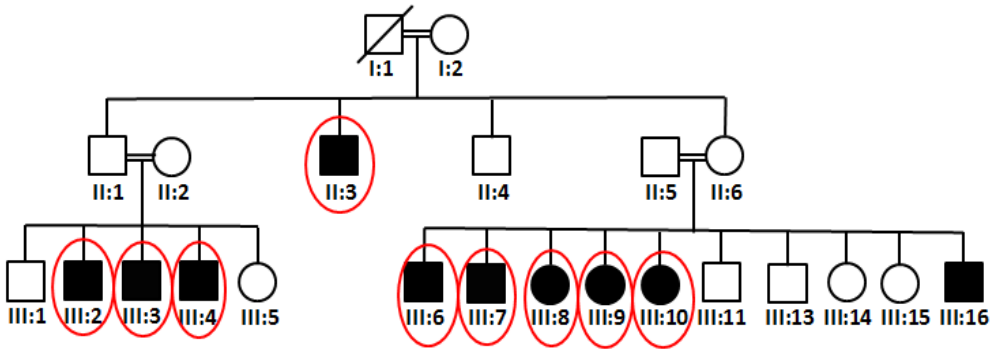

(ii)

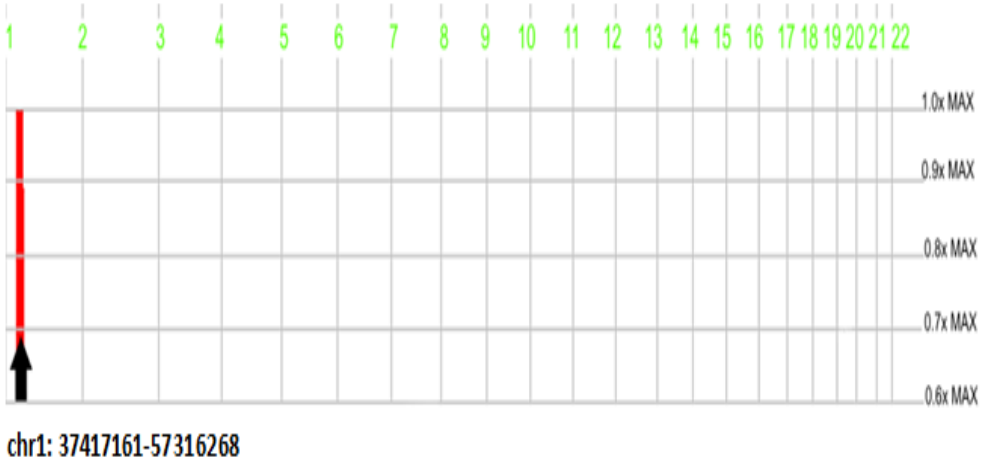

(i) Family pedigree with red circled nine affected cases that were used for SNP genotyping; (ii) Homozygosity plot indicating single autozygous genomic region shared between affected family members (red bar). The position of the *MFSD2A* gene is indicated in an arrow.

3.2.3 Genotyping and whole exome sequencing data analysis

SNP mapping analysis guidance was provided by Dr. Barry Chioza. In order to map the chromosomal location and identify the possible mutated gene responsible for this condition, whole exome sequencing (WES) and whole genome SNP mapping analysis were undertaken in parallel. WES of individual II: 3 revealed novel variants mapping to the candidate region chr1:37417161-57316268 in *MACF1* (chr1:39838200A>G), *MFSD2A* (chr1:40433304C>T) and *EBNA1BP2* (chr1:43637996A>T). The allele frequency of variants was checked using Exome Variant Server (EVS) and Exome Aggregation Consortium (ExAC). Prediction of functional effect of the variants was checked using online tools including Polymorphism Phenotyping v2 (PolyPhen-2), SIFT, Mutation Taster and Provean.

While the *EBNA1BP2* (chr1:43637996A>T) variant was absent in online databases the variant was sequenced in affected and unaffected individuals from the pedigree and found not to co-segregate with the phenotype and be present in homozygous state in unaffected individuals (Figure 3-8; primers in Appendix 6.11). WES data also was analyzed to predict or exclude splice site mutations (using Alamut In-house Software; with a guidance of Dr. Michael N Weedon). Deletion of an intronic base (chr1:43771019A/-) in *TIF1* was predicted to strongly activate a cryptic donor site, indicating the possibility of a deleterious splicing outcome in this gene. However the variant again failed to co-segregate with the disease phenotype, with unaffected individuals II: 5, III: 1, III: 12 and III: 14 being homozygous for this deletion,

excluding the *TIF1* intronic variant as a causative mutation (primers in Appendix 6.11).

Figure 3-8 *EBNA1BP2* variant analysis

A

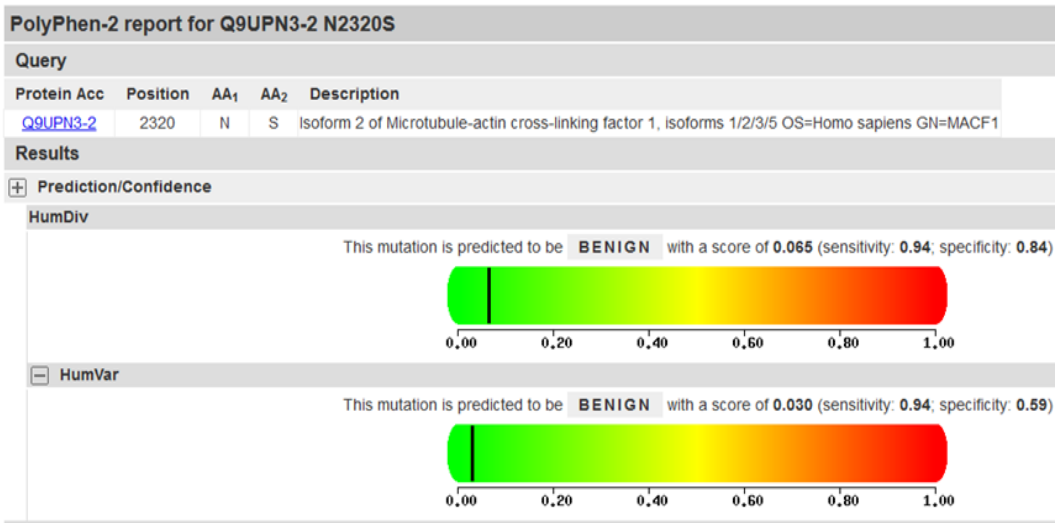

B

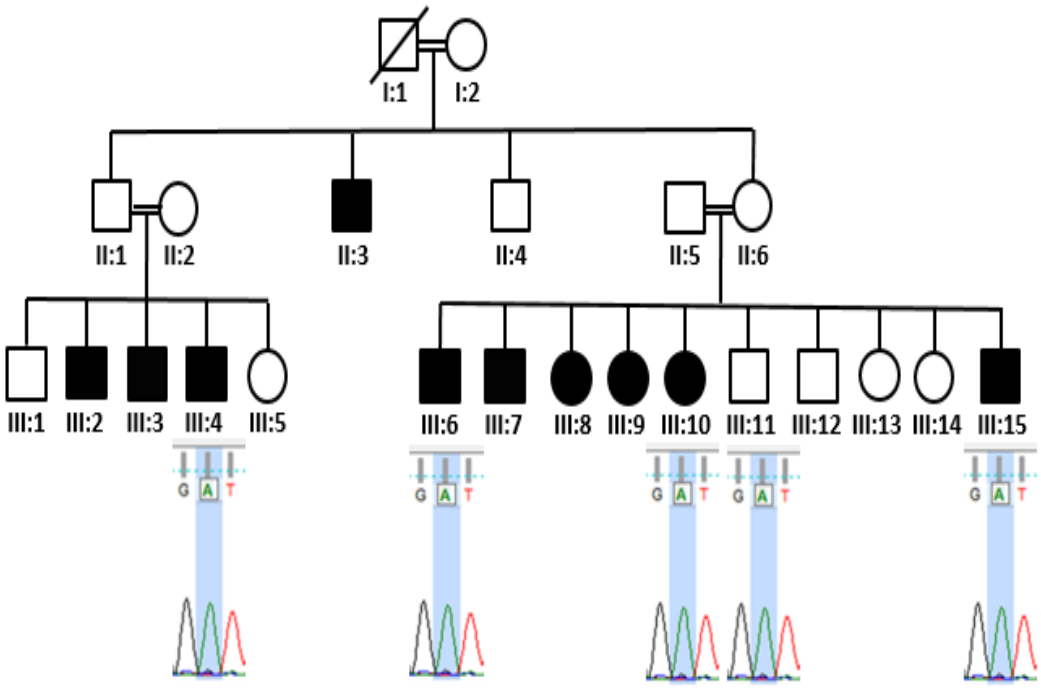

(A) PolyPhen-2 report for the chr1:43637996A>T *EBNA1BP2* variant, predicting the mutation to be 'benign'; (B) Segregation analysis of *EBNA1BP2* variant. Under affected cases III: 4, III: 6, III: 10 and III: 15, and unaffected case III: 11 illustration of chromatogram showing that affected individuals were homozygous to WT allele excluding the variant as a causative mutation.

In addition genes residing within the disease locus which have previously shown to result in neurodevelopmental delay phenotypes (*SNIP1* and *SLC2A1*) were scrutinised for putative mutation. The *SNIP1* gene (chr1:37417161-57316268) has been previously associated with severe neurodevelopmental delay in an Amish family with severe psychomotor retardation, intractable seizures, dysmorphic features, and a 'lumpy' skull surface (Puffenberger et al., 2012; Prof. Crosby: personal communication). This phenotype is different to the clinical presentation that was observed in affected cases of the Pakistani pedigree in regards of neurological and dysmorphological assessment findings. WES of an affected individual, II: 3 did not identified variants *SNIP1* gene. *SNIP1* gene has not been further sequenced.

The *SLC2A1* gene at chr1:43391046 has been associated with developmental delay, mental retardation and mild pyramidal signs were targeted for manual sequencing (primers in Appendix 6.11). Sequencing of ten exons of *SLC2A1* gene on III: 3 affected individual did not reveal any rare deleterious variant.

3.2.4 MFSD2A 40433304C>T variant

The *MFSD2A* (chr1:40433304C>T) gene variant was not present in any genome database. The variant was predicted to be potentially damaging (HumDiv score 0.945) by PolyPhen-2 and highly deleterious (score < −2.5) by PROVEAN mutation analysis software (Figure 3-9, A).

The *MFSD2A* chr1:40433304C>T variant (c.1016C>T) in exon 10 was sequenced in DNA samples extracted from all twenty affected and unaffected family members (primers in Appendix 6.11). The c.1016C>T variant co-segregated with the disease phenotype with all affected individuals being homozygous for the deleterious allele, whilst unaffected individuals and parents were either heterozygous or homozygous for the WT allele (Figure 3-9). In order to exclude c.1016C>T as a common variant specific to the inhabitants of the village in Pakistan where the affected individuals are originally from, 100 controls were screened for c.1016C>T variant. The mutant allele was not detected in any of these controls.

The c.1016C>T variant results in the substitution of the serine at the 339th amino acid (AA) location in MFSD2A protein isomer 2 to leucine. The leucine 339 residue is highly conserved throughout vertebrate evolution including homo sapiens, chimpanzee, mouse, rat, jungle fowl, frog and zebrafish (Figure 3-10, B). Mutation prediction programs locate the MFSD2A serine 339 residue to the transmembrane helix (Figure 3-10, A).

Figure 3-9 MFSD2A c.1016C>T variant analysis

A

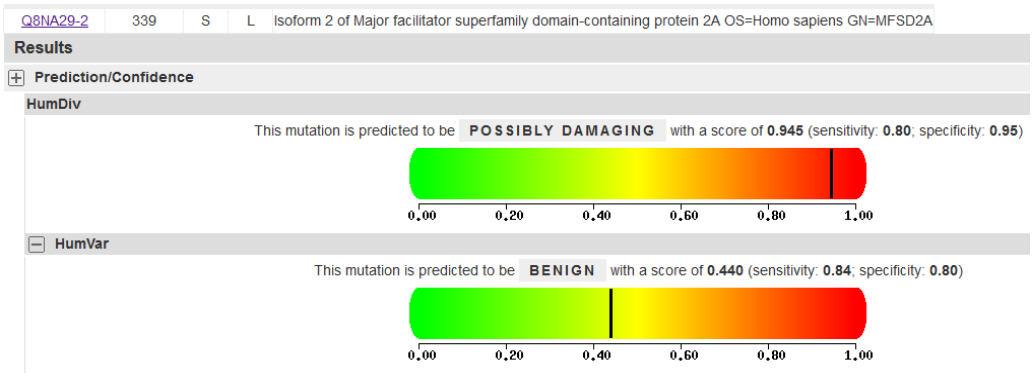

Variant	PROVEAN score	Prediction (cutoff= -2.5)
S339L	-4.660	Deleterious

B

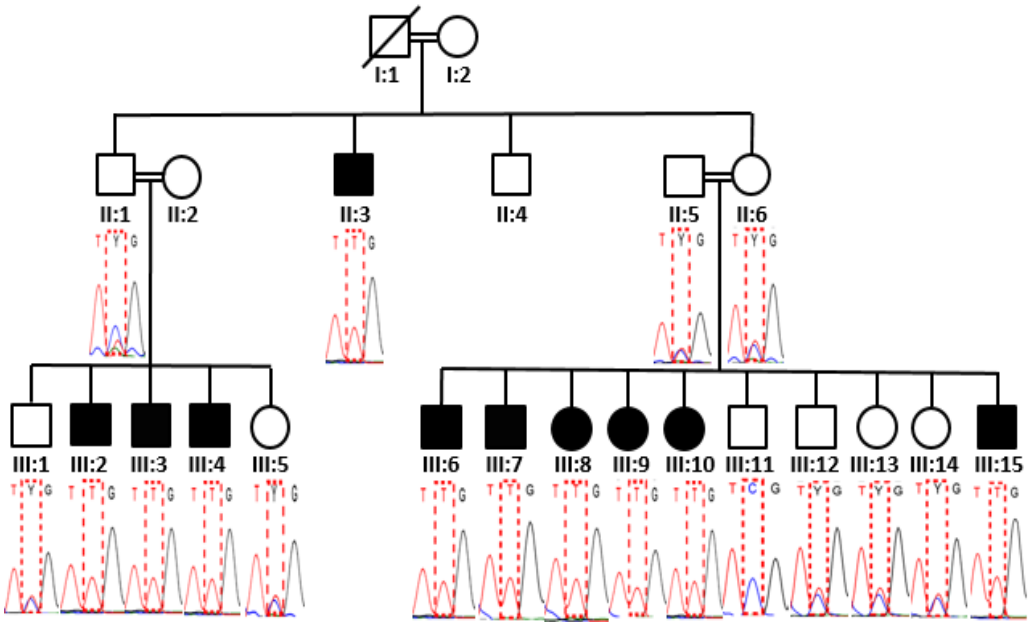

(A) *MFSD2A* 40433304C>T mutation prediction by PolyPhen-2 'possibly damaging' and PROVEAN 'deleterious'; (B) Segregation analysis showed that all affected individuals were homozygous to c.1016C>T variant (chromotograms underneath affected shows highlighted mutant allele T); unaffected individuals were either heterozygous to WT allele (chromotograms underneath unaffected idnividuals II: 1, II: 5, II: 6, III: 1, III: 12, III: 13 and III: 14 cases shows highlighted Y which stands for mutant allele T and WT allele C heterozygosity) or homozygous to WT allele C (III: 11).

Figure 3-10 Ser339Leu residue

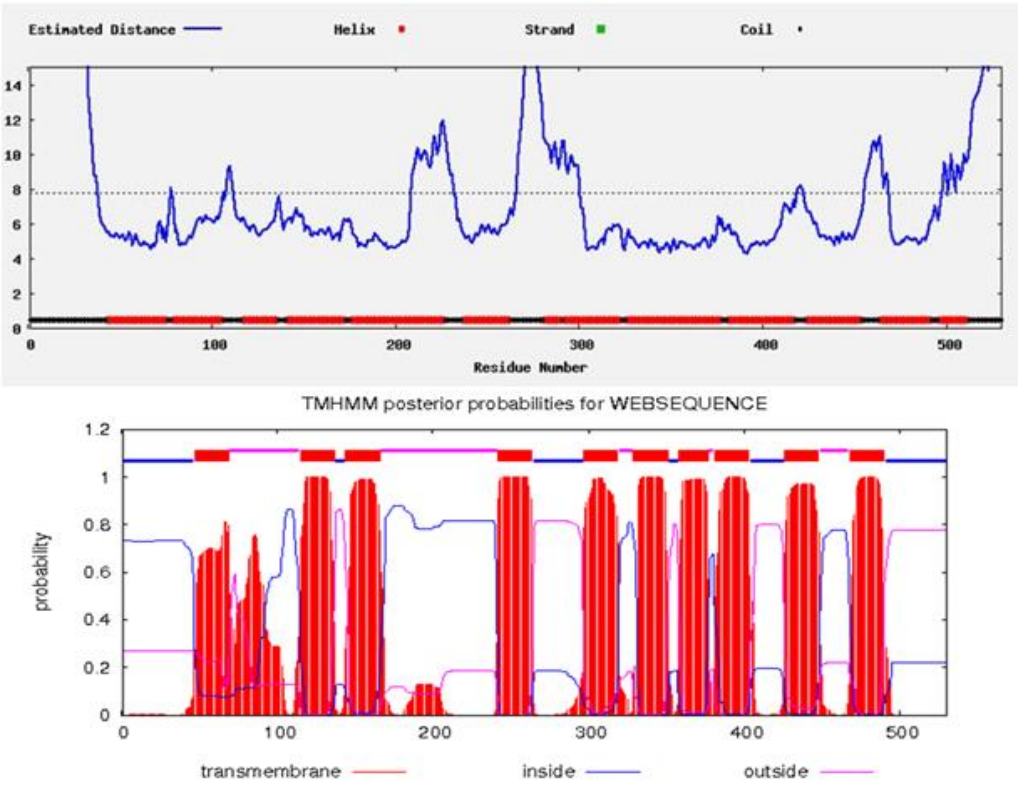

A

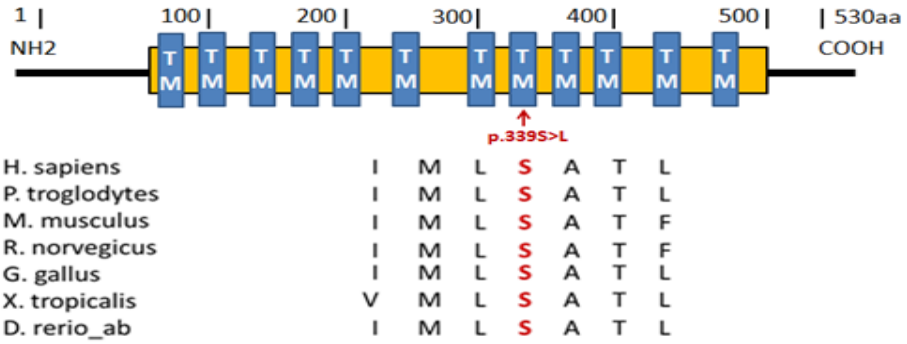

B

(A) I-Tasser and TMHMM prediction of Mfsd2a isomer 2 protein, strongly predicting the Ser339 residue to be transmembrane AA. Blue and red lines in the both graphs demarcate the position of the transmembrane regions, and AA Ser339 lies within the 8th transmembrane domain; (B) Ser339 is highly conservative amongst different vertebrate species. Ser –serine; Leu – leucine; H. sapiens – homo sapiens; P. troglodytes – chimpanzee; M. musculus – mouse; R. norvegicus – rat; G. gallus – jungle fowl; X. tropicalis – frog; D. rerio_ab-zebrafish.

3.2.5 p.Ser339Leu functional outcomes

Dr. Debra Q Y Quek and Dr. Long N Nguyen from Duke–National University of Singapore, performed the immunoblotting and immunofluorescence microscopy, transport study and targeted mass spectrometry analysis.

To determine the consequences of the p.Ser339Leu alteration on Mfsd2a function, the variant was introduced into human *MFSD2A* cDNA, and expressed in HEK293 cells. In HEK293 cells overexpressing mutant MFSD2A, the levels of the glycosylated ~70-kDa species and the total levels of the mutant protein were slightly but non-significantly reduced in comparison to cells overexpressing the wild-type protein (Figure 3-11, A&B). Mutant proteins were stably expressed and localized to the plasma membrane similar to WT on immunofluorescence microscopy (Figure 3-11, C).

To assess transport activity, first HEK293 cells were transfected to express either WT or mutant (Ser339Leu) *MFSD2A* or mock (a negative control), and then the cells were incubated with increasing concentrations of LPC-[^{14}C]DHA, LPC-[^{14}C]oleate or LPC-[^{3}H]palmitate, which previously was characterised as physiological LPC substrates for *MFSD2A* (Nguyen et al., 2014a). Concentration-dependent transport of LPC-[14C]DHA, LPC-[14C]oleate after 30 min in HEK293 cells expressing Ser339Leu Mfsd2a protein was reduced by approximately 50% relative to those observed with WT MFSD2A (Figure 3-12).

Targeted mass spectrometry analysis was performed to detect the lipid profile of affected individuals. Fasting plasma samples were taken by field

workers. Different LPC species as well as total (not albumin bound) LPC concentrations were quantified in the plasma of 4 affected - II: 3, III: 2, III: 3, III: 4, and 2 unaffected- II: 1 and III: 5 and 34 randomly selected regional age-matched controls. Average and standard deviation were calculated with two technical replicates for each LPCs species (targeted mass spectrometry analysis methods were replicated from (Nguyen et al., 2014b). There was a significant increase in total plasma LPC and in the concentration of polysaturated species in patients compared to controls (Figure 3-13).

Figure 3-11 Immunoblotting and immunofluorescence microscopy

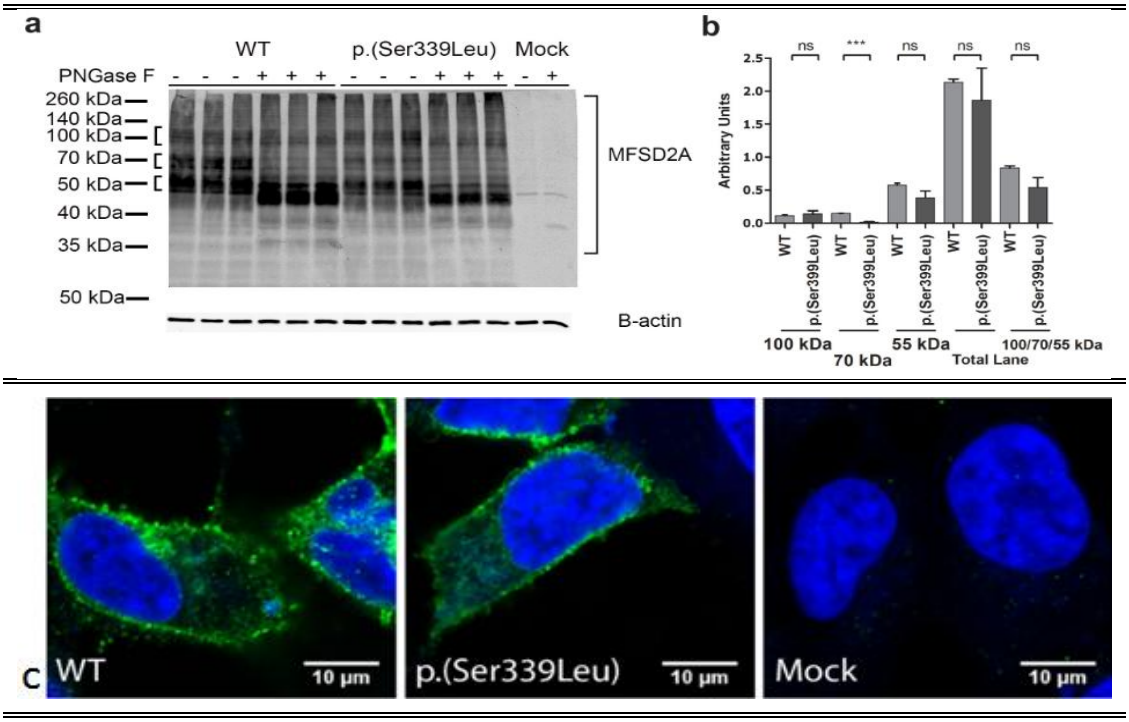

Provided by Dr. Debra Q Y Quek; (A) Immunoblot of Ser339Leu and WT Mfsd2a proteins expressed in HEK293 cells (the small brackets on the left highlight distinct glycosylated species of Mfsd2a). The N-glycosylase PNGase F was used to remove glycans from MFSD2A. Three biological replicates were performed for each WT, mutant and mock immunoblotting. In the mock condition, cells were transfected with empty vector. Overexpression of the Ser339Leu mutant in HEK293 cells resulted in the presence of three main glycosylation protein species of ~55, ~70 and ~100 kDa molecular weights as indicated by the downward shift of the bands in the immunoblotting gel image. In addition, multiple less prominent bands appeared on the immunoblotting image that likely represent Mfsd2a aggregates, as mock-transfected cells completely lacked these protein bands; (B) Quantification of the band intensities separately and the sum of the amounts of the total Mfsd2a (normalized to the band intensity for β-actin); The levels of the glycosylated ~70-kDa species and the total levels of the mutant protein were slightly increased (Values are represented as means ± s.e.m.); (C) Immunofluorescence localization of WT and Ser339Leu proteins expressed in HEK293 cells. MFSD2A-green; nuclei-blue (Hoechst 33342). Scale bars, 10 µm. Mutant proteins were stably expressed and localized to the plasma membrane in a fashion similar to WT

Figure 3-12 LPC transport activity

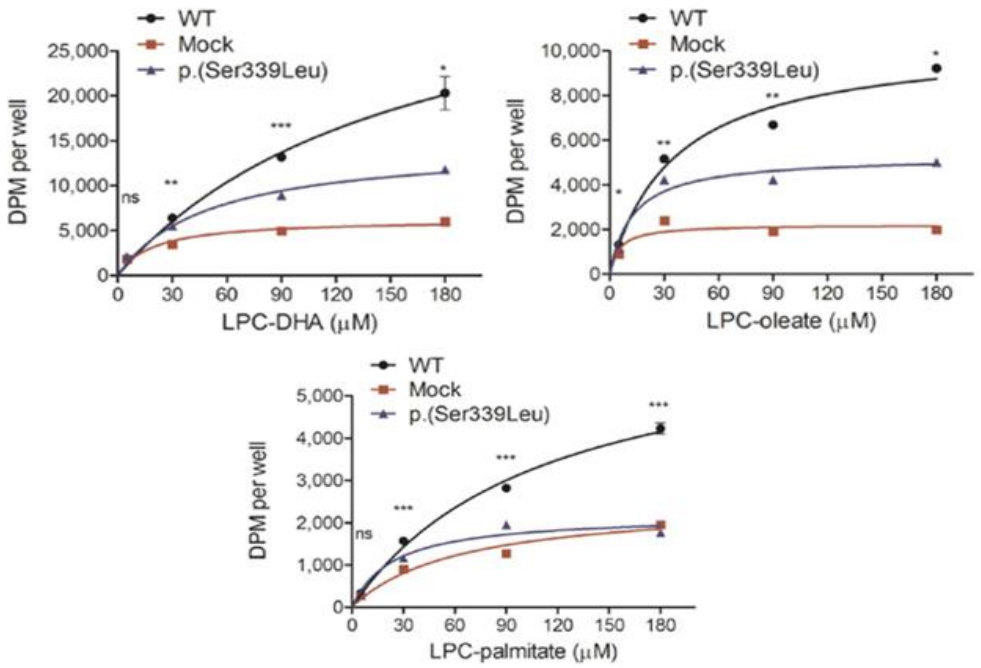

Provided by Dr. Long N Nguyen; HEK293 cells were transfected to express either WT or mutant (Ser339Leu) MFSD2A or mock (a negative control) then the cells were incubated with increasing concentrations of LPC-[14C]DHA, LPC-[14C]oleate or LPC-[3H]palmitate. Concentration-dependent transport of LPC-[14C]DHA, LPC-[14C]oleate after 30 min in HEK293 cells expressing Ser339Leu Mfsd2a protein were reduced by approximately 50% relative to those observed with WT MFSD2A (as measured by disintegrations per minute (dpm) per well). Both mutant lines exhibited transport activity similar to the background level in mock-transfected cells for all LPC lipids tested, indicating impaired LPC transporter activity. Experiments were performed twice with three biological replicates. Values are represented as means ± s.e.m. *P < 0.05, **P < 0.01, ***P < 0.001; NS, not significant. The transport of LPC-[3H] palmitate was similar to that observed in mock-transfected cells.

Figure 3-13 Lipidomic mass spectrometry

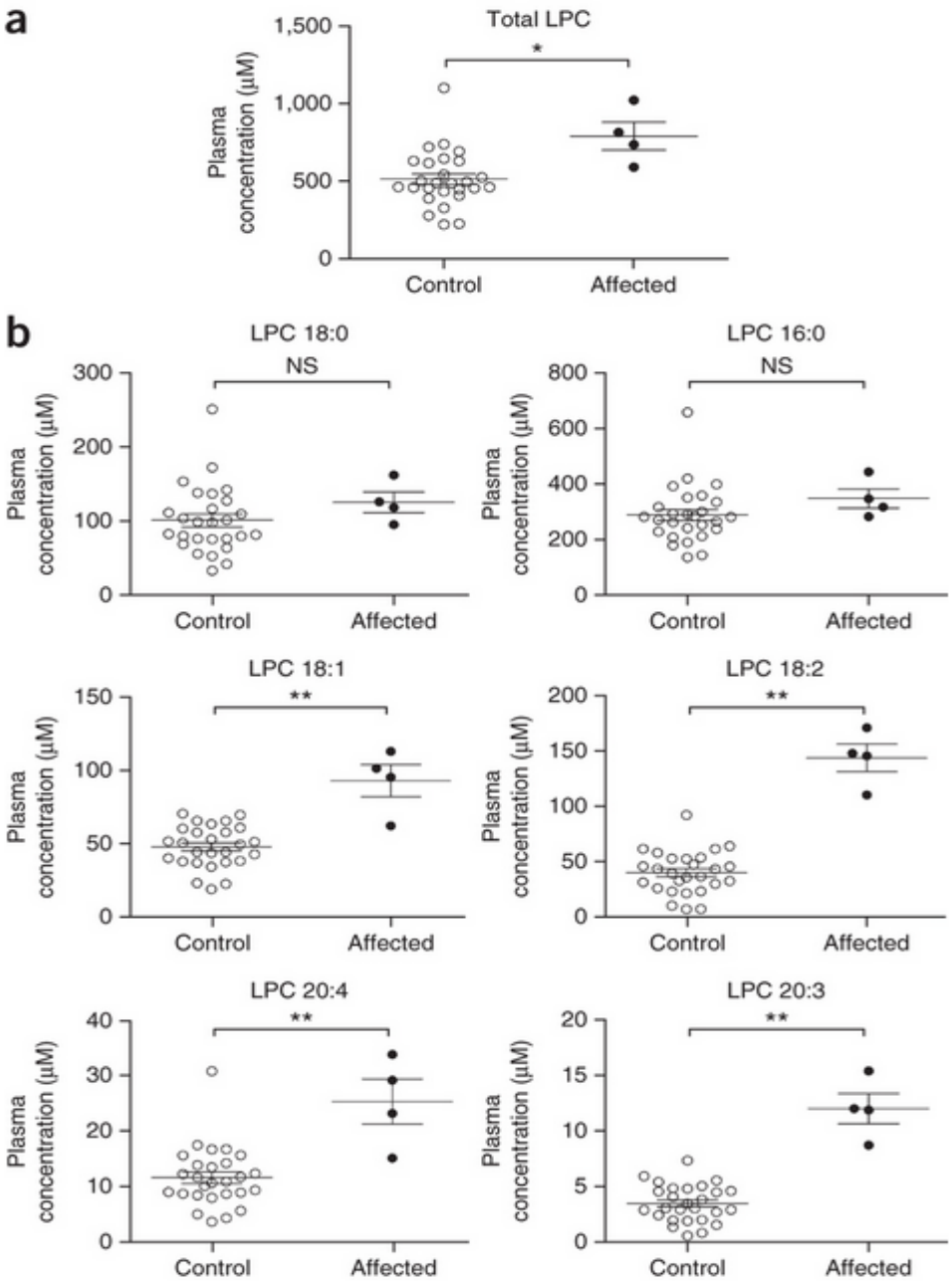

Provided by Dr. Long N Nguyen; (a,b) Total LPC concentration (a) and concentrations of common individual LPC species (b) in plasma from age-matched controls, including 34 unrelated children from the same geographical location, and 1 parent (II:3) and 1 unaffected sibling (III:5) from the pedigree. Analysis was performed once with two technical replicates. Values are represented as means ± s.e.m. *P < 0.05, **P < 0.01; NS, not significant

3.3 Discussion and future work

In this chapter clinical and genetic investigation of an extensive Pakistani pedigree with multiple individuals affected by neurodevelopmental delay with microcephaly inherited in an AR pattern is described. The cardinal features common for all affected cases were significant intellectual disability, absent to limited speech, apraxia, variable degree of upper motor neuron signs and facio-cranial dysmorphic features including microcephaly. More prominent upper motor neuron signs and presence of apraxia in elderly individuals compared to younger ones, may indicate slow progression of neurological features, although MRI contrast imaging of an 11 and 30 year old affected did not show any major structural differences. However, a comprehensive imaging study using voxel-based morphometry and diffusion tensor imaging tract-based spatial statistics analysis is required to detect comparable structural differences among affected cases. There was no mortality amongst individuals affected up to 30 years of age, although further follow-up is required for confirmation. This phenotype was associated with a homozygous *MFSD2A* sequence variant, c.1016C>T affecting a stringently conserved AA residue (p.Ser339Leu).

Although the mechanistic explanation of p.Ser339Leu alteration that eventually leads to the 'non-lethal microcephaly' syndrome is uncertain, it is more likely due to the partial reduction of transport of DHA to the brain than secondary to limited expression in plasma. The small, non-significant reduction in the total amount of MFSD2A Ser339Leu expressed in HEK293 cells may not be likely to account for the disease in affected family members,

as the reduction of MFSD2A protein levels by ~50% in mice heterozygous for a *Mfsd2a*-knockout allele did not result in microcephaly or DHA deficiency in the brain. Consistent with this, the heterozygous parents of the affected individuals did not present with disease (Nguyen et al., 2014a; Berger et al., 2012). The relative changes in the levels of glycosylated species of the Ser339Leu mutant detected by immunoblotting might be indicative of structural changes in the mutant protein. Moreover, the Ser339Leu mutant is localized to the plasma membrane similarly to wild-type MFSD2A further suggesting that the transport function of the Ser339Leu mutant might be impaired.

In order to confirm that the defective LPC transport leads to the reduction of DHA levels and consequently clinical presentation in affected with *MFSD2A* mutation, we sought to identify a surrogate measurement. Since CSF was not available and it was not feasible to measure LPC brain uptake in the affected individuals, we hypothesized that plasma LPC levels would be increased as a consequence of partial inactivation of MFSD2A at the BBB, the major site for MFSD2A expression in the body. Indeed, the plasma level of polyunsaturated LPC species were significantly increased in affected compared to unaffected and regional healthy controls, which were previously identified to be the higher affinity physiological ligands for MFSD2A (Nguyen et al., 2014a). On the other hand, the total plasma LPC level was mildly raised compared to that of controls. This was due to the specific increases in the levels of LPCs containing monounsaturated (LPC 18:1: percent increase of 92%, $p = 0.004$) and polyunsaturated (LPC 18:2, 20:4 and 20:3: percent increases of 254%, $p = 0.002$; 117%, $p = 0.007$; and 238%, $p = 0.002$,

respectively) fatty acyl chains but not in the levels of the most abundant plasma LPCs, which contain saturated acyl chains (C16:0 and C18:0: percent increases of 20%, p = 0.105 and 23%, p = 0.166, respectively). Meanwhile, plasma concentrations of LPCs containing DHA were below quantifiable detection in all subjects, which is consistent with the lack of fish in the diet of the families investigated, who are resident in a geographically land-locked region of Pakistan (Innis, 2007). Although LPCs with saturated fatty acyl chains are the most abundant LPC species in plasma, they are also lower-affinity ligands for MFSD2A than LPCs with unsaturated acyl chains (Nguyen et al., 2014a). The affinities are inversely related to their physiological concentrations, which makes biological sense that the transporter evolved to capture the less abundant LPCs in blood which happen to carry essential fatty acids to the brain. Indeed, LPC-palmitate which is the most abundant LPC species in plasma was not transported by the Ser339Leu mutant protein in a cell-based study because it has low-affinity for MFSD2A (Nguyen et al., 2014a). Whereas, the polyunsaturated LPC species that are less abundant in plasma but have more affinity for MFSD2A were raised in plasma of affected. These findings confirm that partial inactivation of MFSD2A (by p.Ser339Leu alteration) does not result in significant changes in plasma LPC concentrations for lower-affinity ligands but does affect the plasma levels of LPCs that are higher-affinity ligands for MFSD2A.

The studies described here in the extended Pakistani family with non-lethal neurodevelopmental delay and microcephaly were undertaken in parallel with studies of two small families with individuals with a lethal

neurodevelopmental presentation in the lab of Professor Joe Gleeson. These families, one from Libya and the other from Egypt, presented with microcephaly, developmental delay, intellectual disability, hypotonia, upper motor neuron signs and seizures ultimately leading to death within the first few years of life (Guemez-Gamboa et al., 2015). Consistent with the severity of clinical presentation, brain MRI imaging of affected individuals from those pedigrees showed gross hydrocephalus, effacement of the cortical surface and cerebellar/brainstem hypoplasia (atrophy). Two homozygous, highly damaging variants in the *MFSD2A* gene, g.40431005C>T and g.40431162C>T identified in those affected causes significant loss of LPC transporter activity which may explain the high morbidity and mortality of clinical manifestation in those affected (Guemez-Gamboa et al., 2015). Whereas, g.40433304C>T variant identified in affected from pedigree under the investigation partially (by 50%) reduces the transport of DHA to the brain which could be linked to the non-lethal clinical presentation, and less severe motor impairment and an absence of seizures that was observed in our patients.

Although the phenotype of affected individuals from the Pakistani pedigree is substantially milder than the phenotype described in Libyan and Egyptian families, there are overlapping features that are specific for the *MFSD2A* gene mutations (Guemez-Gamboa et al., 2015). Microcephaly, upper motor neuron signs, behavioral disturbances, developmental delay, intellectual disability, absent speech and hydrocephaly or periventricular white matter changes on MRI altogether creates a unique clinical spectrum associated with loss of function of *MFSD2A*. The severe and lethal clinical presentation

of Libyan and Egyptian families correlates with genetic findings of completely inactivating mutations of *MFSD2A.* This results in an increase in the concentrations of all detectable LPC species compared to selective change in the concentration of LPC species caused by partial inactivation of MFSD2A (Guemez-Gamboa et al., 2015). p.Ser339Leu alteration that results in partial inactivation of MFSD2A transporter does not result in significant changes in plasma LPC concentrations for lower-affinity ligands but does affect the plasma levels of LPCs that are higher-affinity ligands for MFSD2A. Consequently our findings indicate that LPCs with mono- and polyunsaturated fatty acyl chains are the major plasma LPC species required for human brain growth.

The physiological mechanism for the partial inactivity arising from the p.Ser339Leu alteration that leads to the defective transport activity remains uncertain. Since the Ser339 residue is located along a transmembrane domain, we speculate that it may face inward into the substrate-binding pocket, and the mutant leucine residue may interfere with substrate binding.

Although it was not feasible to measure brain DHA levels in our patients, notable phenotypic parallels between individuals homozygous for the variant encoding p.Ser339Leu alteration and mice null for Mfsd2a indirectly suggests that those affected individuals would also display a deficiency for DHA in the brain, similarly to *Mfsd2a*-knockout mice (Nguyen et al., 2014a). Mfsd2a transgenic mice deficient for DHA in the brain presented with a phenotype consistent of severe microcephaly, behavioral and cognitive impairment, and progressive worsening of neurological signs with age. The DHA deficiency in

Mfsd2a knockout mice can be explained by the finding that MFSD2A is the primary carrier of DHA to the brain, which does not synthesize DHA. The presentation of microcephaly in both *Mfsd2a*-knockout mice and humans homozygous for the p.Ser339Leu variant suggests the possibility that LPC uptake by the brain provides a preformed phospholipid source for membrane biogenesis. This is possible because LPCs, which are found at low levels in cellular membranes, are converted biochemically into membrane phosphatidylcholine through the action of LPC acyltransferase enzymes (Shindou et al., 2013). Moreover, given that the syndrome exhibited by individuals homozygous for the p.Ser339Leu alteration appears progressive particularly upper motor neuron signs, it seems likely that LPC transport is required in the adult brain to maintain brain function, perhaps by providing LPCs for membrane repair and turnover.

It is difficult to predict the morbidity of the clinical syndrome in affected individuals homozygous for the p.Ser339Leu mutation. Affected individuals homozygous to *MFSD2A* p.Thr159Met and p.Ser166Leu mutations deceased within the first few years of life, as did 40% of Mfsd2a-knockout mice (Guemez-Gamboa et al., 2015; Berger et al., 2012). However, the majority of *Mfsd2aa* and *Mfsd2ab* morphants (a zebrafish model of *Mfsd2a* deficiency) died before neural maturation (Guemez-Gamboa et al., 2015). Since the BBB forms at 3 days post-fertilization in zebrafish (Fleming et al., 2013), it is unlikely that lethality in a zebrafish is caused solely by disruption of neural function or other species-specific effects of *Mfsd2aa/ab* depletion that are unrelated to lipid transport cannot be excluded. Hence, human *MFSD2A* mRNA was co-injected zebrafish zygotes together with *Mfsd2aa*

morpholino (Guemez-Gamboa et al., 2015). It was shown that either zebrafish or human wild-type mRNA largely rescued the lethal phenotype, whereas co-injection with human *MFSD2A* mRNA encoding the Thr159Met or Ser166Leu mutant failed to reverse microcephaly, BBB breakdown and lethality (Guemez-Gamboa et al., 2015).

When considered together, the p.Ser339Leu alteration in *MFSD2A* gene causes the ‘non-lethal microcephaly’ syndrome in individuals homozygous for this variant secondary to the reduction of LPCs with mono/ polyunsaturated fatty acyl chains transport across BBB. The dysmorphological and neurological manifestation of affected individuals homozygous for the p.Ser339Leu mutation presents a unique finding that could further help to link LPCs with mono/polyunsaturated fatty acyl chains and development of the brain regions responsible for speech, intellectual and motor function. Moreover, chr1:40433304C>T variant screening could be used as a diagnostic tool for a neonatal microcephaly and discovery of therapeutic agents that could deliver LPCs with mono/polyunsaturated fatty acyl chains across BBB could prevent development of intellectual disability in those patients.

4

CHAPTER FOUR

A COMPLEX CHROMOSOMAL REARRANGEMENT IN AN INDIAN FAMILY WITH NEURODEVELOPMENTAL DELAY

A COMPLEX CHROMOSOMAL REARRANGEMENT IN AN INDIAN FAMILY WITH NEURODEVELOPMENTAL DELAY

4.1 Introduction

Microscopically visible rearrangements of chromosome 4p16 may result in two rare chromosomal disorders: Wolf–Hirschhorn syndrome (WHS) and partial trisomy 4p syndrome. The deletion of the chromosome 4p16.3 Wolf-Hirschhorn syndrome critical region (WHSCR-2) typically results in a characteristic facial appearance, 'Greek warrior helmet' appearance of the nose, microcephaly, severe intellectual disability, stereotypies and prenatal onset of growth retardation (Battaglia et al., 2000). 4p16 duplication, however, results in partial trisomy 4p syndrome with more variable degree of intellectual disability and dysmorphism, developmental delay without microcephaly or reduction of height (Patel et al., 1995; Partington et al., 1997; Schonewolf-Greulich et al., 2013).

WHS syndrome occurs in approximately 1:50,000 newborns (Bergemann et al., 2005). Most cases are caused by either a de novo isolated deletion or unbalanced de novo translocations involving chromosome 4p. In 20% of WHS cases, however, derivative chromosome 4 originates from a parental translocation (Bergemann et al., 2005; Zollino et al., 2003; Zollino et al., 2004). Different rearrangements of chromosome 4p can cause two contrasting clinical syndromes of WHS with severe intellectual disability, microcephaly, growth failure as well as partial trisomy 4p syndrome with physical overgrowth due to dosage effect of the fibroblast growth factor

receptor gene (*FGFR3*) at WHSCR-2 (Figure 4-1) (Patel et al., 1995; Partington et al., 1997; Schonewolf-Greulich et al., 2013; Gonzalez et al., 1977). Characteristic facial appearance of WHS has been associated with insufficient regulation of Wolf-Hirschhorn syndrome candidate 1 gene (*WHSC1*), responsible for chromatin remodeling (Stec et al., 1998).

Isolated unbalanced translocation that involves chromosomes 4 and 3 is extremely rare compared to the other WSH-associated rearrangements (Schinzel et al., 1978; Petriczko et al., 2012; Grossmann et al., 2009; Han et al., 2012). Clinical presentation of 3p deletion syndrome typically includes cognitive handicap, growth retardation, microcephaly, and facial dimorphism such as ptosis, downslanting palpebral fissures and micrognathia, variable congenital heart defects, postaxial polydactyly, cleft palate, renal and intestinal anomalies (Cargile et al., 2002; Malmgren et al., 2007).

This chapter involves the investigation of a large Indian family with multiple individuals affected by a heterogeous range of neurological features of unknown cause. Our genetic studies defined the causative genomic lesions, entailing the description of the largest pedigree reported exhibiting a complex rearrangement of chromosome 4p16.1, which also occurred in conjunction with a small deletion of chromosome 3p26.3. The family thus comprised individuals with WHS, as well as typical and atypical clinical manifestations of 4p partial trisomy and 3p deletion syndromes.

Figure 4-1 Family with chromosome 4p rearrangement

Photograph of the family with different chromosome 4p rearrangements causing WHS with typical facial dysmorphic features, microcephaly and growth failure (seated fourth from the left); contrasting with another affected individual with physical overgrowth, macrocephaly, prominent glabella due to partial 4p trisomy (seated third from the left).

(Partington et al., 1997)

4.2 Results

4.2.1 Clinical report

The extended pedigree investigated originates from Kerala, Southern India, with a total of nineteen individuals including ten affected and nine unaffected individuals (Figure 4-2). All nineteen individuals have been assessed by Dr. Alakbarzade, Dr. Christos and Professor Patton. Developmental milestones and dysmorphic features of the three patients with the chromosomes 4p16 deletion and 3p26.3 duplication are summarized in Table 4-2 and Table 4-3. Photo of affected V: 1 illustrates a characteristic facial appearance, 'Greek warrior helmet' that is commonly seen in patients with WHS (Figure 4-3, E).

V: 1 and V: 2 are the only affected siblings in the pedigree and are born from an unaffected parent with a balanced chromosome 4p and 3p translocation. V: 1 had a history of febrile seizures and status epilepticus and developed stereotypic body movements such as bending from side to side, body rocking and repeated hand washing in addition to severe neurodevelopmental delay. Her neurological examination at 12 years of age revealed increased muscle tone and reflexes in lower limbs. Her younger sibling (V: 2) with a history of generalized tonic-clonic seizures that developed at age 17 months demonstrated more severe developmental delay (Table 4-1). Her neurological examination conducted at age 8 revealed left lower motor neuron facial palsy, reduced tone (upper limbs), and increased tone in the lower extremities with exaggerated reflexes. MRI imaging of the brain showed hypo-dense lesions in frontal lobes white matter (only report is available).

Figure 4-2 The pedigree of the family with chromosomal rearrangement

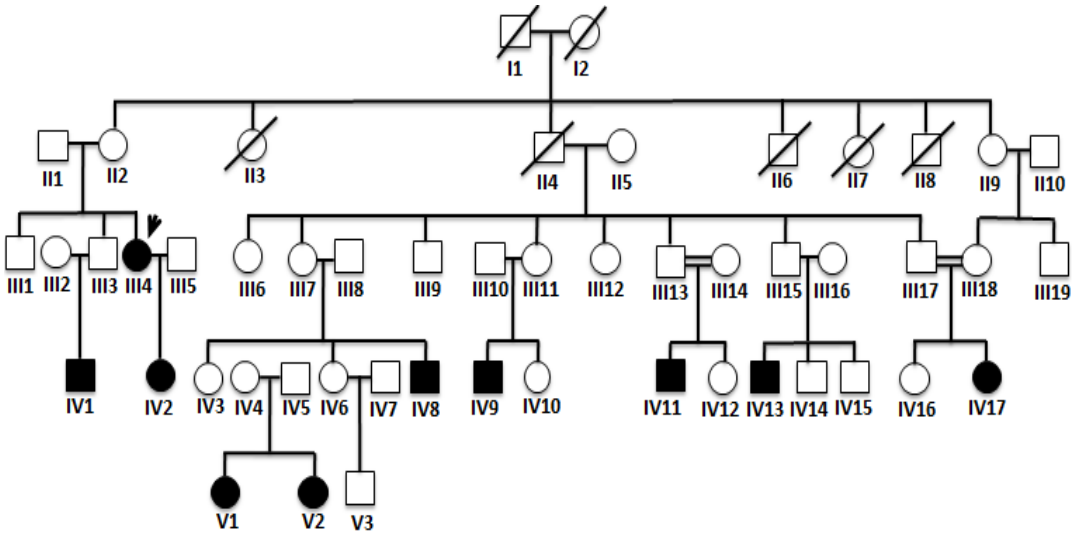

In the pedigree nineteen individuals including ten affected (III:4, IV:1, IV:2, IV:8, IV:9, IV:11, IV:13, IV:17, V:1 and V:2) and nine unaffected (II:2, II:9, III:3, III:7, III:11, III:13, III:15, III:18 and IV:4) individuals that have been clinically and genetically investigated. The index case III:4 is indicated by an arrow. All nine clinically unaffected individuals demonstrated normal motor, social and cognitive development in relative to their social and educational background. All nine were found to possess balanced translocation of chromosome 3 and 4. All third generation unaffected (III:3, III:7, III:11, III:13, III:15 and III:18) individuals inherited likely chromosome 3 and 4 balanced translocation from their parents (affected individuals clinical manifestation are described in Table 4-1 and Table 4-2). All affected individuals from three generations possessed an unbalanced chromosome 3 and 4 translocation. Only three affected V:1, V:2 and IV:13 had 4p deletion and 3p partial trisomy, while III:4, IV:1, IV:2, IV:18, IV:19, IV:11 and IV:17 had 3p deletion and partial 4p trisomy. Only IV:2 affected inherited unbalanced translocation from affected III:4 parent with unbalanced translocation.

A maternal cousin of siblings V: 1 and V: 2, IV: 13 had similarly, history of generalized tonic-clonic seizures developed at age 12 months which is currently under control on phenytoin. She had swallowing difficulties, drooling, urinary incontinence and behavioral problems such as body rocking movements and self-harm which complicated neurodevelopmental delay. Her neurological examination revealed strabismus, reduced muscle tone and brisk deep tendon reflexes. MRI imaging of the brain showed dysgenesis of the corpus callosum (images are not available).

Developmental milestones and dysmorphic features of two affected individuals with severe intellectual disability, and chromosome 4p16.1 duplication and 3p26.3 microdeletion are described in (Table 4-4). Individual IV: 11 were born pre-term to consanguineous parents. Compared to other affected individuals with a chromosome 4p16.1 duplication and 3p26.3 microdeletion (Table 4-3) he presented with more severe developmental delay, learning disability and malformations (Figure 4-3, A and B). He developed complex partial seizures and stereotypic behavioral abnormalities including rocking, hand wringing, repeated hand washing, head banging and self-harm in late childhood. Neurological examination revealed strabismus, gaze evoked nystagmus, limb and gait ataxia, exaggerated knee and ankle jerks and up-going plantar reflexes.

The other affected with severe clinical presentation and chromosomes 4p16.1 duplication and 3p26.3 microdeletion, III: 4 is the eldest affected of the pedigree (Figure 4-3, C and D). Her medical history is also significant for medically resistant secondarily generalized tonic-clonic seizures. Systemic

and neurological examination at 40 years of age revealed severe kyphosis, gaze evoked nystagmus, dysarthric speech, reduced upper limb deep tendon reflexes, absent knee and ankle jerk, hypotonia, and an ataxic gait.

A summary of five affected individuals with mild clinical manifestations and distinctive dysmorphic features of chromosomes 4p16.1 duplication and 3p26.3 microdeletion is on Table 4-3. All five individuals had delayed motor and language developmental milestones and mild intellectual disability. IV: 2 inherited unbalanced chromosomes 4p and 3p translocation from her mother with severe clinical presentation of chromosomes 4p16.1 duplication and 3p26.3 microdeletion. Her neurological examination at age 16 only revealed dysarthria, and absent knee and ankle jerks.

A potentially distinct chromosome 4p and 3p translocation phenotype was seen in individual IV: 8 with upper and lower motor neuron signs and limb ataxia, and MRI showing mild cerebral atrophy. Neurological examination of IV: 9, IV: 1 and IV: 17 were within normal limits.

Table 4-1 Prenatal and postnatal developmental milestones of the three patients with the chromosomes 4p16 deletion and 3p26.3 duplication

Characteristics	**V: 1**	**V: 2**	**IV: 13**
Age*	12 y/5m	8y/8m	12y
Gender	F	F	M
Weight at birth**	1.5 kg	1.5 kg	1.8 kg
Motor developmental milestones	Floppy at birth; Sitting at 4 years***; Sitting and standing with support; Unable to walk	Floppy at birth****; Standing and walking with support*****	Floppy at birth; Independently roll from back to front; Sitting, standing with support; Unable to walk
Social developmental milestones	Poor eye contact; Absent speech; Verbalize only sounds	Sufficient eye contact; Speech limited to a few words	Absent eye contact; Poor response to noise; Speech limited to a few words
Height (cm/SDS)	109 /-5.9	110 /-5.3	128 /-0.3
Head circumference (cm/SDS)	43 /-8.8	42 /-8.0	48 /-4.2
Limitation in adaptive/ Intellectual functioning	Yes/Severe******	Yes/Severe	Yes/Severe

y-years; m-months when growth parameters were measured; F-female, M-male; *Exact age when height and head circumference were measured; **Length and head circumference at birth is not available; ***Sitting at age 4; ****Required ventilation for a month post-delivery; *****Started to walk at age 2; SDS standard deviation score was calculated using WHO website parameters using age on examination; above age; http://www.who.int/childgrowth/standards/en; (-2 SDS) normal average; ******Severity is classified using outlines given by DSM-5 (Appendix 6.1).

Table 4-2 Dysmorphic features of the three patients with the chromosomes 4p16 deletion and 3p26.3 duplication

Dysmorphic features	**V: 1**	**V: 2**	**IV: 13**
Cranio-facial	Highly arched eyebrows; Flat nose bridge; Bullous nose; Prominent eyes; Hypertelorism; Short philtrum; Downturned mouth**;** Micrognathia	Highly arched eyebrows; Flat nose bridge; Bullous nose; Prominent eyes; Hypertelorism; Short philtrum; Downturned mouth; Micrognathia; Left preauricular sinus; Small earl lobule; 'Cauliflower' shaped left ear; Pointed pinna	A high arched palate, cleft lip; Highly arched eyebrows; Flat nose bridge; Bullous nose; Prominent eyes; Hypertelorism; Short philtrum; Downturned mouth; Micrognathia; Flat occiput
Limb	Tapering-long fingers; Single transverse palmar crease; Hypermobile MCPJ of thumb; Overlapping fingers; Pes planus	Overlapping, tapered fingers, Flexion contracture of PIPJ; Inability to abduct the thumb, Single transverse palmar crease; Hypermobile MCPJ of thumb; Rocker bottom feet; Prominent talus and medial malleolus	Overlapping, tapered fingers; flexion contracture of PIPJ; Inability to abduct the thumb, Single transverse palmar crease; Hypermobile MCPJ of thumb; Fixed flexion deformity of the elbows; Rocker bottom feet; Prominent talus and medial malleolus
Organ*	Agenesis of the right kidney	N/A	Right kidney malformation

*Abdominal ultrasound findings; MCPJ- metacarpophalangeal joints; PIPJ- proximal interphalangeal joints; N/A-not available

Table 4-3 Summary of the five patients with mild clinical presentation and chromosomes 4p16.1 duplication and 3p26.3 microdeletion

Case	IV:8	IV:9	IV:2	IV:1	IV:17
Age*	20y/5m	16y/7m	16y/1m	11y/7m	7y/9 m
Sex	M	M	F	M	F
ID**	Mild	Mild	Mild	Mild	Mild
Height (cm/SDS***)	179/0.2	172/-0.4	151/-2.0	143/-0.3	122/ -0.4
Head circumference (cm/SDS**)	55/-1.3	53.5/-1.9	53/-1.7	51/-2.4	51/ -1.5
Dysmorphic features					
Face	Prominent supraorbital ridges & glabella	Prominent supraorbital ridges, glabella & midface; prognathism small eyes	Prominent supraorbital ridges, glabella & midface; prognathism	NAD	NAD
Nose/Mouth	Bulbous nose	Bulbous nose High arched palate	Bulbous nose	Flat nasal bridge	NAD
Ear	Low set ears	Enlarged ears, malformed helix	Enlarged, low set ears	Low set ears	NAD
Hands & feet	Fixed-flexed deformity of 2,3,&4 toes	Long digits	NAD	Clindact ily	NAD

y-years; m-months when growth parameters were measured; F-female, M-male; *Exact age when height and head circumference were measured; **ID-Intellectual deficit; ***SDS standard deviation score was calculated using WHO website parameters (http://www.who.int/childgrowth/standards/en/); above (-2 SDS) normal average; severity of ID were evaluated according to Appendix 6.1; NAD-no abnormality detected

Table 4-4 Summary of the two patients with severe clinical presentation and chromosomes 4p16.1 duplication and 3p26.3 microdeletion

Case	III:4	IV:11
Age*	40y	14y/1m
Sex	F	M
Weigh at birth**	N/A	1.2 kg
Motor developmental milestones	Walking with support	Floppy at birth; Standing and walking with support***
Language and social developmental milestones	Limited vocabulary Unable to read or write Poor eye contact	Absent speech; Poor eye contact
Height (cm/SDS****)	157/-1.1	130/-3.8
Head circumference (cm/SDS****) Head shape	52/-2.5 Normocephaly	49/-4.1 Trigonocephaly
Limitation in adaptive/ Intellectual functioning	Yes/Severe*****	Yes/Severe
Dysmorphic features		
Face	Prominent supraorbital ridges & glabella; prominent midface; prognathism; strabismus	Hypertelorism, Prominent midface; Highly arched eyebrows Cleft lip
Nose/Mouth	Bulbous nose; thin vermillion of the upper lip; High arched palate; cleft lip; gum hypertrophy	Broad high nasal bridge; bulbous nose; Short philtrum
Ear	NAD	Low set ears; malformed helix
Hands & feet	Camptodactyly Pes cavus; Inversion deformity of feet	Camptodactyly; #

y-years; m-months when growth parameters were measured; F-female, M-male; N/A-not available; NAD-no abnormality detected *Exact age when height and head circumference were measured; **Length and head circumference at birth is not available; *** Started to walk with support at age 3;****Severity is classified using outlines given by DSM-5; *****SDS standard deviation score was calculated using WHO website parameters (http://www.who.int/childgrowth/standards/en/) ; above (-2 SDS) normal average; # other body dysmorphic features - sacral dimple and hypospadius

Figure 4-3 Photo of affected individuals with chromosomal rearrangement

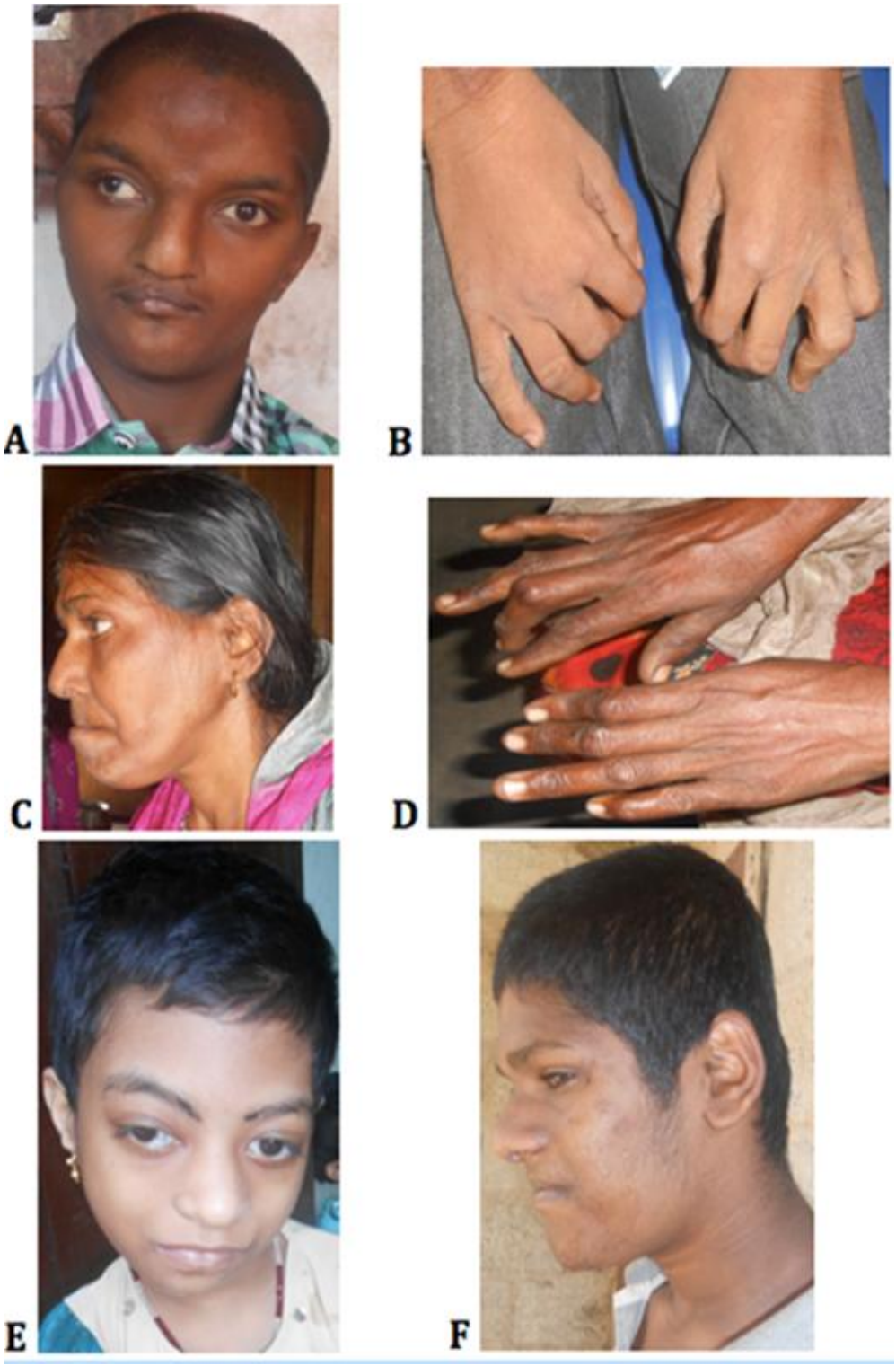

(A)(B) case IV: 11; (C)(D) case III: 4; (E) case V: 1; (F) case IV: 9

4.2.2 *Microarray and fluorescence in situ hybridization (FISH) analysis*

In order to perform gene mapping linkage studies, and assess family members for CNVs and chromosomal abnormalities, DNA samples from family members were genotyped using the Illumina HumanCytoSNP-12 v2.1 microarrays. This revealed the presence of a chromosomal rearrangement involving chromosomes 3p and 4p, in different combination in family members (Table 4-5). In three affected individuals (IV: 13; V: 1; V: 2) a 3p26.3 (0–2144867) x3duplication and 4p16.3-16.1 (0–10308871) x1 deletion was identified. In seven affected individuals (III: 4; IV: 8; IV: 9; IV: 2; IV: 11; IV: 1; IV: 17), including two (III: 4 and IV: 11) with more severe phenotype than others a reciprocal 3p26.3 (0–2118422) x1deletion and 4p16.3-16.1 (0–10290552) x3duplication was detected (Figure 4-4).

In order to confirm the presence of the unbalanced chromosomal rearrangement and define balanced translocation FISH was performed by Dr Abhi Kulkarni. Three samples, V: 2, IV: 9 and III: 3 were available for study. Kreatech probes D4S33060 and D3S4558 were designed for target regions of 4p16.3 and 3pter, respectively. FISH confirmed the presence 4p16.3-16.1 deletion and 3p26.3 duplication in case V: 2, 4p16.3-16.1 duplication and 3p26.3 deletion in case IV: 9 and detected balance translocation between 4p16.3-16.1 and 3p26.3 in case III: 3 (Figure 4-5, Figure 4-6 and Figure 4-7).

Table 4-5 cDNA copy alterations identified using micro-array copy number analysis

Cases	ISCN description
V: 1 V: 2 IV: 13	Del 4p16.3-16.1 (0-9919593)x1 Dup 3p26.3 (0-2161551)x3
III: 4 IV: 1 IV: 2 IV: 8 IV: 9 IV: 11 IV: 17	Dup 4p16.3-16.1 (0-9901274)x3 Del 3p26.3 (0-2135106)x1

ISCN- International System for Chromosome Nomenclature

Figure 4-4 KaryoStudio analysis output

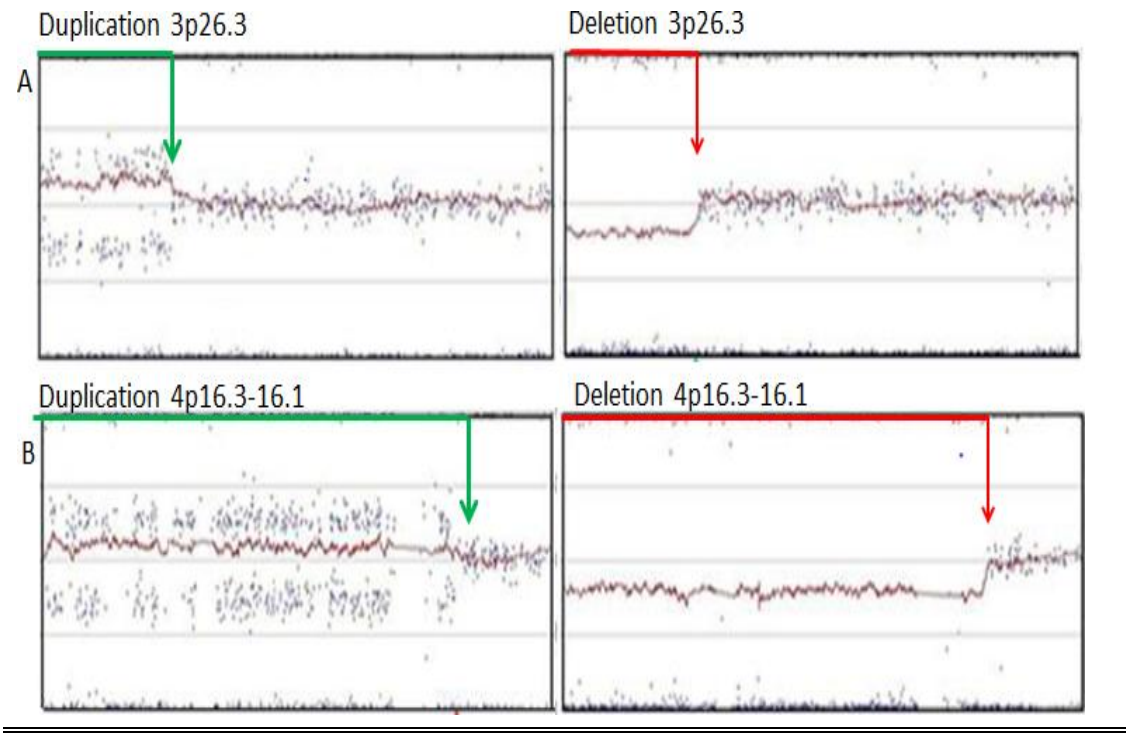

Example of beadarray analysis of SNP data, used to identify the chromosomal subregion duplication and deletion events present in family members. (A) Chromosome 3p26.3 region; (B) Chromosome 4p16.3-16.1 region; The midline shows a 1:1 DNA ratio to the reference genome; Deleted regions are segments below the midline (red line boundaries), and duplications (gains) are above the midline (green line boundaries) (log 2 scale)

Figure 4-5 FISH karyotype analyses of V: 2

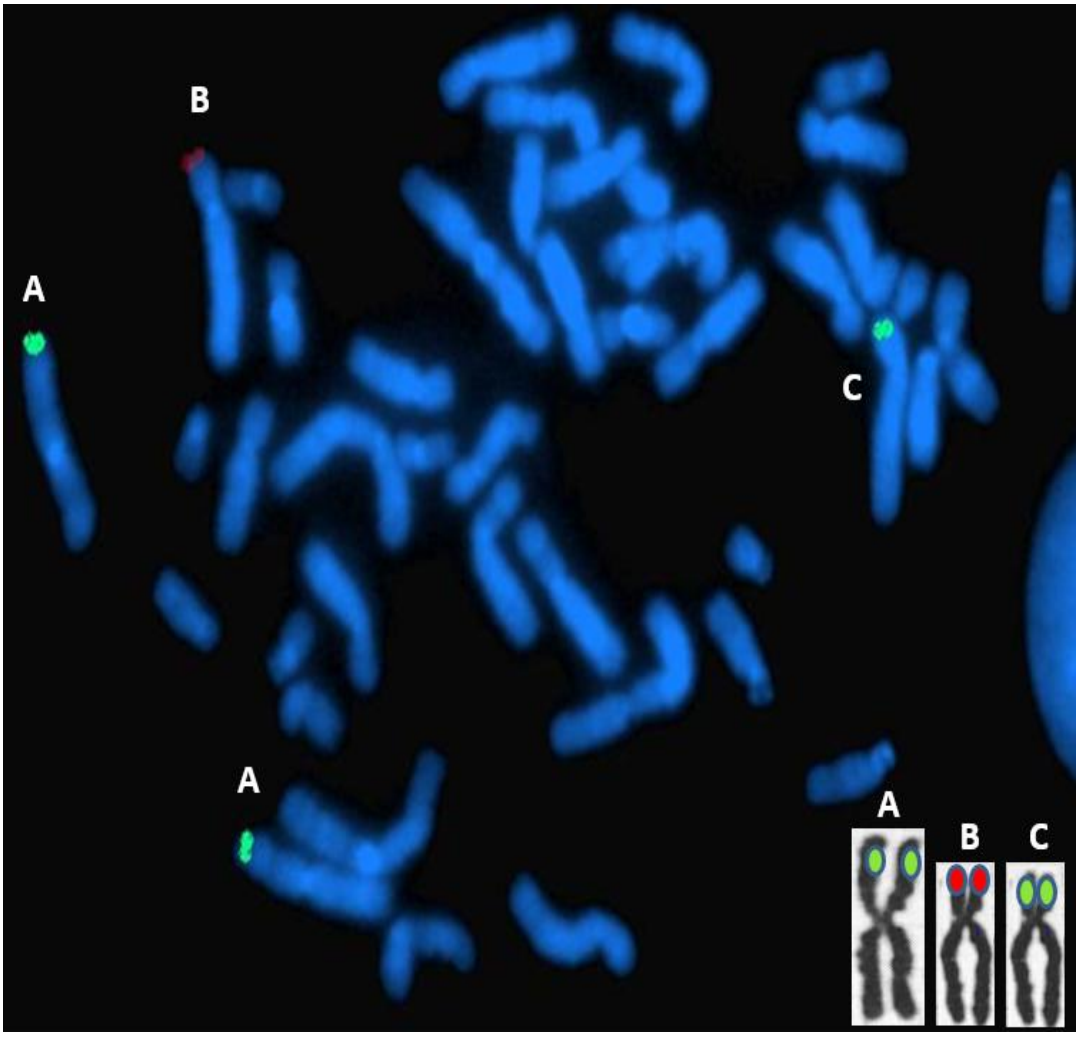

Kreatech probe D3S4558 was used for chromosome 3p26.3 or 3pter (green dot) (A) and D4S33060 was used for chromosome 4p16.3-16.1 or 4pter (red dot) (B); FISH microscopy of a V: 2 case shows that 4pter probes did not attach to the derivative chromosome 4p16.3-16.1 (C) instead 3pter probes attached to the derivative chromosome 4p16.3-16.1 (C) as well as to the chromosome 3p26.3 (A); This indicates chromosome 4p16.3-16.1 deletion (partial monosomy) and 3p26.3 duplication (partial trisomy) in the V: 2 case.

Figure 4-6 FISH karyotype analyses of IV: 9

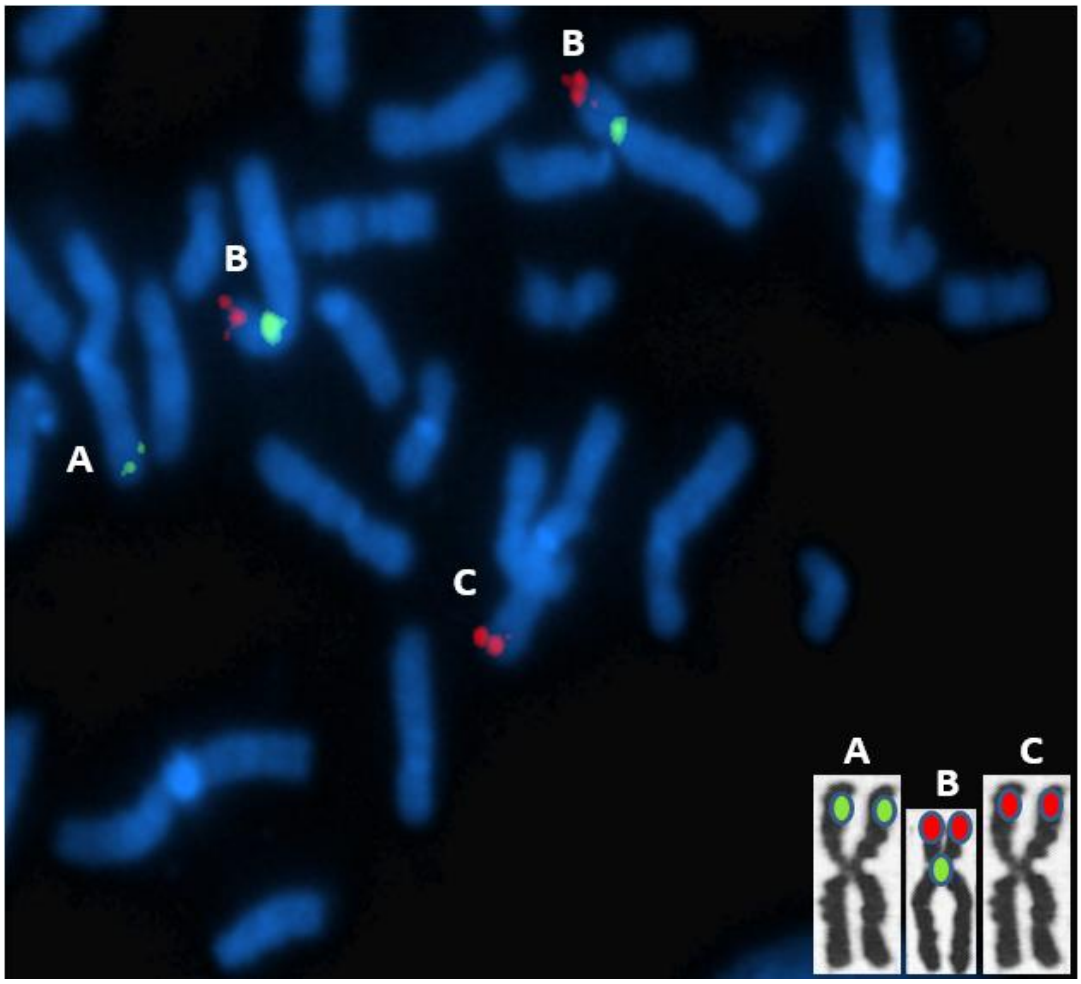

Kreatech probe D3S4558 was used for chromosome 3p26.3 or 3pter (green dot) (A), D4S33060 was used for chromosome 4p16.3-16.1 or 4pter (red dot) and green markers were used for chromosome 4 centromere (B) to distinguish chromosome 4 and 3; FISH microscopy of a IV: 9 case shows that 3pter probes did not attach to the derivative chromosome 3p26.3 (C) instead 4pter probes attached to the derivative chromosome 3p26.3 (C) as well as to the chromosome 4p26.3 (B); This indicates chromosome 3p26.3 deletion (partial monosomy) and 4p16.3-16.1 duplication (partial trisomy) in the IV: 9 case.

Figure 4-7 FISH karyotype analyses of III: 3

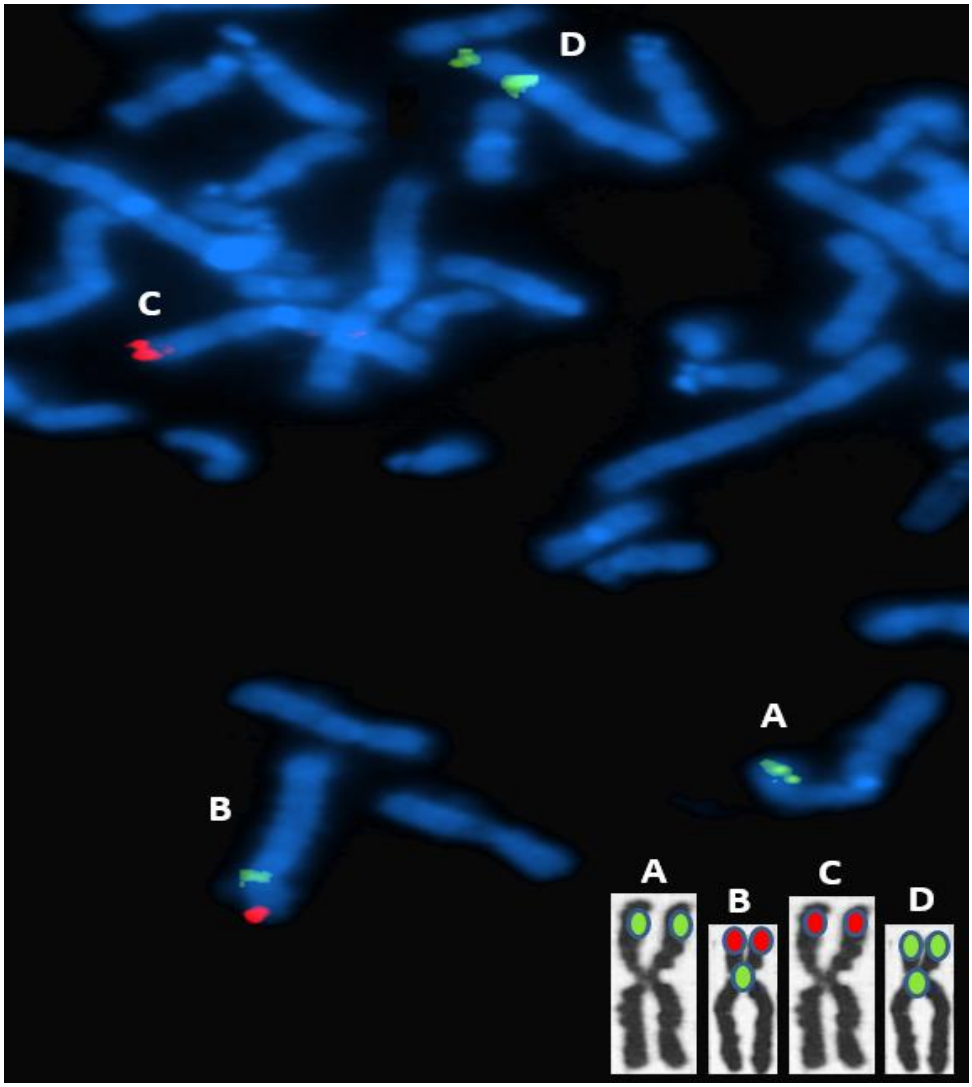

Kreatech probe D3S4558 was used for chromosome 3p26.3 or 3pter (green dot) (A), D4S33060 was used for chromosome 4p16.3-16.1 or 4pter (red dot) and green markers were used for chromosome 4 centromere (B and D) to distinguish chromosome 4 and 3; FISH microscopy of a III: 3 case shows that 3pter probes attached to the derivative chromosome 4p16.3-16.1 (D) and 4pter probes attached to the derivative chromosome 3p26.3 (C); This indicates balanced translocation between 4p16.3-16.1 and 3p26.3 in the III: 3 case.

4.3 Discussion

This chapter describes a large Indian pedigree with diverse neurodevelopmental and dysmorphological clinical manifestations reflecting three rare chromosomal disorders that were found to relate a complex reciprocal translocation involving chromosome 4 and 3. Nine of the ten affected family members (II: 2; III: 7; III: 10; III: 12; III: 14; III: 17 and IV: 4) were born from a healthy parent with a possible balanced chromosome 4 and 3 translocation (in III: 3 case it was confirmed by FISH), while a single affected individual (IV: 2) inherited her imbalanced chromosomal complement from her affected mother (III: 4) who herself displayed the same 4p16.1 duplication and 3p.26.3 microdeletion (Figure 4-2). This is the first reported case study of WHS-associated chromosomal rearrangements involving 4p partial trisomy and 3p deletion syndromes in the same family.

WHS results from deletion of the chromosome 4p region with a 'core phenotype' of a typical facial appearance, severe mental retardation, growth delay and seizures (Zollino et al., 2008). Three affected with the chromosomes 4p16 deletion identified by SNP genotyping displayed the typical clinical features of WHS including severe delay in all developmental milestones, severe learning disability, a characteristic facial appearance (hypertelorism and flat nose bridge, that is 'Greek warrior helmet' appearance) and seizures (Table 4-1, Table 4-2 and Figure 4-3, E). The high arched eyebrows and prominent nasal tip that were also seen in all three cases may relate to the progression of these facial features with age, as has been previously suggested (Battaglia et al., 2000). The other facial, hand and

feet malformations described in Table 4-2, stereotypic behavioral disturbances (in all three cases) as well as dysgenesis of corpus callosum (in IV: 13 case) have previously been associated with chromosome 4p deletion. (Battaglia et al., 2000; Verbrugge et al., 2009).

At a molecular level, the likely critical region responsible for core phenotype of WHS lies within the terminal 1.9 Mb region on 4p16.3, coined as a WHSCR-2 (Zollino et al., 2003). Candidate genes mapping to WHSCR-2 have been suggested to cause particular clinical aspects of WHS (Stec et al., 1998; Wright et al., 1999). Deletion of *WHSC1* gene has been related to both facial characteristics and growth delay in WHS cases (Wright et al., 1997; Zollino et al., 2003; Rodriguez-Revenga et al., 2007). The origin of seizures in WHS however is not clear. Although leucine zipper/EF-hand-containing transmembrane protein 1 gene (*LETM*1), mapping entirely within WHSCR-2 is proposed to play an important role in the pathogenesis of seizures, genotype–phenotype correlation analyses suggested that deletion of *LETM1* alone may not be sufficient in causing seizures (Nowikovsky et al., 2004; Schlickum et al., 2004; Frazier et al., 2006; Jiang et al., 2009; DiMauro et al., 1999; Zollino et al., 2014). The loss of the terminal 1.5 Mb region with breakpoint at about 300 kb from the *LETM1* locus, preserving *LETM1* has been associated with development of a seizure disorder (Zollino et al., 2014). All three presented cases with chromosome 4p deletion have history of seizures (V: 2 and IV: 13 generalized tonic clonic seizures and V: 1 febrile seizure). Increased muscle tone (in V: 1, and V: 2) and exaggerated deep tendon reflexes suggestive of upper motor neuron involvement in all three

cases contrast to reduced muscle tone a common neurological examination finding in WHS cases (Zollino et al., 2008).

Above described 'classical' severe and uniform syndromic presentation seen in the three WHS patients caused by deletion of the chromosome 4p region is relatively different from gains of the same region, which results in more variable clinical manifestations in terms of severity of presentation and dysmorphic features. The majority of the seven patients with chromosomes 4p16.1 duplication and 3p26.3 microdeletion displayed dysmorphic features previously described for trisomy of 4p syndrome, including prominent supraorbital ridges, bulbous nose, prognathism, camptodactyly or clindactyly, and low-set ears (Table 4-4 and Figure 4-3). However limitation in adaptive and intellectual functioning as well as growth milestones and developmental delay were variable in severity at presentation (Table 4-3). HC and height were within normal limits in 90% of cases with relatively mild clinical presentation of learning disability and developmental delay (above -2 SDS). Overexpression or inactivating mutations of two genes mapped to the chromosomal region involved, *FGFR3* and *WHSC1*, have been reported to be associated with overgrowth features such as macrocephaly, campodactyly and tall stature (Toydemir et al., 2006; Nimura et al., 2009). *FGFR3* is a physiological negative regulator of bone growth, and has been associated with dysmorphic syndromes involving bone growth including overgrowth syndrome CATSHL (campodactyly, tall stature, and hearing loss) (Toydemir et al., 2006). Although none of the seven cases with chromosomes 4p16.1 duplication presented with tall stature or macrocephaly, normal limits (defined by WHO, above -2 SDS) of HC and

height observed in those cases may be related to partial effect of *FGFR3* overexpression. Haploinsufficiency of *WHSC1* has previously been shown in mice models to result in developmental delay, that was observed in seven cases with chromosomes 4p16.1 duplication in variable degree (Nimura et al., 2009).

Two of the seven chromosome 4p duplication cases (III: 4 and IV: 11) demonstrated rather different clinical manifestations including severe intellectual disability, significantly reduced growth milestones (HC and height), generalized tonic-clonic seizures and cerebellar signs, compared with relatively mild learning difficulties in the remaining five cases (IV: 8; IV: 9; IV: 2; IV: 1 and IV: 17). Although serum phenytoin level has not been checked, cerebellar signs and gum hypertrophy seen in the two severely affected cases may relate to its long term use. The craniofacial dysmorphism in one of the two partial 4p trisomy cases (IV: 11), including high arched eye brows, hypertelorism, trigonocephaly as well as marked reduction in growth milestones (including microcephaly) and behavioral changes, are not easily explained or recognized in partial 4p trisomy syndrome (Table 4-4 and Figure 4-3). While this may reflect as yet unrecognized clinical variability in this disorder, it is more likely to be due to the complexity of the chromosome imbalance in these cases or phenotypical expression of chromosome 3 microdeletion. Although the chromosome 3pter rearrangement identified in seven cases somewhat smaller compared with rearrangements previously reported as part of chromosome 3p duplication syndrome, the 2.7Mb microdeletion in chromosome 3p26.3 includes the contactin 4 (*CNTN4*) and cell adhesion molecule L1-like (*CHL1*) genes, which have been associated

with a 3p duplication syndrome dysmorphic features and intellectual disability (Conte et al., 1995; Kotzot et al., 1996; Dijkhuizen et al., 2006; Pohjola et al., 2010; Frints et al., 2003; Shrimpton et al., 2006). Deletion of *CNTN4* has also been related to microcephaly, trigonosephaly, hypertelorism, growth retardation and ear abnormalities. However these clinical features were present in only two of the seven chromosome 3p26.3 microdeletion cases (III: 4 & IV: 11) presented here, indicating that other factors including age of examination, other genes in the 3pter region, epigenetic phenomena, expression or regulatory variation and the unmasking of recessive variants residing on the other unperturbed allele, may also be required for the development of these features.

5

CHAPTER FIVE

LINGO1 GENE DUPLICATION AS A LIKELY CAUSE OF DYSTONIC TREMOR

LINGO1 GENE DUPLICATION AS A LIKELY CAUSE OF DYSTONIC TREMOR

5.1 Introduction

Leucine-rich repeat and Ig domain containing Nogo receptor interacting protein-1 (*LINGO1)* is selectively expressed in neurons and oligodendrocytes within the CNS (Barrette et al., 2007; Inoue et al., 2007; Llorens et al., 2008). Lingo-1 protein has been found to interact with inhibitory myelin proteins including Nogo-A, myelin associated glycoprotein and oligodendrocyte myelin glycoprotein (Schwab, 2004). All three of these myelin-associated inhibitor factors are able to bind to and activate the same axonal multi-protein receptor complex. The proteins that generate this receptor complex are the ligand binding Nogo-66 receptor (NgR1) and two signal transducing binding partners, the p75 neurotrophin receptor (p75) and Lingo1 (Yiu and He, 2003; Mi et al., 2004). Interaction of myelin-associated inhibitors with the p75/NgR1/LINGO-1 complex can activate RhoA which is a negative regulator for neuronal survival, axonal regeneration, oligodendrocyte maturation and neuronal myelination (Figure 5-1) (Llorens et al., 2011; McGee and Strittmatter, 2003; Mi et al., 2008; Yiu and He, 2006; Lee et al., 2007; Jepson et al., 2012; Lööv et al., 2012).

LINGO1 has been associated with different neurological disorders including multiple sclerosis (MS), ET, Parkinson's disease (PD), cerebral ischemia, spinal injury etc. (Xing et al., 2015; Delay et al., 2014; Miller and Mi, 2007; Chen et al., 2015). Moreover, antagonism of LINGO1 function in an animal model of MS has been shown to improve morphometrically evident

remyelination, axonal integrity, clinical scores, and locomotor behavior (Mi et al., 2007; Wang et al., 2014).

Genome wide association studies have identified *LINGO1* as potential ET susceptibility gene (Table 5-1). However, while risk variants located in the intron of the *LINGO1* gene and coding exons have been identified to map within the linkage disequilibrium block risk SNP haplotype, sequencing of the coding region of the gene in patients and families has not identified pathogenic variants (Stefansson et al., 2009; Tan et al., 2009; Clark et al., 2010; Vilarino-Guell et al., 2010a; Thier et al., 2010). Therefore, it has been suggested that unidentified intronic variants associated with ET either directly influence or are in linkage disequlibrium with mutations affecting LINGO1 protein expression levels via altering gene transcription or translation (Wang et al., 2006; Zhou et al., 2012). *LINGO1* (*rs11856808*) has also been shown to play a protective role by decreasing the risk for PD (Chen et al., 2015).

Recently, a number of studies have been conducted to explore the role of LINGO1 protein in the pathogenesis of ET. LINGO1 protein levels in the cerebellar cortex of ET cases have shown that the LINGO1 protein level is significantly increased in ET patients compared to healthy individuals (Kuo et al., 2013; Delay et al., 2014). Distal processes of basket cells (BC) which are highly enriched with LINGO1 protein have been found to become elongated in ET cerebellum compared to control brains (Figure 5-2) (Ango et al., 2004; Kuo et al., 2013). Interestingly, LINGO1 levels remain similar in other brain region of ET cases and controls, providing evidence that the cerebellum could plays a central role in ET pathogenesis.

Figure 5-1 Mechanism of LINGO1 mediated axonal overgrowth inhibition

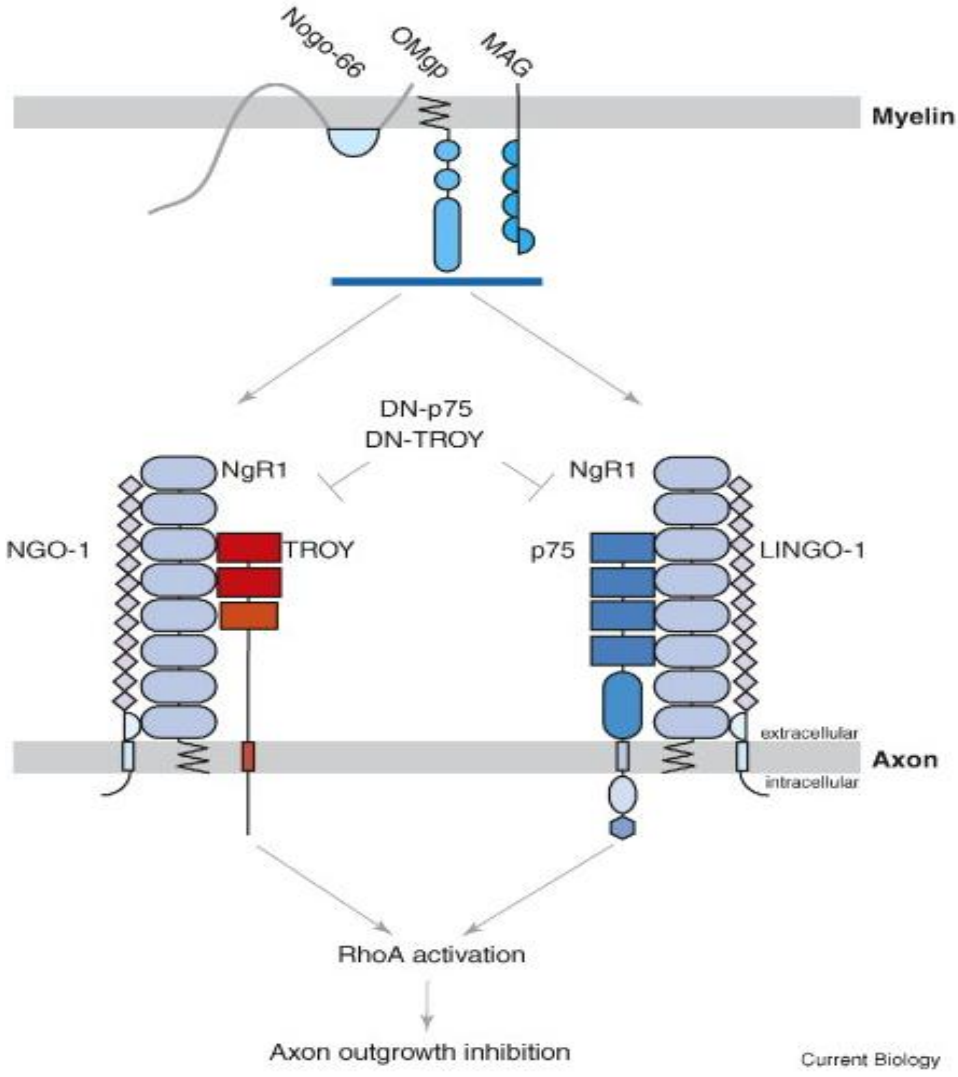

Illustration of the myelin associated inhibitor factors (Nogo-66, myelin associated glycoprotein (MAG) and oligodendrocyte myelin glycoprotein (OMgp)) and a shared receptor NgR1 which results in the axonal degeneration. An interaction between NgR1, LINGO1 and p75, as well as NgR1, LINGO1 and TROY can transduce signaling upon binding of myelin associated inhibitor factor to NgR1, leading to RhoA activation and axon outgrowth inhibition.

(Mandemakers and Barres, 2005)

Table 5-1 *LINGO1* variants detected by genome-wide association studies of ET

Study references	*LINGO1/2* variants	Total ET HET N^0	Control N^0	Cohort source	Overall results
(Stefansson et al., 2009)	*LINGO1* rs9652490G	733/338*	15.582	Iceland, Austrian, German, US	$p < 1.2 \times 10^{-9}$
(Thier et al., 2010)	*LINGO1* rs9652490T rs11856808	332/177	574	German, French	$p = 9.1 \times 10^{-3}$ $p = 1.0 \times 10^{-3}$
(Clark et al., 2010)	*LINGO1* rs9652490G	257/88	265	US	$p = 0.03$
(Vilarino-Guell et al., 2010a)	*LINGO1* rs9652490A/A	356/NS**	428	North American	$p = 0.014$
(Radovica et al., 2012)	*LINGO1* rs9652490A/G	141/77	130	Latvian	$p = 0.04$
(Tan et al., 2009)	*LINGO1* rs9652490G	190/75	733	Singapore	$p = 0.068$
(Vilarino-Guell et al., 2010b)	*LINGO1* rs8028808T/T *LINGO2* rs1412229 T/T	1247	642	North American	$p = 0.008$ $p = 0.015$
(Wu et al., 2011)	*LINGO2* rs10812774C/C	327/NA	499	Chinese, Singapore	$p = 0.01$

* Number of hereditary essential tremor (HET) in discovery sample which was 452; ** Not specified

Figure 5-2 Elongated LINGO1 labeled basket cell processes in ET brains.

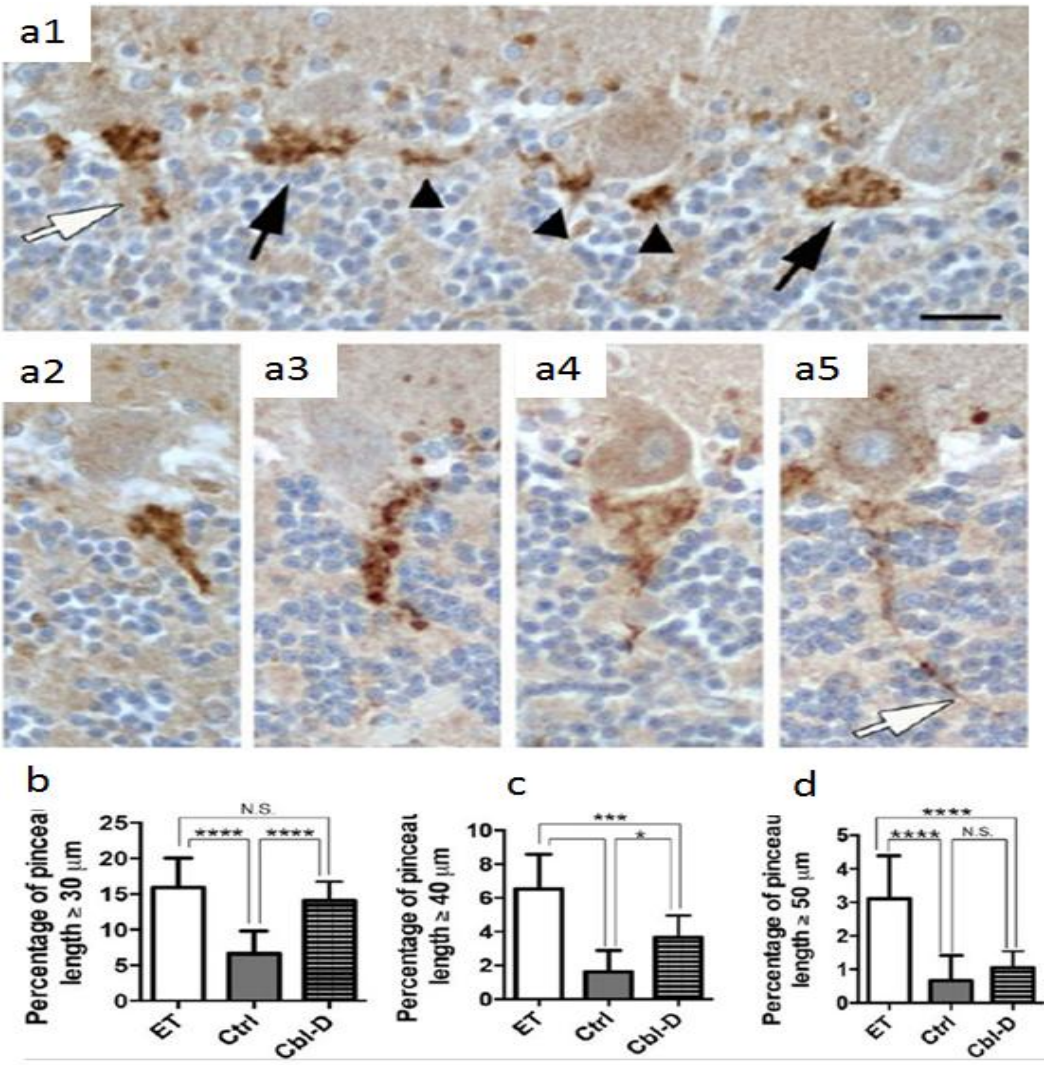

Variable appearance of LINGO1 labeled basket cell processes (pinceau) in paraffin sections, ranging from very short segments (a1, arrowheads), cone-shaped structure (a1, black arrows), or more elongated forms (a1, white arrow, a2-a5). LINGO1 labeled pinceau measuring ≥30 μm (b), ≥40 μm (c) or ≥50 μm (d) in length were more frequently seen in ET cases. In comparison with other cerebellar degenerative disorders (Cbl-D), the percentage of LINGO1 labeled pinceau ≥30 μm was similar in ET cases and Cbl-D cases (b). However, ET cases had a significantly higher percentage of LINGO1 labeled pinceau ≥40 μm or ≥50 μm than Cbl-D cases (c,d), and pinceau ≥50 μm are relatively specific to ET (d). *$p \leq 0.05$, ***$p \leq 0.001$, ****$p \leq 0.0001$ (Kuo et al., 2013).

5.2 Results

5.2.1 Clinical report

We investigated an extensive Indian pedigree (Figure 5-3) from a small remote village of Kerala in Southern India. An in-person evaluation of eleven affected individuals with a history of tremor (III: 5, IV: 8, III: 9, III: 15, II: 6, II: 8, II: 9, II: 11, IV: 1, IV: 2 and V: 1) was conducted either by Dr. Thomas Iype at Trivandrum Medical College Hospital, Kerala, or by Dr. Vafa Alakbarzade and a consultant neurologist Dr. Christos Proukakis in the individual's homes. The evaluation included comprehensive history including past medical history of thyroid disease and medication history, drawing Archimedes spirals (a set of four Archimedes spirals, two right and two left) and a structured videotaped neurological examination which included a detailed assessment of postural, kinetic, intention and rest tremors in the limbs, as well as dystonia and other movement disorders (Louis et al., 2014; Louis et al., 2013; Louis et al., 2008). Upper limb hyperkinetic movements were assessed with the patient sitting and the arms outstretched. The patient was instructed to alternately open and close, and then to pronate and supinate the hands. Additional motor tasks included drinking from a cup with each hand and pouring water from one cup to another. Lower limb hyperkinetic movements were assessed with the patient sitting in a chair (feet resting on the ground and with the legs extended 90 degrees) and also whilst walking. Abnormal posturing or movements of the affected limb whilst the patient performed tasks such as writing, drawing and drinking with both limbs were also observed. The videotapes and Archimedes spirals (Figure 5-

4) were assessed by senior neurologists specializing in movement disorders, Prof Tom Warner and Professor Elan D. Louis.

In summary, affected individuals demonstrated asymmetrical posturing and irregular postural tremor bilaterally in upper limbs with onset from childhood to late adulthood (16-54 years of age). Additional findings on neurological examination of case III: 5 who is a 46 year old male, with a history of tremor of upper limbs started at age of 16 was a ‘yes-yes’ tremor of head.

On examination of II: 11, the eldest of all affected, 80 years of age reduced shoulder range of movements secondary to pain, unilateral upper limb rest tremor and bradykinesia was noted in addition to dystonic posturing with ‘thumbs up’, ‘dinner fork’ of fingers, left sided terminal tremor and irregular postural tremor bilaterally in upper limbs. Four cases without history of tremor were also evaluated including II: 1, II: 3, III: 11 and IV: 5. Neurological examination of IV: 5, 22 year old lady revealed mild symmetric postural tremor, nil else. II: 1, II: 3 and III: 11 cases had no abnormal neurological examination findings.

Venous blood from the forearm has been collected to EDTA- as well as PAX tubes and skin biopsy was performed in three cases, III: 5, IV: 2 and II: 11 (for FISH).

Figure 5-3 Pedigree of the family with dystonic tremor

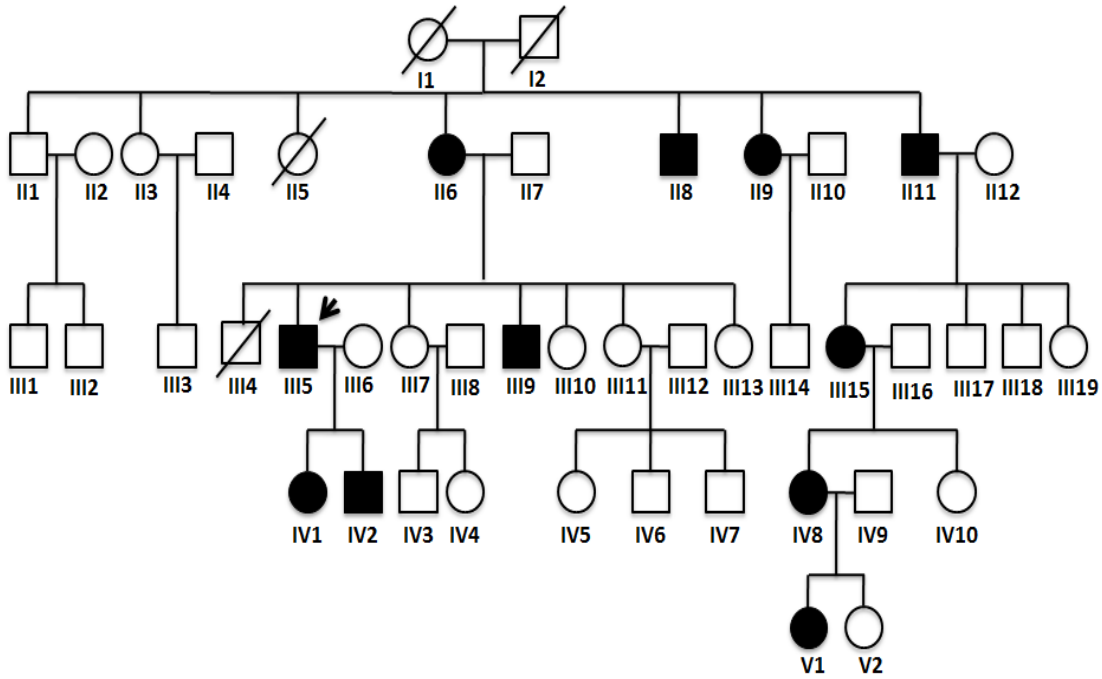

Proband is indicated by an arrow. All affected individuals demonstrated dystonic tremor; case III: 5 presented asymmetrical posturing, postural tremor, head tremor; case II: 11 presented with asymmetrical posturing, postural tremor, possibly with 'frozen shoulder syndrome' and Parkinsonism. Four cases without history of tremor including II: 1, II: 3, III: 11 and IV: 5 were examined.

Figure 5-4 Archimedes spiral drawing of affected

Archimedes spiral on a pre-drawn pattern with the dominant hand

5.2.2 Illumina330K SNP, FISH and WES analysis

In order to perform gene mapping linkage studies and assess family members for CNVs DNA samples from eleven affected individuals were genotyped using the Illumina Illumina330K SNP microarrays. Quantitative trait linkage analysis (using MERLIN software) of the data under a model of AD inheritance with full penetrance revealed a single linkage peak with LOD score of 3.8 at chromosome 15q region (Figure 5-5). The flanking markers for the linked region were rs6494503 (chr15:65,241,569-65,242,069) and rs7164668 (chr15:93,479,041 -93,479,541). The size of the region is 28 Mb with total of 1721 genes mapping to the region, including *LINGO1* gene. Literature search (OMIM and PubMed) of the genes did not reveal previous association with hereditary dystonia.

Guidance for FISH analysis was provided by Prof Andrew Crosby. WES analysis of both V: 1 and IV: 2 affected family members revealed 19 potentially deleterious sequence variants mapping to chr15:65,241,569-93,479,541. The allele frequency these 19 variants was checked using online genomic databases (dbSNP, Exome Variant Server, ExAC), four of which have been described previously with frequencies of <1% (5:133326592, 5:180582411, 6:35428390 and 7:6470196). None of the 19 sequence variants were found to co-segregate with the disease phenotype; excluding them as a causative (Primers for the variants in Appendix 6.11).

Figure 5-5 Graphical summary of linkage curve

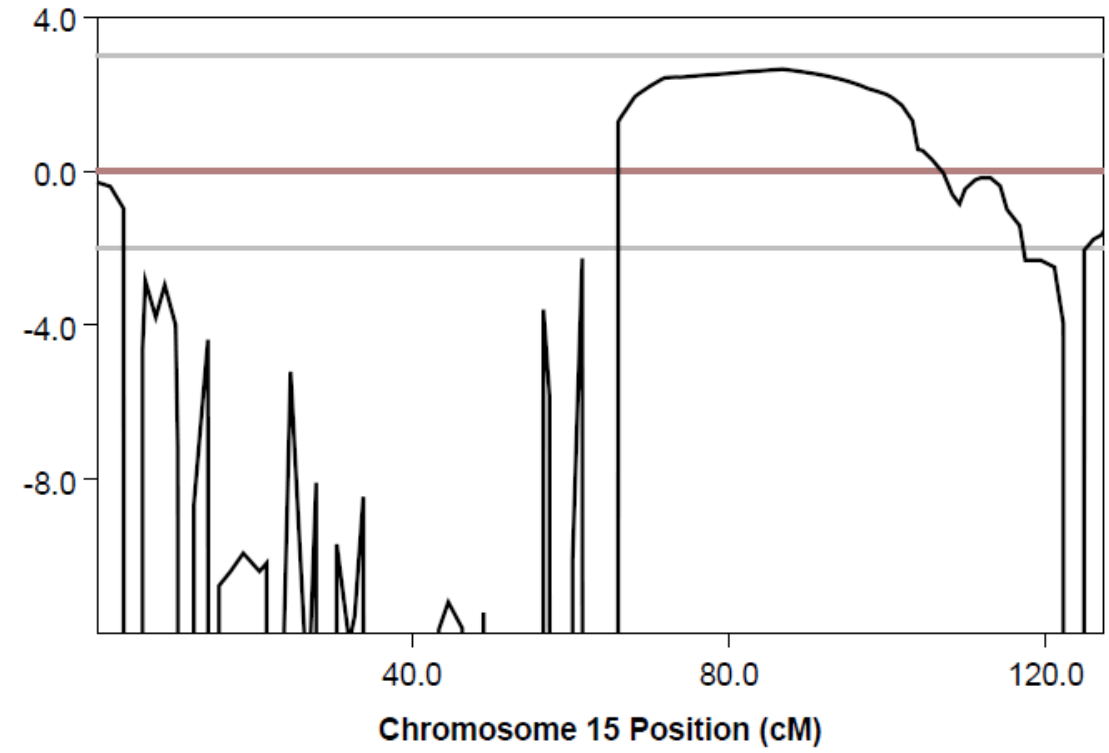

LOD score calculations for genetic markers on chromosome 15 identifies linkage peak between markers rs6494503 (chr15:65,241,569-65,242,069) and rs7164668 (chr15:93,479,041 -93,479,541). X axis indicates estimated multipoint LOD score and y axis particular chromosomal location (cM)

Illumina330K SNP image data was also analyzed in the Illumina's KaryoStudio and Illumina GenomeStudio software to generate genotype calls, B allele frequency and logR2 ratio values. To minimize false positive CNV calls, filtering approaches were applied to exclude smaller repeats (<100 kb) and common CNVs from Database of genomic variants. Illumina's KaryoStudio software transformed the signal intensity data for Illumina330K probes into logR2 ratio and B allele frequency (BAF) measures that could be used to generate CNV calls by PennCNV and QuantiSNP. This identified a region on chromosome 15q with a distinct BAF pattern and increased logR2 ratio of >0.5 among eleven affected individuals (III: 5, III: 9, II: 11, IV: 1, IV: 2, V: 1, II: 6, II: 9, II: 8 and III: 15), indicative of a genomic duplication (Figure 5-6). A genomic duplication at chromosome 15q was absent in three unaffected family members (II: 1; II: 3 & III: 11), as well as on our existing healthy control data from South Indian Illumina330K samples. The CNV identified corresponds to a 400-650kb region (variation in estimates of size between family members is due to inter-sample CNV data variability) on chromosome 15q24 containing around 12 genes, including *LINGO1* (Table 5-2). *LINGO1* gene

In order to detect the origin of the duplicated chromosomal material FISH was performed (Method described in Appendix 6.10). A probe was designed to the chr15:78146252-78322027 region (BlueFISH probe RP11-114H24). FISH analysis of two affected IV: 2 and II: 11 detected one signal clearly larger than other indicating tandem duplication (Figure 5-7).

Figure 5-6 KaryoStudio 330K illuminabead analysis

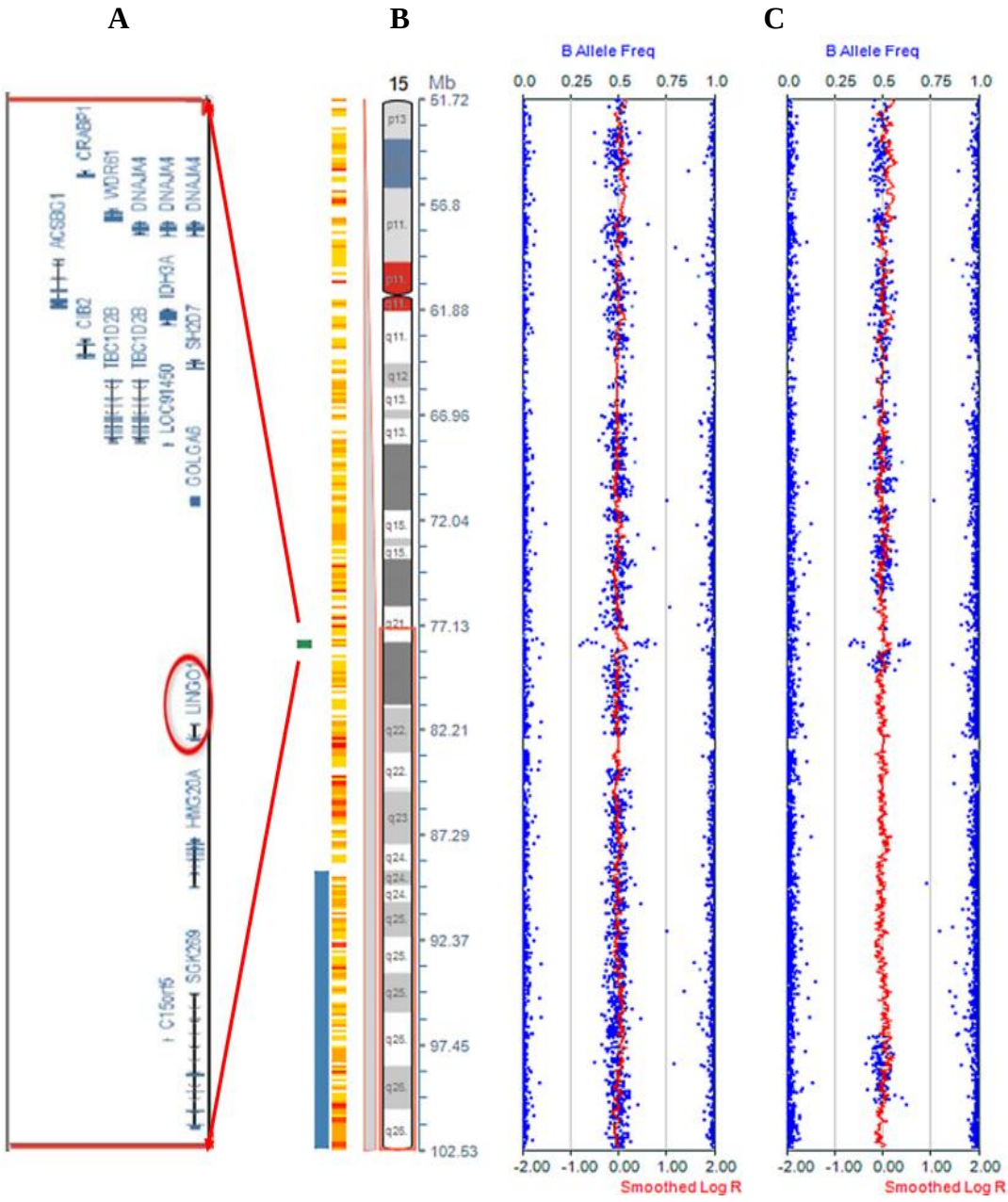

KaryoStudio SNP genotype analysis shows increased smoothed log2 ratio (red line) and relative intensity of allele frequency of the SNP genotype calls, B allele frequency (blue dots) that represents a heterozygous gain in copy number in the two affected individuals (C); a genomic duplication at chromosome 15q24.3-25.1 (green square) (B) contains around 12 genes, including *LINGO1* (A).

Table 5-2 The size, position and gene coverage of the duplicated CNV segment

ID	Duplicated segment position	Cytobands	Genes
III: 15	15: 77672118-78327269	q24.3 q25.1	LOC101929457 ***LINGO1*** LOC253044 LOC101929478 CSPG4P13 DNM1P9 LOC645752 LOC101929509 LOC440292 ADAMTS7P3 LOC91450 TBC1D2B
V: 1	15: 77787469-78327269	q24.3 q25.1	
IV: 2	15: 77787469-78327269	q24.3 q25.1	
III: 9	15: 77816944-78327269	q24.3 q25.1	
III: 5	15: 77915103-78327269	q24.3 q25.1	
II: 11	15: 77921042-78327269	q24.3 q25.1	
IV: 1	15: 77921042-78346867	q24.3 q25.1	
II: 9	15: 77921042-78327269	q24.3 q25.1	
IV: 8	15: 77921042-78327269	q24.3 q25.1	

Illumina's KaryoStudio software data of initially analysed 9 affected individuals showing duplicated segment position with is slightly different among affected most likely due to inter-sample CNV data variability; cytobans of duplicated segment and 12 genes mapped to the duplicated regions, including *LINGO1* gene

Figure 5-7 FISH analysis of IV:2

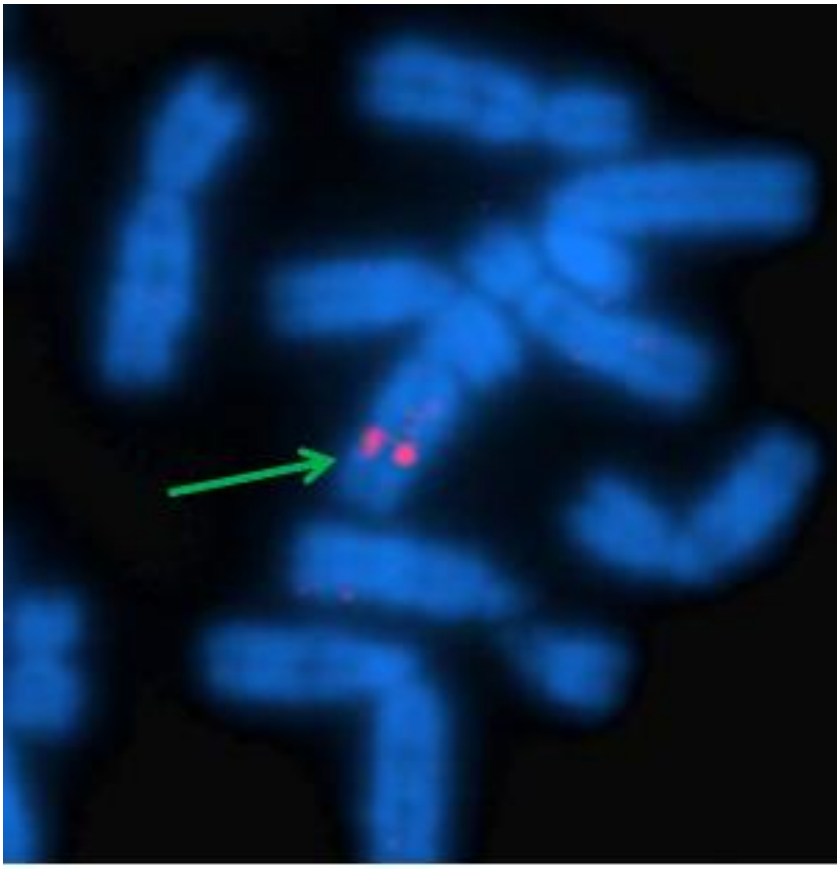

chr15:78146252-78322027 region signal (in two red dotes on two homologous daughter chromosomes). One red dote that indicated by green arrow is visibly larger than other red dot, indicating that the probe designed for the chr15:78146252-78322027 region hybridised twice to one of the daughter chromosomes, indicating tandem duplication of chr15:78146252-78322027 region in a heterozygous manner.

5.2.3 Whole genome sequencing and breakpoint region amplification

Guidance for genomic library preparation was provided by Dr Richard Caswell. In order to map precisely the CNV breakpoints and confirm the nature, orientation and chromosomal position of the duplication (direct repeat or inverted repeat) pair reads (PR) NGS was performed. PR sequencing data analysis of a patient III: 15 identified four read pairs mapping approximately 550kb apart, in reverse-forward rather than forward-reverse orientation, suggesting a tandem duplication event (Figure 1-10). The exact coordinates of the duplication event were detected in 1 and 4 reads spanning the breakpoint on each side, respectively, spanning chromosome15 (hg19): 77775483-78331797 confirming the size of the duplication as 556,315 bp (Figure 5-8). Read count across the region indicates an average coverage increase from approximately 7.5 x to 10x with an expected 50% increase in the number of reads for a heterozygous duplication. A total of 13 genes, including *LINGO1* gene, map within the 556 kb region.

In order to confirm and analyze the chromosome 15: 77775483-78331797 duplication event, conventional PCR was performed across the identified breakpoints in all affected as well as unaffected individuals from the pedigree (Figure 5-3) and 100 age matching healthy controls from the same geographical region.

Sequence of chr15: 77775483-78331797 was obtained from UCSC web browser and the flanking sequence was used to design primers (Figure 5-9). 5’ end sequence of the region was converted to reverse complement and

marked as a reverse primer. 3' end sequence of the region was marked as a forward primer. In theory, DNA sample amplification with those primers was suggestive of duplication and contrary would exclude the duplication event at chr15: 77775483-78331797.

Forward primer, TCTCCGAGTCTACAGGCCAA (Tm 64.9^{0}C) (chr15: 78331133-78331152) and reverse primer, GCAGCAATCACAAAGCCACA (Tm67.4^{0}C) (chr15: 77775980-77775999) were designed using Primer3 plus web browser with the breakpoint product size of 1184 base pairs. Thermocycler program was adjusted with regards of the final annealing temperature (TD) being 62° and extension time of 1: 30 seconds. The breakpoint product which contained the duplication region containing the *LINGO1* gene confirmed the SNP data and cosegregated with individuals with DT, and was absent in unaffected individuals as well as 100 age matching healthy controls from the same geographical region (Figure 5-9).

Figure 5-8 Single-base pair level coordinates of the breakpoint event

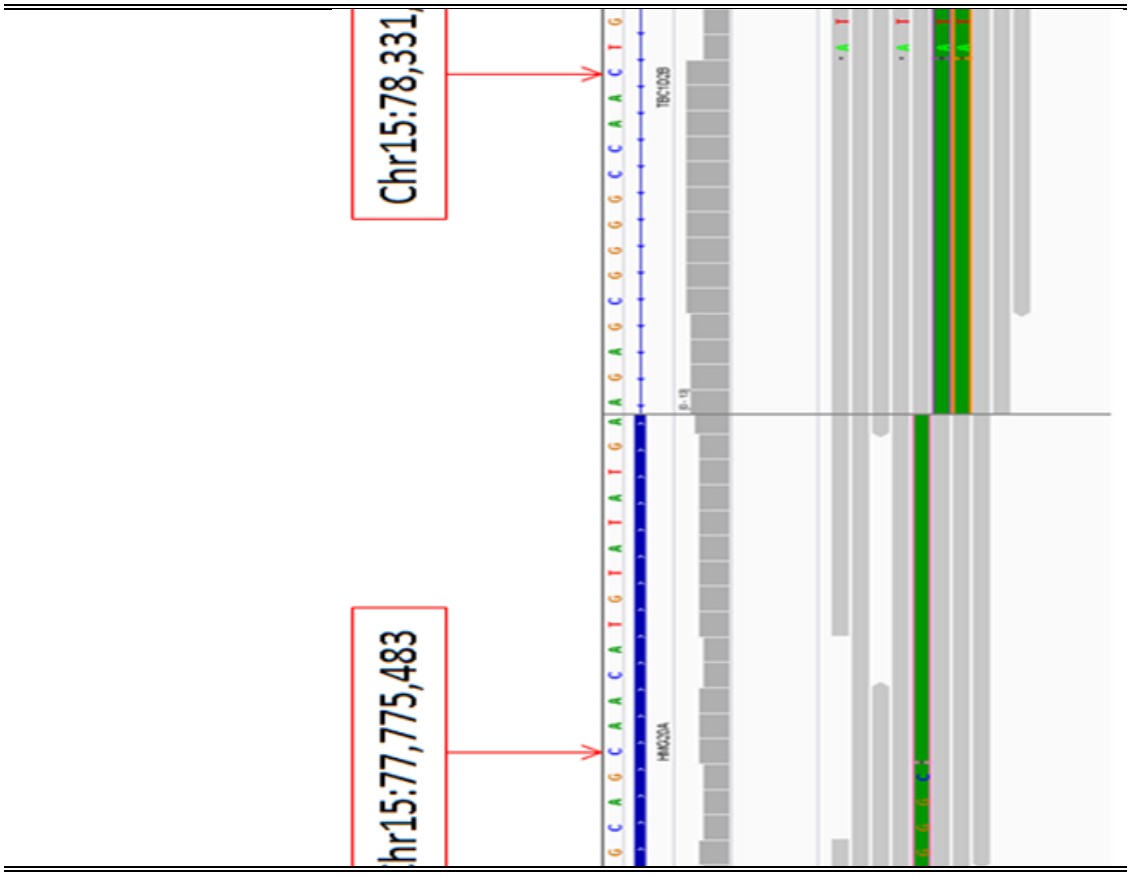

Image demonstrated the single-base pair level coordinates of the breakpoint event detected in 1 and 4 pair read sequences (in green) spanning the breakpoint on each side.

Figure 5-9 Breakpoint region PCR

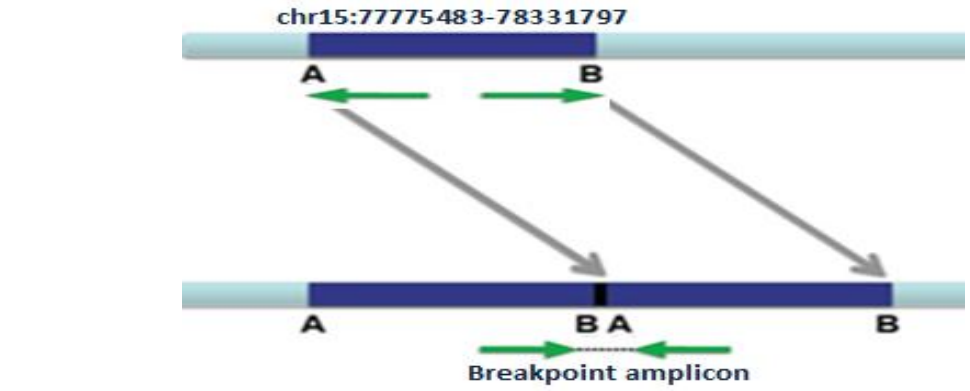

(i)

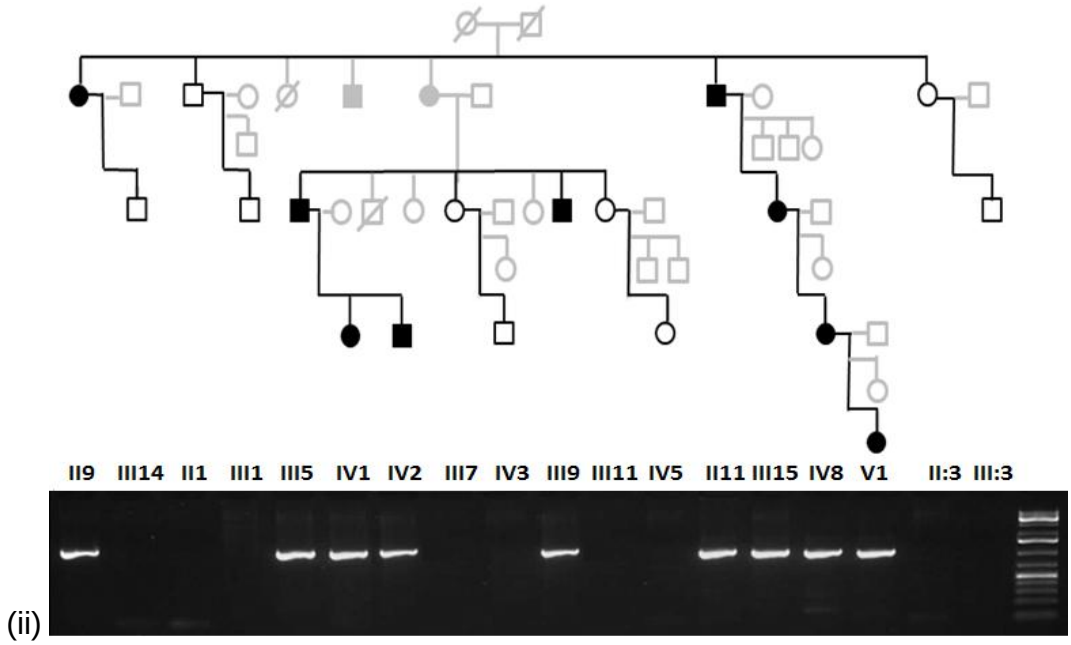

(ii)

(i) illustration shows the principles of primer designing for the breakpoint region. chr15: 77775483-78331797 region (blue bar A-B) flanking sequences were obtained (green arrows). In theory, tandem duplication results in the B sequence being the 5' end or forward primer, and the A sequence (duplicated event) being the reverse primer. Amplification of a PCR product between B and A (lines between green arrows) indicate a tandem duplication; (ii) image is a rearranged pedigree (Figure 5-3) reconfigured to reflect sample loading position for the PCR gel image. As can be seen all eleven affected individuals possess the tandem duplication which is absent in all unaffected family members.

5.2.4 CNV analysis of ET brain samples

In order to assess a possible association between *LINGO1* gene duplication and ET which has been associated to Lingo-1 protein overexpression (Kuo et al., 2011), post-mortem cerebellar samples of ET with Lingo-1 overexpression was obtained from the New York Brain Bank. DNA was extracted from two patients with ET and three patients with Alzheimer's disease and seven age matching controls. Illumina Illumina330K SNP microarray screening of twelve DNA sampled did not identify chromosome 15q24 containing *LINGO1* gene duplication.

5.2.5 Quantitative real-time PCR

The expression level of LINGO1 in blood samples from the DT family was assessed by quantitative real-time PCR. LINGO1 transcript was not expressed in blood of the cases with dystonic tremor, nor in blood of healthy controls compared to endogenous control gene expression (GAPDH, B2M and GUSE) known to be expressed in blood (Real time amplification plot in Appendix 0). This suggests that LINGO1 is not expressed in blood. In order to exclude LINGO1 TaqMan custom probe defects, control brain mRNA was used for quantitative real-time PCR, which showed quantifiable expression of LINGO1.

5.3 Discussion and future work

This chapter describes studies of a multi-generational pedigree with ten individuals affected with adolescent to adult onset DT. Dystonia involved predominantly upper-limbs. Since upper limb and head tremor was the initial symptom and sign along with only mild dystonic posturing (such as “thumbs up” or “dinner fork”) which was only detected in detailed examination by movement disorders specialists, patients were originally misdiagnosed as ET. As previously discussed (Section 1.3.1), ET may be frequently misdiagnosed as DT and therefore these cases again highlight the caveats in the current classification of DT with the requirement of clear dystonic posturing for diagnosis, which in mild cases can be missed on examination leading to misdiagnosis (Deuschl et al., 1998; Quinn et al., 2011). Similar to presented pedigree, tremor has been found to be a prominent clinical feature of other AD dystonias such as DYT24 (Section 1.3.3). Heterozygous mutations in *ANO3* gene results in an asymmetric arm, head and voice tremor without clear dystonic posturing (Stamelou et al., 2013).

All affected individuals presented with isolated tremulous dystonia without other neurological disorders, excluding case II: 11 with combined dystonia and Parkinsonism (Figure 5-3). Since only one case presented with Parkinsonism, further follow-up of the rest affected cases is required before concluding that Parkinsonism may present a late-onset features of the DT syndrome in this pedigree. On the other hand, because the incidence and prevalence of PD increases with advancing age, being present in 1% of people over the age of 65 years, the Parkinsonism in case II: 11 who is the

eldest affected could be idiopathic PD unrelated to this DT condition (Tanner and Goldman, 1996).

Linkage analysis of affected individuals identified co-segregation of chromosome 15q22.31-26.1 with this DT phenotype (Figure 5-5). This locus has not been previously associated with AD dystonia (Table 1-3). Further genetic investigation identified a chromosome 15q24 duplication containing around 12 genes, including *LINGO1* (Figure 5-6). Neither chr15q duplication nor the *LINGO1* gene has previously been suggested as a possible cause of dystonia.

In order to investigate the chromosome 15q24 region further in patients with ET, including *LINGO1* duplication, genomic DNA extracted from the cerebellum of ET patients previously shown to have LINGO1 overexpression and investigated by genome-wide SNP genotyping (Delay et al., 2014). However, no chromosome 15q24 region duplication was identified, excluding *LINGO1* duplication as a cause of increased LINGO1 protein expression in ET patients' cerebellum. On the other hand, it does not exclude the fact that LINGO1 protein overexpression could result from *LINGO1* intronic variants that increase risk of ET (Table 5-1).

LINGO1 expression seems to be very specific to the brain, probably due to its tightly-regulated expression pattern. Consequently, no meaningful regulated LINGO1 expression in blood or fibroblasts has been identified by real-time quantitative PCR (section 5.2.5). This makes correlating sequence variants with transcription levels in patients problematical. Therefore we are undertaking LINGO1 CSF biomarker studies from healthy control individuals,

in order to detect the relative level of LINGO1 in CSF. Five different LINGO1 peptides at a quantifiable level (without any enrichment) have already been detected. The Indian family may indicate that a ~1.5 fold increase in transcription is sufficient to produce DT; hence transcription of *LINGO1* is presumably tightly regulated ordinarily and may be regulated to within a relatively tight window of expression level from person to person. Hence, the detection of LINGO1 peptide variability as a biomarker may help to identify LINGO1 levels relative to other CSF proteins/markers in healthy individuals, and consequently may help to assess altered levels LINGO1 in patients with DT. On the other hand, this is still not an ideal way of correlating with genetic findings, as if the DT mechanism involves increased expression in particular brain regions only, it may still not be overexpressed in CSF.

Recent evidence of LINGO1 overexpression in the cerebellum of ET patients opens an interesting debate about whether *LINGO1* gene dosage effect could contribute to the pathogenesis of DT as well (Kuo et al., 2011; Delay et al., 2014). In the cerebellum, LINGO1 specifically is enriched in the axonal processes of basket cells (BC) (Kuo et al., 2013). BCs are critical for initiation of Purkinje cells (PC) action potentials by delivering GABAergic inhibitory input and modulating PC output (Clark et al., 2005; Foust et al., 2010; Ogawa and Rasband, 2008; Somogyi and Hamori, 1976; Xie et al., 2010). Although a few basket cell axonal terminals provides GABAergic inhibitory input to PC, axonal processes of BCs become abnormally elongated and creates a plexus around PCs as an effect of LINGO1 protein overexpression, as seen in ET cerebellum (Ango et al., 2004; Kuo et al., 2013; Babij et al., 2013). It has been recently suggested that a functionally distorted cerebellar

output due to an abnormal burst firing pattern in PCs may be responsible for tremor occurrence in dystonic patients (Defazio et al., 2013). Moreover, stimulation applied to the main target of cerebellar projections toward thalamus has been reported to improve tremor in patients with dystonia (Hedera et al., 2013).

Since *LINGO1* is a negative regulator for neuronal survival and axonal regeneration, *LINGO1* activating mutations consequently may be expected to be pathogenic. Our genetic data is consistent with this hypothesis as the chromosome 15 duplicated genomic segment, which segregates with the disease phenotype, would be expected to result in an additional (trisomic) intact functional copy of *LINGO1* in all affected family members. While the outcome of the duplication of the other genes located within this region requires further exploration, our data suggests that hypermorphic mutation of *LINGO1* may be the pathogenic cause.

Although further follow-up genetic and functional studies are required, this data suggests that dosage effect of *LINGO1* gene leads to loss cerebellar inhibitory output via increased density of BC processes, and in turn more inhibition of inhibitory PCs. This could lead to dystonic tremor, since cerebellar dysfunction or abnormal interactions of cerebellar and basal ganglia networks has been suggested as a pathogenic mechanism leading to dystonia (Section 1.3.2). In fact, decreased or inhibited cerebellar inhibitory output has been demonstrated to cause postural-, kinetic tremor as well as motor incoordination in *$Gaba_A$ α1* knockout mice (Kralic et al., 2005).

More follow-up investigations are now required in order to validate clinical and genetic findings. Firstly long-term follow-up examinations of all affected could assist to categorize dystonic syndrome into isolated or combined dystonia. Electrophysiological studies are required to characterise the tremor in these patients and define laboratory criteria for the diagnosis of tremor in dystonic patients. Conventional neuroimaging is also required to exclude possible structural abnormalities associated with DT in these cases.

A key genetic follow-up study is screening other families with dystonia or dystonic tremor for chromosome 15q region duplication from South Kerala and other geographic areas, to identify a possible regional specific founder mutation. Further detection of the region or regions that could affect LINGO1 expression levels also required to identify possible transcription factor mutations. Since *LINGO1* is known to be associated with ET, but no coding mutations have been found, transcription factor mutation could be initiator in possible LINGO1 protein overexpression yet to be identified. To confirm this hypothesis, whole genome sequencing of cerebellar samples with LINGO1 protein overexpression, as well as dystonic patients and ET patients with association to *LINGO1* (rs9652490 risk allele), is planned. We may well find in some patients causative rare/de novo sequence variants in/around *LINGO1*. This selective approach to the inclusion criteria of samples for the further exploration of novel/rare variants in and around *LINGO1* may raise a likelihood of identification of the group ‘dystonic tremor’ or ‘essential tremors’ caused by *LINGO1* gene activation, as opposed to other groups with non-*LINGO1* background. This finding also may provide a link between to different phenotypic tremor disorders. Depending on NGS findings, further

transcriptomic studies are required to identify the effect of mutations to LINGO1 transcript level which can finally nail down the genetic basis of the role of *LINGO1* in dystonia, and would represent a major finding. Finally, more postmortem cerebellar tissue investigation of patients with DT is required for LINGO1 protein immunochemistry.

In this study, for the first time we demonstrate *LINGO1* gene copy number gain in DT patients and suggest disease mechanism primarily triggered by *LINGO1* dosage.

6

CHAPTER SIX

APPENDICES

APPENDICES

6.1 Severity of intellectual disability

Severity of intellectual disability

Severity level*	Proportion of individuals with ID ¶	Adaptive skill domains		
		Conceptual domain Δ	Social domain Δ	Practical domain Δ
Mild	85 percent	Children require academic supports to learn skills expected for age. Adults may have difficulties with functional academic skills such as planning, reading, and money management.	Social skills and personal judgement are immature for age. The individual is at risk of being manipulated by others (gullibility).	Most individuals are independent in daily living activities, employable in jobs requiring simple skills, and often able to live independently. They typically need support for making decisions in health care, nutrition, shopping, finances, and raising a family.
Moderate	10 percent	For children, conceptual and academic skills lag well behind those of peers. For adults, academic skills are typically at an elementary level. Complex tasks such as money management need substantial support.	Successful friendships with family/friends are possible using spoken language, but the individual is limited by deficits in social and communicative skills. Social cues, social judgment, social and life decisions regularly need support.	Most individuals are capable of personal care activities with sufficient teaching and support, and achieve independent self-care with moderate supports, such as available in a group home. Adults may be employable in a supported environment.
Severe	3 to 4 percent	Individuals have little understanding of written language, or number, time, and money concepts. Caretakers provide extensive supports for problem-solving.	Individuals benefit from healthy supportive interactions with family/familiar people and may use very basic single words, phrases, or gestures pertinent to their direct experience.	Individuals are trainable in some basic activities of daily living with significant ongoing support and supervision.
Profound	1 to 2 percent	Individuals may use objects in a goal-directed fashion for self-care and recreation.	Although understanding of symbolic communication is very limited, individuals may understand some gestures and emotional cues, and can express themselves non-verbally.	Individuals are typically dependent upon support for all activities of everyday living. Co-occurring sensory or physical limitations are common.

This table paraphrases the severity levels of ID as outlined by the American Psychiatric Association in the Diagnostic and Statistical Manual, 5th Edition (DSM-5). The American Association on Intellectual and Developmental Disabilities (AAIDD) uses a scheme that is similar except that it focuses on support needs, which are classified as intermittent, limited, extensive, and pervasive.

ID: intellectual disability.
* DSM-5-defined categories of severity.
¶ Estimates are based on IQ-derived levels of severity (which differ from DSM-5 defined categories of the same name).
Δ Examples of the needs and supports of each adaptive domain, with increasing categories of severity.

Adapted from the following sources:

1. *American Psychiatric Association. Intellectual Disability (Intellectual Developmental Disorder). In: Diagnostic and Statistical Manual of Mental Disorders, Fifth Edition, American Psychiatric Association.*
2. *American Association of Intellectual and Developmental Disabilities (AAIDD), Definition of Intellectual Disability, available at: http://aaidd.org/intellectual-disability/definition (Accessed on July 11, 2013).*

6.2 Consent form in Malayalam

സമ്മതപത്രം

തിരുവനന്തപുരം മെഡിക്കൽ കോളേജിൽ പാരമ്പര്യനാഡീജന്യ രോഗങ്ങളെക്കുറിച്ച് ഒരു പഠനം നടക്കുന്ന വിവരം ഞാൻ ഡോക്ടറിൽ നിന്നും അറിയുകയുണ്ടായി. രോഗത്തിന്റെ അവസ്ഥ മനസ്സിലാക്കുന്നതിലേയ്ക്കായി ഡി.എൻ.എ പരിശോധനയ്ക്ക് ഒരു ചെറിയ അളവിലുള്ള (10 ml) രക്തം എടുക്കുന്നു എന്നും അറിയിച്ചിട്ടുണ്ട്. ഈ പഠനത്തിന്റെ ഭാഗമായി പുതിയതായി മരുന്നുകളോ ചികിത്സയോ ഒന്നും എന്നിൽ പരീക്ഷിക്കുന്നതല്ല എന്നും, ഈ പഠനവുമായി ഞാൻ സഹകരിച്ചില്ലെങ്കിലും എന്റെ ചികിത്സയിൽ ഒരുമാറ്റവും വരുത്തുന്നതല്ല എന്നും എന്നെ അറിയിക്കുകയുണ്ടായി. ഈ വസ്തുതകളെല്ലാം മനസ്സിലാക്കിക്കൊണ്ട് ഈ പഠനത്തിൽ പങ്കുചേരാൻ ഞാൻ എന്റെ സമ്മതം അറിയിക്കുന്നു.

ആത്മാർത്ഥതയോടെ

രോഗിയുടെ പേര് : .....

ഒപ്പ് : .....

ഡോക്ടറുടെ പേര് : .....

ഒപ്പ് : .....

സ്ഥലം : .....

തീയതി : .....

Translation: I was informed by the doctor that a study is underway on familial neurological deceases and consent was requested for partaking in the study. I was informed that a blood sample may be collected for genetic testing and my pictures taken as part of the study may be used for publication. I was informed that I can withdraw at any point of the study and it will not have any effect on my treatment process. Also I was informed that no new treatment method of medication will be tested on me. Understanding the fact I am providing my willingness to partake in the study Sincerely Sign Place & date.

6.3 Web links for performed protocols

1. Link to DNA extraction guide:

https://www.promega.co.uk/~/media/files/resources/protocols/technical%20manuals/101/reliaprep%20blood%20gdna%20miniprep%20system%20protocol.pdf

2. Link to RNA extraction guide:

http://www.preanalytix.com/sites/default/files/handbooks/PAXgene-Blood-RNA-Kit-Handbook-Version-2-EN_FDA_762164.pdf

3. Link to SNP genotyping protocol:

https://support.illumina.com/content/dam/illumina-support/documents/myillumina/67f59f89-51ee-44d6-b1bb-a53dcb5bd01e/infinium_hd_ultra_user_guide_11328087_revb.pdf.

4. Link for MERLIN software tutorial:

http://csg.sph.umich.edu/abecasis/Merlin/tour/parametric.html

5. Link for DNA extraction from brain samples:

https://www.qiagen.com/us/shop/sample-technologies/dna-sample-technologies/genomic-dna/magattract-hmw-dna-kit-48/

6. Link for BigDye XTerminator® purification kit protocol:

https://www3.appliedbiosystems.com/cms/groups/mcb_support/documents/generaldocuments/cms_042772.pdf

6.4 Next generation sequencing-genomic library preparation

Incubations and PCR reactions was performed on DNA Engine Tetrad, NGS lab. First day of experiment stock gDNA (III: 15 from figure 5-3 pedigree) of volume ~ 20 µl was re-quantified using Qubit assay (1 µl gDNA used in dsDNA BR): concentration 290ng/µl, total 5510 ng, input volume 10.34, and input 2998.6 ng. DNA shearing: ~3 µg gDNA (10.34 µl stock) diluted to 80 µl total volume with TE in Anachem lo-bind tube; fragmented 11 minutes, low power (6-place head, MolGen Bioruptor). DNA purified on 120 µl AMPure, eluted in 50 µl ddH2O. Fragmented DNA analysed on Agilent Tapestation 2200 (D1000 screen tape).

On the next step purified ligation product was mixed directly with 10 µl gel loading buffer and run on 1.2% prep gel (5.5 h @70 V). Then gel slices were excised in a range of 400-450 bp (library 'a') and 450-500 bp (library 'b', back-up sample). DNA was purified using Qiagen QIAquick gel extraction kit (code 28704) and eluted in 30 µl EB. Product then was analyzed on Agilent Tapestation 2200 (HS D1000 screentape).

On the last step, amplification was performed using 50 ng adapter-ligated DNA in 50 µl reaction. The adapters are standard Illumina paired-end adapters, except that they are made by Sigma for a fraction of the cost. DNA was purified on 90 µl AMPure beads and eluted in 30 µl water. Libraries underwent preliminary quantitation by Qubit assay (dsDNA HS; Life Technologies). 2 µl aliquots were then diluted to ~2 ng/µl and run in duplicate on HS D1000 screentape. Both libraries have amplified as expected -

sequencing carried out on library WG_06a. Library WG_06a was diluted to give ~10 nM final concentration. The diluted library was re-analyzed in triplicate (as 2x dilution) on HS D1000 screentape for the size selection.

Genomic library preparation workflow

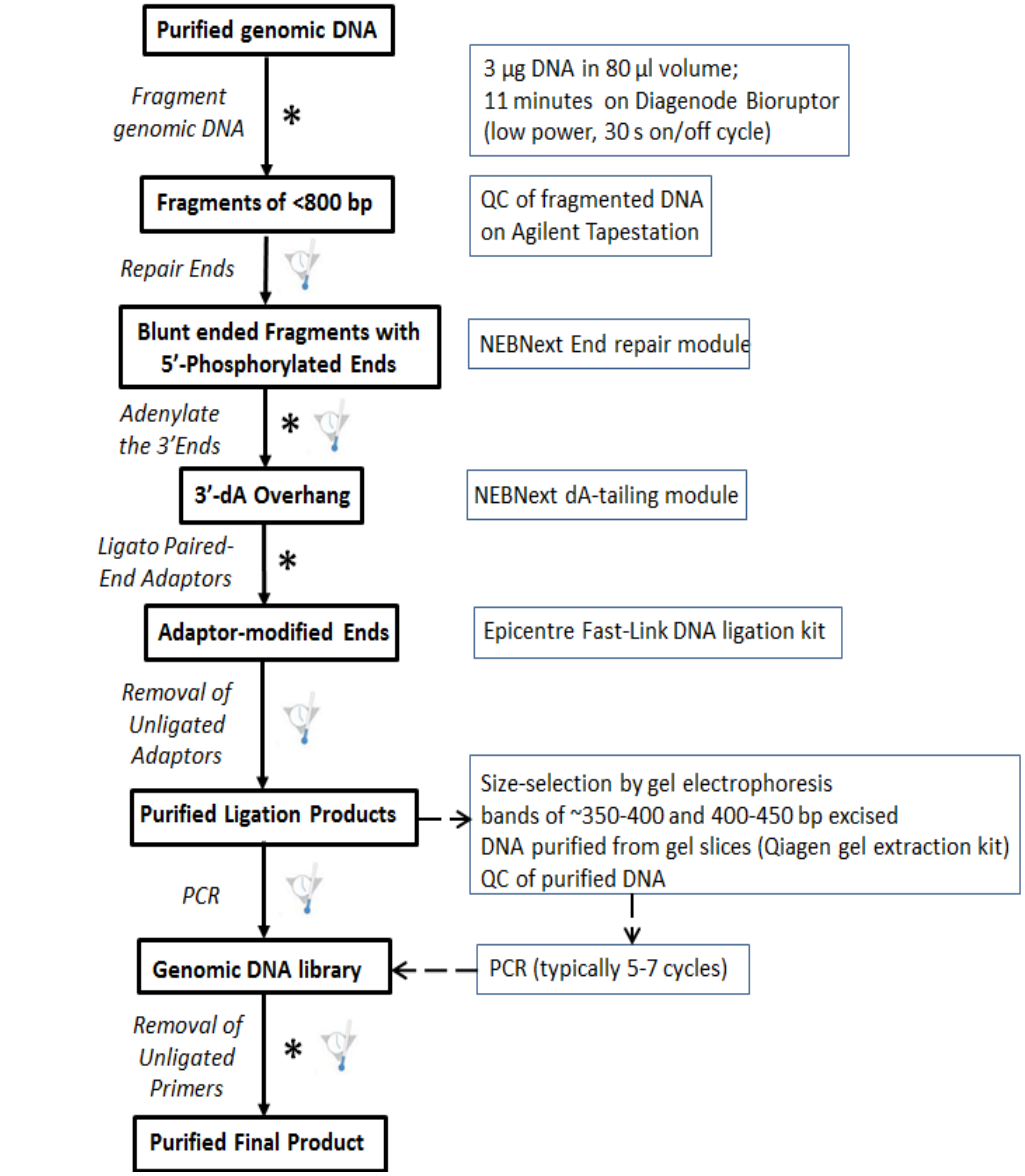

* purification step using AMPureXP SPRI beads
From an Illumina library prep manual, with some exceptions (e.g. the gel purification step, usage of alternative reagents for flexibility etc.,)

6.5 Antibodies, plasmids, cell culture and recombinant PNGase F treatment of MFSD2A

A polyclonal MFSD2A antibody was raised in rabbits against the c-terminal peptide H-CSDTDSTELASIL-OH (NeoMPS, San Diego, CA). Serum was purified on polyA/G resin followed by affinity purification against the peptide immobilized on Sulfolink resin (ThermoScientific). Other antibodies used in these studies were β-actin (Sigma), Tom20 (Santa Cruz), Cox4 (Cell Signal), and UCP1 (Abcam).

Human *MFSD2A* cDNA was subcloned into pcDNA3.1 Mammalian Expression Vector (Invitrogen), which were then expressed in Human Embryonic Kidney 293 cells (HEK293 cells).

HEK293 cells are a specific cell line originally derived from human embryonic kidney. Mycoplasma negative HEK293 cells were ordered from the American Type Culture Collection. HEK293 cells were cultured in DMEM (Invitrogen) with 10% fetal bovine serum and penicillin/streptomycin at 37°C with 5% CO_2. Sub-confluent cells were transiently transfected for 12 hours using Lipofectamine 2000 (Invitrogen) 24–48 hours prior to experimentation (Berger et al., 2012).

Glycosylation is among the most abundant of all post-translational modifications (Khoury et al., 2011). The glycosidase PNGase F is used extensively for studying glycoproteins. First isolated from *Elizabethkingia miricola*, PNGase F catalyzes the cleavage of N-linked oligosaccharides between the innermost GlcNAc and asparagine residues of high mannose, hybrid and complex oligosaccharides from N-linked glycoproteins (Elder and

Alexander, 1982). For treatment with PNGase F, 1 µl of 10× Glycoprotein Denaturing Buffer (New England BioLabs), 2 µl of 10× G7RB, 2 µl of 10% NP-40 and 1,000 U of PNGase F (New England BioLabs) were added to 7 µl of HEK293 whole-cell lysate (30 µg protein). The reaction was incubated for 2 h at 37 °C.

6.6 MFSD2A protein turnover assays and protein extraction

For a protein turnover, cycloheximide (0.1 µg/µl) in fresh media was added to wells at the beginning of an experiment. Where indicated, 100 µM chloroquine (in H_2O) or 10 µM MG-132 (in DMSO) was added 2 hours prior to addition of cycloheximide and maintained in the media throughout the end of the experiment. To biotinylate surface proteins, cells were washed on ice three times with cold phosphate buffered saline (PBS) and incubated with freshly made maleimide-PEG_2-Biotin (ThermoScientific) in PBS for one hour. Excess biotin was washed away three times in cold PBS with 1 mM dithiothreitol.

Cell cultures were ground with a dounce homogenizer on ice in RIPA buffer with EDTA-free cOmplete protease inhibitor cocktail (Roche) and then cell cultures were washed with cold PBS and scraped with cold RIPA buffer. Protein concentration was measured with a Bradford assay (BioRad). Equal volumes of protein extract and streptavidin agarose slurry (Pierce ThermoScientific) were mixed and washed three times. Samples were rotated overnight at 4°C, washed three times, and mixed with a volume of SDS-Laemmli buffer. The supernatant was analyzed by SDS-PAGE.

6.7 Immunoblotting and immunohistochemistry

Immunoblotting is a technique that uses antibodies to identify target proteins among a number of unrelated protein species. It involves identification of protein target via antigen-antibody specific reactions. Proteins are typically separated by electrophoresis and transferred onto nitrocellulose membranes. Immunofluorescence microscopy is a method to assess both the localization and endogenous expression levels of proteins of interest. It utilizes fluorescent-labeled antibodies to detect specific target antigens.

PNGase treated and untreated HEK293 whole-cell extracted protein samples (40 µg protein/lane) were separated by SDS-PAGE. Then samples were transferred to nitrocellulose membranes (Bio-Rad) and incubated overnight with above described rabbit polyclonal antibody against *MFSD2A.* Immunoblots were quantified; with data representing means ± s.e.m. Statistical analysis was performed using a Student's *t* test.

Cells were fixed with 4% paraformaldehyde (PFA) at 4 °C overnight, cryopreserved in 30% sucrose and frozen in TissueTek OCT (Sakura) and blocked with 5% goat serum, permeabilized with 0.5% Triton X-100. Then stained with the following primary antibodies: α-MFSD2A (1:500; Cell Signaling Technologies (under development)) (green in colour) and hoechst 33342 (eBioscience) for nuclei staining (blue in colour).Slides were mounted in Fluoromount G (EMS) and visualized by epifluorescence, light, or confocal microscopy. Scale bars, 10 µm.

6.8 Transport assay

Radiolabeled LPC-[^{14}C]DHA (docosahexaenoate), LPC-[^{14}C]oleate and LPC-[^{3}H]palmitate were purchased from Avanti Polar Lipids. Non-radiolabeled LPC-DHA was synthesized as described previously (Berger et al., 2012). Uptake assays of radiolabelled LPCs (fluorescent LPCs) were tested using HEK293 cells overexpressing WT) or mutant (Ser339Leu) MFSD2A.

HEK293 cells at 90–95% confluency were transfected using lipofectamine 2000 (invitrogen) with pcDNA3.1Mfsd2a (WT), pcDNA3.1Mfsd2a (Ser339Leu), or pcDNA3.1 (mock) plasmids as described above. For concentration and time dependent assays, 24 h post transfection of those HEK293 cells plasmids were washed once with serum-free pre-warmed DMEM medium before addition of a mixture of 25 μM radiolabelled LPC palmitate and 250 μM cold competitors, which were dissolved in 12% BSA. Total BSA concentration was kept constant in samples with or without cold competitors. Assays were performed at 37 °C for 30 min. The reduced reaction time was necessary in order to limit potential negative effects of detergents and bioactive lipids on cell survival. Experiments were performed in 12-well plates with triplicates and at 37 °C. Uptake activity is expressed in dpm per well. For sodium dependent assay, radiolabelled LPCs were diluted in transport buffer (5 mM KCl, 10 mM Hepes, pH 7.4) with 150 mM NaCl or 150 mM choline chloride. For sodium concentration dependent assays, any reductions in the concentration of NaCl were replaced by choline chloride in order to maintain a constant cation molarity of 150 mM.

To prepare LPC palmitate dissolved in ethanol, 0.75 µCi LPC [^{3}H]palmitate were diluted in LPC palmitate in chloroform. Mixture was dried and dissolved in 50 µl ethanol before adding 6ml of transport buffer with 150 mM sodium as described above to have 50 µM LPC palmitate. To prepare LPC palmitate micelles, 0.75 µCi LPC [^{3}H]palmitate was diluted in LPC palmitate in chloroform. This mixture then was dried and dissolved in 6 ml of transport buffer with 150 mM sodium to have 100 µM LPC palmitate and sonicated on ice for 5 min. Activated charcoal was added and spun to remove the monomers of LPC palmitate. Transport assays were similarly performed with HEK293 cells overexpressing with pcDNA3.1MFSD2A or pcDNA3.1plasmid as control for 30 mins at 37 °C (Nguyen et al., 2014b).

6.9 Lipidomic analysis of plasma samples

Extracting lipids from the complex biological system is usually the first step for lipid analysis. After extraction, the proteins and some minerals are removed, therefore, the biological system becomes simple, which facilitates lipid analysis. A simple and reproducible extraction method is necessary for cross-validation of lipid data obtained in different laboratories. Hence, a methanol-based protocol which only utilizes a single methanol (MeOH) solvent and involves a single step of centrifugation was used for lysophospholipids extraction (Zhao and Xu, 2010).

A single and duplicate plasma samples each for 4 affected- II: 3, III: 2, III: 3, III: 4, 2 unaffected- II: 1 and III: 5 (pedigree on the figure 7), were used for LPC analysis. Plasma samples from 34 age-matched healthy children (male and female) between 0.1 and 18 years old (mean = 4.3 years, s.d. = ±4.4 years), and II: 1 (father) and III: 5 unaffected sibling in the pedigree were used as controls. All extractions were performed either in siliconized tubes or in glass tubes. 2 µl plasma samples were resuspended in 198 µl of methanol containing 453 pmol/ml LPC 20:0 as an internal standard (Avanti Polar Lipids) and were then vortexed for 30 s and sonicated for 30 min on ice. Then samples were centrifuged at 20,000g for 10 min at 4 °C to remove debris. 2 µl from each supernatant was injected into a liquid chromatography–tandem mass spectrometry (LC-MS/MS) instrument.

Mass spectrometry (MS) is the most important technology for lipid analysis. The targeted MS lipids analysis focuses on known lipids, and develops a

specific method with a high sensitivity for the quantitative analysis of these specific lipids.

To identify a surrogate measurement for defective LPC transport, plasma LPC concentrations in several of the patients, their unaffected siblings and random age-matched controls living in the same geographical region as the affected family members were measured using a targeted MS approach. Samples were randomized for injection into the LC-MS/MS instrument. Each sample was analyzed in technical duplicates. Analysis for each sample was followed by injection with a blank to avoid carry-over. The stability of the signal throughout the analysis was monitored by regular injection of a quality control sample. Chromatographic analysis was undertaken on a 1290 Liquid Chromatography System (Agilent Technologies) using a Kinetex HILIC stationary phase (Phenomenex). The dimentions were: column length-150 mm; column internal diameter-2.1 mm; particle size-2.6 µm; pore size-100Å.

Gradient elutions were performed with two solvents, A and B. Solvent A consists 95% acetonitrile, 5% 10 mM ammonium formate and 0.1% formic acid, and solvent B contains 50% acetonitrile, 50% 10 mM ammonium formate and 0.1% formic acid. A gradient was ranged from 0.1 to 75% solvent B in 6 min, 75 to 90% solvent B in 1 min, and 90 to 0.1% solvent B in 0.1 min followed by 0.1% solvent B for 3 min. Total run time was 10.1 min. Under these conditions, LPC species elute in ~4.9 min with a flow rate of 0.5 ml/min.

There are several detection modes in a 6460 triple quadrupole MS (Agilent Technologies). Multiple Reaction Monitoring (MRM) mode was used for LPC

species quantification with gas temperature of 300 °C, gas flow of 5 l/min, sheath gas flow of 11 l/min and capillary voltage of 3,500 V. MRM transitions were from precursor ions to the choline head fragment (mass/charge ratio (m/z) = 184) with a collision energy of 29 V. 36 transitions were monitored simultaneously with a dwell time of 20 ms. Quantification data were extracted using MassHunter Quantitative Analysis (QQQ) software, and data were manually curated to ensure correct peak integration. Areas under the curve (AUCs) for the extracted ion chromatogram peaks for each MRM transition and lipid species were normalized to an internal standard. The total LPC concentration and concentrations for individual LPC species from human samples are expressed in μM. A Mann-Whitney non-parametric, non-paired, two-tailed t test was used to determine statistical significance.

6.10 Fluorescence in sity hybridization (FISH)

In FISH, a fluorophore labeled probe is hybridized to the targeted DNA sequence, enabling it to be efficiently tracked by fluorescence microscopy. Homogeneous DNA probes are hybridized to fixed pro-metaphase as well as interphase chromosome spreads on a glass slide.

Probe designing as well as FISH analysis were performed by the investigators at the Microarrays and Molecular Genotyping Department, St Georges NHS Hospital Trust. In order to increase the resolution (<1Mb), blood cultures were harvested at the more extended pro-metaphase chromosomal cycles. Simultaneously 100 interphase cells on the same slide were analyzed where a proportion of interphase nuclei show three distinct signals supporting array finding of duplication. In pro-metaphase, hybridized probe for one particular chromosomal region is seen as a double signal indicating presence of both chromatids. In case of tandem duplication, one of the chromosomal signals has greater intensity compared to other, while in case of the deletion only one signal can be seen. The advantage of the FISH is that it can sufficiently identify whether the investigated gene is involved in duplication or deletion by targeting it with pre-designed probes.

In case of the chromosomal translocations different fluorescent dyes were used for the different DNA probes simultaneously for the cases of suspected translocations (from microarray data) to identify specific sequences in relation to each other. In some cases fluorophore dyes were used for labeling the centromere of chromosomes in cases of chromosomal

translocations in order to distinguish the chromosomes from each other under the microscope. The advantage of the FISH analysis over microarray analysis (quantification of genotypes), is that it can detect whether one of the parent of affected with unbalanced translocation carries a balanced translocation, which will explain the inheritance pattern of the chromosomal aberration.

6.11 Primers

Whole exome sequencing analysis of both V: 1 and IV: 2 affected family members with dystonic tremor (Figure 5-3) revealed 19 potentially deleterious variants. Primers (below) were designed for co-segregation analysis.

Primers for the 19 gene variants identified from the WES analysis

Variant Position	Primer Name	Primer Sequence (5'-3')	Primer Length	Prod. Size (bp)
Chr2:99722076	Chr2:99722076-F	GCTGCATGCATGTTGATGTA	20	390
	Chr2:99722076-R	TGCTGTCTCTTGAGCAATCTG	21	
Chr2:101014379	Chr2:101014379-F	CGCCTGGAACTCATCAGAAA	20	282
	Chr2:101014379-R	GTCAAACCAGCCCTCTTGTG	20	
Chr3:122632502	Chr3:122632502-F	AAAGTGGCCTGGATTCTCCT	20	399
	Chr3:122632502-R	TTGCACGTCTTGAACTCCTG	20	
Chr4:106967749	Chr4:106967749-F	GCTCACCTTGTGAAGATGAAA	21	219
	Chr4:106967749-R	ACGGAAATGCAACAATCTGG	20	
Chr5:112176900	Chr5:112176900-F	GCTCCCAAATAATGAAGATAGAGTC	25	246
	Chr5:112176900-R	TTAGCTGATTGTTGGTTGGAG	21	
Chr5:133326592	Chr5:133326592-F	GCACCGAGATTACTGTGGAAG	21	226
	Chr5:133326592-R	CCACCTGCAACATCAGAGAA	20	
Chr5:180582411	Chr5:180582411-F	TGGCATACAAATTGGCCTCT	20	274
	Chr5:180582411-R	GGCCAGCTTCAACAAGGATA	20	
Chr6:35428390	Chr6:35428390-F	GGGAGTTGGAGCAGCAGATA	20	242
	Chr6:35428390-R	CCTCCATGCACTGAAGGACT	20	
Chr6:57013144	Chr6:57013144-F	TTTCCAGTAATAGAGACCAGTAACCA	26	226
	Chr6:57013144-R	GCTGCTCCTCCTCATCACTC	20	
Chr7:5643038	Chr7:5643038-F	ATGGACCTGTCTGCCAATCA	20	255
	Chr7:5643038-R	AAGTAGCAGCTGGCATTCCT	20	
Chr7:6470196	Chr7: 6470196-F	CAACGAAGGAGCAGGAAGAG	20	283
	Chr7: 6470196-R	AAGGGAAATATGGCTATGGAG	21	
Chr8:145980092	Chr8:145980092-F	GAGTTCTCCCCACTGAAGGTAA	22	205
	Chr8:145980092-R	CACGGCTCCAGAGGAGAGTA	20	
Chr14:22309851	Chr14:22309851-F	CAGCAACAGTGCTTCTCAGTCT	22	245
	Chr14:22309851-R	CCAGCAGGTTTGGGTACAGA	20	
Chr14:23947231	Chr14:23947231-F	GCCCTTCCCTCTAGATGTCC	20	218
	Chr14:23947231-R	TTCCACATGTCCAAAGCAAA	20	
Chr14:55462336	Chr14:55462336-F	TGAGTTTTTCTAAATCATTCACTTTTA	27	385
	Chr14:55462336-R	TTTCCTCTAAGCACCACTTAGC	22	
Chr15:49030501	Chr15:49030501-F	TCATAAGGCTGATAGATTAAAGTCAGA	27	244
	Chr15:49030501-R	AAAGAGGCAGGGCTCACAAT	20	
Chr16:88783601	Chr16:88783601-F	GAGAATGCGGTTGTGTGACC	20	268
	Chr16:88783601-R	CACATGCTCACCTCATAGCC	20	
Chr18:6997812	Chr18:6997812-F	TTGTCTTGTAGCCTGTGATGATG	23	246
	Chr18:6997812-R	GGGAGGACACATGGAATGAC	20	
Chr22:47188431	Chr18:47188431-F	TCCTTCAGTCCTGTGGGTTC	20	283
	Chr18:47188431-R	GAAACCAGTCTCCTCCCTGA	20	

EBNA1BP2 chr1:43637996A>T variant primers

FORWARD PRIMER	5'-TCTGCTGAAGACCAAGGCAG-3'
REVERSE PRIMER	5'-AGGACACAATCACGGTCACT-3'

TIF1 intronic variant chr1:43771019A/- primers

FORWARD PRIMER	5'- GAAAACCAGGCCGCTGAC-3'
REVERSE PRIMER	5'- ACAGAAGGAAGGCAGCTCAG-3'

SLC2A1 gene primers

FORWARD PRIMER FOR EXON 1	5'-GTCGGAGTCAGAGTCGCAG-3'
REVERSE PRIMER FOR EXON 1	5'-GTAAGGCGGGCAGGAGTC-3'
FORWARD PRIMER FOR EXON 2	5'-CCTGCCCTGTAGTAACCTGC-3'
REVERSE PRIMER FOR EXON 2	5'-GCATGTGTGATGTGCAACAG-3'
FORWARD PRIMER FOR EXON 3&4	5'-GGAAAAGGAAGACTGGGTCC-3'
REVERSE PRIMER FOR EXON 3&4	5'-AGATCCGAGAGCCACTGAAG-3'
FORWARD PRIMER FOR EXON 5&6	5'-CACAAAGTAGGGAAGGCCAC-3'
REVERSE PRIMER FOR EXON 5&6	5'-ACACTTGACCAGAGGGCTTG-3'
FORWARD PRIMER FOR EXON 7&8	5'-GGTCCCACATCCACTGCTAC-3'
REVERSE PRIMER FOR EXON 7&8	5'-TATGAAGCCCAGGCAAACTC-3'
FORWARD PRIMER FOR EXON 9	5'-CAGGAGCAGCTACCCTGGAT-3'
REVERSE PRIMER FOR EXON 9	5'-CCCGCACGCATGACCCCACA-3'
FORWARD PRIMER FOR EXON 10	5'-ACAGCCAGGATGTAGGGTC-3'
REVERSE PRIMER FOR EXON 10	5'-GGTTTGGAAGTCTCATCCAGC-3'

MFSD2A transcript primers

Forward primer for *MFSD2A* cDNA	5'-TGCTGTCATCCTGATCCTGG-3'
Reverse primer for *MFSD2A* cDNA	5'- AATGACATCAGGCAGCATGG-3'
Product size 465 bp	

MFSD2A 40433304C>T variant primer

Forward primer	5'-TCAGAGGTTTGAGAGGGCAG-3'
Reverse primer	5'-TCCCCAGTTTTGAAGCTCCT-3'
PCR product size	571 bp

6.12 Real time amplification plot

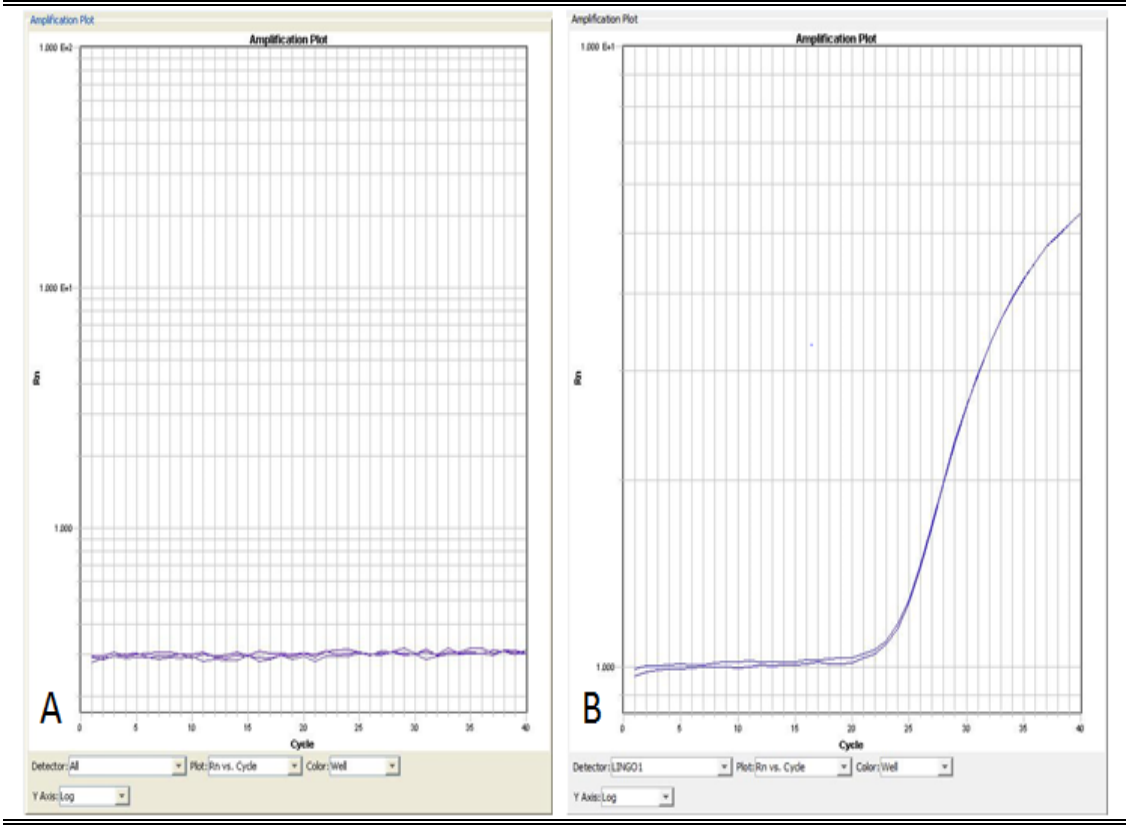

PCR amplifications plot on the ABI 7900HT platform (Life technologies, Foster City, USA). A demonstrated LINGO1 transcript expression in blood of cases with dystonic tremor. Absence of upsloping curve shows that there is no quantifiable expression of Lingo1 transcript in blood. (B) LINGO1 expression in sample from post-mortem hippocampus, with significant expression that gradually builds up exponentially along with increased amplification.

BIBLIOGRAPHY

American Speech-Language-Hearing Association 1993. Definitions of communication disorders and variations. Ad Hoc Committee on Service Delivery in the Schools. American Speech-Language-Hearing Association. *ASHA Suppl,* 35**,** 40-1.

The International HapMap Project 2003. The International HapMap Project. *Nature,* 426**,** 789-96.

ABBRUZZESE, G., MARCHESE, R., BUCCOLIERI, A., GASPARETTO, B. & TROMPETTO, C. 2001. Abnormalities of sensorimotor integration in focal dystonia: a transcranial magnetic stimulation study. *Brain,* 124**,** 537-45.

ABECASIS, G.R., ALTSHULER, D., AUTON, A., BROOKS, L.D., DURBIN, R.M., GIBBS, R.A., HURLES, M.E. & MCVEAN, G.A. 2010. A map of human genome variation from population-scale sequencing. *Nature,* 467**,** 1061-73.

ABECASIS, G.R., CHERNY, S.S., COOKSON, W.O. & CARDON, L.R. 2002. Merlin--rapid analysis of dense genetic maps using sparse gene flow trees. *Nat Genet,* 30**,** 97-101.

AITMAN, T.J., DONG, R., VYSE, T.J., NORSWORTHY, P.J., JOHNSON, M.D., SMITH, J., MANGION, J., ROBERTON-LOWE, C., MARSHALL, A.J., PETRETTO, E., HODGES, M.D., BHANGAL, G., PATEL, S.G., SHEEHAN-ROONEY, K., DUDA, M., COOK, P.R., EVANS, D.J., DOMIN, J., FLINT, J., BOYLE, J.J., PUSEY, C.D. & COOK, H.T. 2006. Copy number polymorphism in Fcgr3 predisposes to glomerulonephritis in rats and humans. *Nature,* 439**,** 851-5.

ALAKBARZADE, V., HAMEED, A., QUEK, D.Q.Y., CHIOZA, B.A., BAPLE, E.L., CAZENAVE-GASSIOT, A., NGUYEN, L.N., WENK, M.R., AHMAD, A.Q., SREEKANTAN-NAIR, A., WEEDON, M.N., RICH, P., PATTON, M.A., WARNER, T.T., SILVER, D.L. & CROSBY, A.H. 2015. A partially inactivating mutation in the sodium-dependent lysophosphatidylcholine transporter MFSD2A causes a non-lethal microcephaly syndrome. *Nat Genet,* advance online publication.

ALBANESE, A. 2003. The clinical expression of primary dystonia. *J Neurol,* 250**,** 1145-51.

ALBANESE, A., BHATIA, K., BRESSMAN, S.B., DELONG, M.R., FAHN, S., FUNG, V.S., HALLETT, M., JANKOVIC, J., JINNAH, H.A., KLEIN, C., LANG, A.E., MINK, J.W. & TELLER, J.K. 2013. Phenomenology and classification of dystonia: a consensus update. *Mov Disord,* 28**,** 863-73.

ALCANTARA, D. & O'DRISCOLL, M. 2014. Congenital microcephaly. *Am J Med Genet C Semin Med Genet,* 166C**,** 124-39.

ALKAN, C., COE, B.P. & EICHLER, E.E. 2011. Genome structural variation discovery and genotyping. *Nat Rev Genet,* 12**,** 363-76.

ALKURAYA, F.S. 2012. Discovery of rare homozygous mutations from studies of consanguineous pedigrees. *Curr Protoc Hum Genet,* Chapter 6**,** Unit6 12.

ALMASY, L., BRESSMAN, S.B., RAYMOND, D., KRAMER, P.L., GREENE, P.E., HEIMAN, G.A., FORD, B., YOUNT, J., DE LEON, D., CHOUINARD, S., SAUNDERS-PULLMAN, R., BRIN, M.F., KAPOOR, R.P., JONES, A.C., SHEN, H., FAHN, S., RISCH, N.J. & NYGAARD, T.G. 1997. Idiopathic torsion dystonia linked to chromosome 8 in two Mennonite families. *Ann Neurol,* 42**,** 670-3.

ALVAREZ-BUYLLA, A. & TEMPLE, S. 1998. Stem cells in the developing and adult nervous system. *J Neurobiol,* 36**,** 105-10.

ANDERSON, R. 2010. Multiplex fluorescence in situ hybridization (M-FISH). *Methods Mol Biol,* 659**,** 83-97.

ANDREONE, B.J., LACOSTE, B. & GU, C. 2015. Neuronal and vascular interactions. *Annu Rev Neurosci,* 38**,** 25-46.

ANGO, F., DI CRISTO, G., HIGASHIYAMA, H., BENNETT, V., WU, P. & HUANG, Z.J. 2004. Ankyrin-based subcellular gradient of neurofascin, an immunoglobulin family protein, directs GABAergic innervation at purkinje axon initial segment. *Cell,* 119**,** 257-72.

ANKALA, A., TAMHANKAR, P.M., VALENCIA, C.A., RAYAM, K.K., KUMAR, M.M. & HEGDE, M.R. 2015. Clinical applications and implications of common and founder mutations in Indian subpopulations. *Hum Mutat,* 36**,** 1-10.

ARGYELAN, M., CARBON, M., NIETHAMMER, M., ULUG, A.M., VOSS, H.U., BRESSMAN, S.B., DHAWAN, V. & EIDELBERG, D. 2009. Cerebellothalamocortical connectivity regulates penetrance in dystonia. *J Neurosci,* 29**,** 9740-7.

ARMULIK, A., GENOVE, G., MAE, M., NISANCIOGLU, M.H., WALLGARD, E., NIAUDET, C., HE, L., NORLIN, J., LINDBLOM, P., STRITTMATTER, K., JOHANSSON, B.R. & BETSHOLTZ, C. 2010. Pericytes regulate the blood-brain barrier. *Nature,* 468**,** 557-61.

ASHWAL, S., MICHELSON, D., PLAWNER, L. & DOBYNS, W.B. 2009. Practice parameter: Evaluation of the child with microcephaly (an evidence-based review): report of the Quality Standards Subcommittee of the American Academy of Neurology and the Practice Committee of the Child Neurology Society. *Neurology,* 73**,** 887-97.

ASSOCIATION, A.P. (ed.) 2013. *Diagnostic and Statistical Manual of Mental Disorders, Fifth Edition* American Psychiatric Publishing.

AURELI, M., GRASSI, S., PRIONI, S., SONNINO, S. & PRINETTI, A. 2015. Lipid membrane domains in the brain. *Biochim Biophys Acta,* 1851**,** 1006-16.

BABIJ, R., LEE, M., CORTES, E., VONSATTEL, J.P., FAUST, P.L. & LOUIS, E.D. 2013. Purkinje cell axonal anatomy: quantifying morphometric changes in essential tremor versus control brains. *Brain,* 136**,** 3051-61.

BAHL, S., VIRDI, K., MITTAL, U., SACHDEVA, M.P., KALLA, A.K., HOLMES, S.E., O'HEARN, E., MARGOLIS, R.L., JAIN, S., SRIVASTAVA, A.K. & MUKERJI, M. 2005. Evidence of a common founder for SCA12 in the Indian population. *Ann Hum Genet,* 69**,** 528-34.

BAILEY, J.A., GU, Z., CLARK, R.A., REINERT, K., SAMONTE, R.V., SCHWARTZ, S., ADAMS, M.D., MYERS, E.W., LI, P.W. & EICHLER, E.E. 2002. Recent segmental duplications in the human genome. *Science,* 297**,** 1003-7.

BALINT, B. & BHATIA, K.P. 2014. Dystonia: an update on phenomenology, classification, pathogenesis and treatment. *Curr Opin Neurol,* 27**,** 468-76.

BARRETTE, B., VALLIERES, N., DUBE, M. & LACROIX, S. 2007. Expression profile of receptors for myelin-associated inhibitors of axonal regeneration in the intact and injured mouse central nervous system. *Mol Cell Neurosci,* 34**,** 519-38.

BATTAGLIA, A., CAREY, J.C., VISKOCHIL, D.H., CEDERHOLM, P. & OPITZ, J.M. 2000. Wolf-Hirschhorn syndrome (WHS): a history in pictures. *Clin Dysmorphol,* 9**,** 25-30.

BATTAGLIA, A., FILIPPI, T. & CAREY, J.C. 2008. Update on the clinical features and natural history of Wolf-Hirschhorn (4p-) syndrome: experience with 87 patients and recommendations for routine health supervision. *Am J Med Genet C Semin Med Genet,* 148C**,** 246-51.

BELL, R.D., WINKLER, E.A., SAGARE, A.P., SINGH, I., LARUE, B., DEANE, R. & ZLOKOVIC, B.V. 2010. Pericytes control key neurovascular functions and neuronal phenotype in the adult brain and during brain aging. *Neuron,* 68**,** 409-27.

BELL, R.D., WINKLER, E.A., SINGH, I., SAGARE, A.P., DEANE, R., WU, Z., HOLTZMAN, D.M., BETSHOLTZ, C., ARMULIK, A., SALLSTROM, J., BERK, B.C. & ZLOKOVIC, B.V. 2012. Apolipoprotein E controls cerebrovascular integrity via cyclophilin A. *Nature,* 485**,** 512-6.

BEN-ZVI, A., LACOSTE, B., KUR, E., ANDREONE, B.J., MAYSHAR, Y., YAN, H. & GU, C. 2014. Mfsd2a is critical for the formation and function of the blood-brain barrier. *Nature,* 509**,** 507-511.

BERGEMANN, A.D., COLE, F. & HIRSCHHORN, K. 2005. The etiology of Wolf-Hirschhorn syndrome. *Trends Genet,* 21**,** 188-95.
BERGER, J.H., CHARRON, M.J. & SILVER, D.L. 2012. Major facilitator superfamily domain-containing protein 2a (MFSD2A) has roles in body growth, motor function, and lipid metabolism. *PLoS One,* 7**,** e50629.
BETSHOLTZ, C. 2014a. Physiology: Double function at the blood-brain barrier. *Nature,* 509**,** 432-3.
BETSHOLTZ, C. 2014b. Physiology: Double function at the blood-brain barrier. *Nature,* 509**,** 432-433.
BITTLES, A.H. 2007. Congenital heart disease and consanguineous marriage in South India. *Ann Hum Biol,* 34**,** 682-3; author reply 683.
BLANCHARD, A., EA, V., ROUBERTIE, A., MARTIN, M., COQUART, C., CLAUSTRES, M., BEROUD, C. & COLLOD-BEROUD, G. 2011. DYT6 dystonia: review of the literature and creation of the UMD Locus-Specific Database (LSDB) for mutations in the THAP1 gene. *Hum Mutat,* 32**,** 1213-24.
BLANCHETTE, M. & DANEMAN, R. 2015. Formation and maintenance of the BBB. *Mech Dev*.
BLINDER, P., TSAI, P.S., KAUFHOLD, J.P., KNUTSEN, P.M., SUHL, H. & KLEINFELD, D. 2013. The cortical angiome: an interconnected vascular network with noncolumnar patterns of blood flow. *Nat Neurosci,* 16**,** 889-97.
BOSTAN, A.C., DUM, R.P. & STRICK, P.L. 2010. The basal ganglia communicate with the cerebellum. *Proc Natl Acad Sci U S A,* 107**,** 8452-6.
BRASHEAR, A., DELEON, D., BRESSMAN, S.B., THYAGARAJAN, D., FARLOW, M.R. & DOBYNS, W.B. 1997. Rapid-onset dystonia-parkinsonism in a second family. *Neurology,* 48**,** 1066-9.
BRECKENRIDGE, W.C., GOMBOS, G. & MORGAN, I.G. 1972. The lipid composition of adult rat brain synaptosomal plasma membranes. *Biochim Biophys Acta,* 266**,** 695-707.
BRESSMAN, S.B., RAYMOND, D., FUCHS, T., HEIMAN, G.A., OZELIUS, L.J. & SAUNDERS-PULLMAN, R. 2009. Mutations in THAP1 (DYT6) in early-onset dystonia: a genetic screening study. *Lancet Neurol,* 8**,** 441-6.
BRESSMAN, S.B., SABATTI, C., RAYMOND, D., DE LEON, D., KLEIN, C., KRAMER, P.L., BRIN, M.F., FAHN, S., BREAKEFIELD, X., OZELIUS, L.J. & RISCH, N.J. 2000. The DYT1 phenotype and guidelines for diagnostic testing. *Neurology,* 54**,** 1746-52.
BRIGHINA, F., ROMANO, M., GIGLIA, G., SAIA, V., PUMA, A., GIGLIA, F. & FIERRO, B. 2009. Effects of cerebellar TMS on motor cortex of patients with focal dystonia: a preliminary report. *Exp Brain Res,* 192**,** 651-6.
BUTTS, T., GREEN, M.J. & WINGATE, R.J. 2014. Development of the cerebellum: simple steps to make a 'little brain'. *Development,* 141**,** 4031-41.
CAMARGO, C.H., CAMARGOS, S.T., CARDOSO, F.E. & TEIVE, H.A. 2015. The genetics of the dystonias--a review based on the new classification of the dystonias. *Arq Neuropsiquiatr,* 73**,** 350-8.
CAMARGO, C.H., CAMARGOS, S.T., RASKIN, S., CARDOSO, F.E. & TEIVE, H.A. 2014. DYT6 in Brazil: Genetic Assessment and Clinical Characteristics of Patients. *Tremor Other Hyperkinet Mov (N Y),* 4**,** 226.
CARGILE, C.B., GOH, D.L., GOODMAN, B.K., CHEN, X.N., KORENBERG, J.R., SEMENZA, G.L. & THOMAS, G.H. 2002. Molecular cytogenetic characterization of a subtle interstitial del(3)(p25.3p26.2) in a patient with deletion 3p syndrome. *Am J Med Genet,* 109**,** 133-8.
CARMELIET, P. & RUIZ DE ALMODOVAR, C. 2013. VEGF ligands and receptors: implications in neurodevelopment and neurodegeneration. *Cell Mol Life Sci,* 70**,** 1763-78.

CARRIE, I., CLEMENT, M., DE JAVEL, D., FRANCES, H. & BOURRE, J.M. 2000. Phospholipid supplementation reverses behavioral and biochemical alterations induced by n-3 polyunsaturated fatty acid deficiency in mice. *J Lipid Res,* 41**,** 473-80.

CARVER, J.D., BENFORD, V.J., HAN, B. & CANTOR, A.B. 2001. The relationship between age and the fatty acid composition of cerebral cortex and erythrocytes in human subjects. *Brain Res Bull,* 56**,** 79-85.

CASSETTA, E., DEL GROSSO, N., BENTIVOGLIO, A.R., VALENTE, E.M., FRONTALI, M. & ALBANESE, A. 1999. Italian family with cranial cervical dystonia: clinical and genetic study. *Mov Disord,* 14**,** 820-5.

CASTROP, F., DRESEL, C., HENNENLOTTER, A., ZIMMER, C. & HASLINGER, B. 2012. Basal ganglia-premotor dysfunction during movement imagination in writer's cramp. *Mov Disord,* 27**,** 1432-9.

CHARLESWORTH, G., PLAGNOL, V., HOLMSTROM, K.M., BRAS, J., SHEERIN, U.M., PREZA, E., RUBIO-AGUSTI, I., RYTEN, M., SCHNEIDER, S.A., STAMELOU, M., TRABZUNI, D., ABRAMOV, A.Y., BHATIA, K.P. & WOOD, N.W. 2012. Mutations in ANO3 cause dominant craniocervical dystonia: ion channel implicated in pathogenesis. *Am J Hum Genet,* 91**,** 1041-50.

CHEN, Y., CAO, B., YANG, J., WEI, Q., OU, R.W., ZHAO, B., SONG, W., GUO, X. & SHANG, H. 2015. Analysis and meta-analysis of five polymorphisms of the LINGO1 and LINGO2 genes in Parkinson's disease and multiple system atrophy in a Chinese population. *J Neurol,* 262**,** 2478-83.

CHOW, B.W. & GU, C. 2015. The Molecular Constituents of the Blood-Brain Barrier. *Trends Neurosci,* 38**,** 598-608.

CHRISTIANSON, A. & MODELL, B. 2004. Medical genetics in developing countries. *Annu Rev Genomics Hum Genet,* 5**,** 219-65.

CLARK, B.A., MONSIVAIS, P., BRANCO, T., LONDON, M. & HAUSSER, M. 2005. The site of action potential initiation in cerebellar Purkinje neurons. *Nat Neurosci,* 8**,** 137-9.

CLARK, L.N., PARK, N., KISSELEV, S., RIOS, E., LEE, J.H. & LOUIS, E.D. 2010. Replication of the LINGO1 gene association with essential tremor in a North American population. *Eur J Hum Genet,* 18**,** 838-43.

CLOT, F., GRABLI, D., BURBAUD, P., AYA, M., DERKINDEREN, P., DEFEBVRE, L., DAMIER, P., KRYSTKOWIAK, P., POLLAK, P., LEGUERN, E., SAN, C., CAMUZAT, A., ROZE, E., VIDAILHET, M., DURR, A. & BRICE, A. 2011. Screening of the THAP1 gene in patients with early-onset dystonia: myoclonic jerks are part of the dystonia 6 phenotype. *Neurogenetics,* 12**,** 87-9.

COE, B.P., YLSTRA, B., CARVALHO, B., MEIJER, G.A., MACAULAY, C. & LAM, W.L. 2007. Resolving the resolution of array CGH. *Genomics,* 89**,** 647-53.

COLLINS, A. 2007. *Linkage Disequilibrium and Association Mapping: Analysis and Applications*, Humana Press.

CONNOR, W.E. 2000. Importance of n-3 fatty acids in health and disease. *Am J Clin Nutr,* 71**,** 171S-5S.

CONNOR, W.E., NEURINGER, M. & LIN, D.S. 1990. Dietary effects on brain fatty acid composition: the reversibility of n-3 fatty acid deficiency and turnover of docosahexaenoic acid in the brain, erythrocytes, and plasma of rhesus monkeys. *J Lipid Res,* 31**,** 237-47.

CONTE, R.A., PITTER, J.H. & VERMA, R.S. 1995. Molecular characterization of trisomic segment 3p24.1-->3pter: a case with review of the literature. *Clin Genet,* 48**,** 49-53.

COOPER, G.M., ZERR, T., KIDD, J.M., EICHLER, E.E. & NICKERSON, D.A. 2008. Systematic assessment of copy number variant detection via genome-wide SNP genotyping. *Nat Genet,* 40**,** 1199-203.

CRADDOCK, N., HURLES, M.E., CARDIN, N., PEARSON, R.D., PLAGNOL, V., ROBSON, S., VUKCEVIC, D., BARNES, C., CONRAD, D.F., GIANNOULATOU, E., HOLMES, C., MARCHINI, J.L., STIRRUPS, K., TOBIN, M.D., WAIN, L.V., YAU, C., AERTS, J., AHMAD, T., ANDREWS, T.D., ARBURY, H., ATTWOOD, A., AUTON, A., BALL, S.G., BALMFORTH, A.J., BARRETT, J.C., BARROSO, I., BARTON, A., BENNETT, A.J., BHASKAR, S., BLASZCZYK, K., BOWES, J., BRAND, O.J., BRAUND, P.S., BREDIN, F., BREEN, G., BROWN, M.J., BRUCE, I.N., BULL, J., BURREN, O.S., BURTON, J., BYRNES, J., CAESAR, S., CLEE, C.M., COFFEY, A.J., CONNELL, J.M., COOPER, J.D., DOMINICZAK, A.F., DOWNES, K., DRUMMOND, H.E., DUDAKIA, D., DUNHAM, A., EBBS, B., ECCLES, D., EDKINS, S., EDWARDS, C., ELLIOT, A., EMERY, P., EVANS, D.M., EVANS, G., EYRE, S., FARMER, A., FERRIER, I.N., FEUK, L., FITZGERALD, T., FLYNN, E., FORBES, A., FORTY, L., FRANKLYN, J.A., FREATHY, R.M., GIBBS, P., GILBERT, P., GOKUMEN, O., GORDON-SMITH, K., GRAY, E., GREEN, E., GROVES, C.J., GROZEVA, D., GWILLIAM, R., HALL, A., HAMMOND, N., HARDY, M., HARRISON, P., HASSANALI, N., HEBAISHI, H., HINES, S., HINKS, A., HITMAN, G.A., HOCKING, L., HOWARD, E., HOWARD, P., HOWSON, J.M., HUGHES, D., HUNT, S., ISAACS, J.D., JAIN, M., JEWELL, D.P., JOHNSON, T., JOLLEY, J.D., JONES, I.R., JONES, L.A., et al. 2010. Genome-wide association study of CNVs in 16,000 cases of eight common diseases and 3,000 shared controls. *Nature,* 464**,** 713-20.

CUSTER, D.A., VEZINA, L.G., VAUGHT, D.R., BRASSEUX, C., SAMANGO-SPROUSE, C.A., COHEN, M.S. & ROSENBAUM, K.N. 2000. Neurodevelopmental and neuroimaging correlates in nonsyndromal microcephalic children. *J Dev Behav Pediatr,* 21**,** 12-8.

DANEMAN, R., ZHOU, L., KEBEDE, A.A. & BARRES, B.A. 2010. Pericytes are required for blood-brain barrier integrity during embryogenesis. *Nature,* 468**,** 562-6.

DE BRUIN, C. & DAUBER, A. 2015. Insights from exome sequencing for endocrine disorders. *Nat Rev Endocrinol,* 11**,** 455-64.

DE CARVALHO AGUIAR, P., SWEADNER, K.J., PENNISTON, J.T., ZAREMBA, J., LIU, L., CATON, M., LINAZASORO, G., BORG, M., TIJSSEN, M.A., BRESSMAN, S.B., DOBYNS, W.B., BRASHEAR, A. & OZELIUS, L.J. 2004. Mutations in the Na+/K+ -ATPase alpha3 gene ATP1A3 are associated with rapid-onset dystonia parkinsonism. *Neuron,* 43**,** 169-75.

DE VRIES, B.B., PFUNDT, R., LEISINK, M., KOOLEN, D.A., VISSERS, L.E., JANSSEN, I.M., REIJMERSDAL, S., NILLESEN, W.M., HUYS, E.H., LEEUW, N., SMEETS, D., SISTERMANS, E.A., FEUTH, T., VAN RAVENSWAAIJ-ARTS, C.M., VAN KESSEL, A.G., SCHOENMAKERS, E.F., BRUNNER, H.G. & VELTMAN, J.A. 2005. Diagnostic genome profiling in mental retardation. *Am J Hum Genet,* 77**,** 606-16.

DEFAZIO, G., CONTE, A., GIGANTE, A.F., FABBRINI, G. & BERARDELLI, A. 2015. Is tremor in dystonia a phenotypic feature of dystonia? *Neurology,* 84**,** 1053-9.

DEFAZIO, G., GIGANTE, A.F., ABBRUZZESE, G., BENTIVOGLIO, A.R., COLOSIMO, C., ESPOSITO, M., FABBRINI, G., GUIDUBALDI, A., GIRLANDA, P., LIGUORI, R., MARINELLI, L., MORGANTE, F., SANTORO, L., TINAZZI, M., LIVREA, P. & BERARDELLI, A. 2013. Tremor in primary adult-onset dystonia: prevalence and associated clinical features. *J Neurol Neurosurg Psychiatry,* 84**,** 404-8.

DELAY, C., TREMBLAY, C., BROCHU, E., PARIS-ROBIDAS, S., EMOND, V., RAJPUT, A.H., RAJPUT, A. & CALON, F. 2014. Increased LINGO1 in the cerebellum of essential tremor patients. *Mov Disord*.

DELONG, M.R. & WICHMANN, T. 2007. Circuits and circuit disorders of the basal ganglia. *Arch Neurol,* 64**,** 20-4.

DEUSCHL, G., BAIN, P. & BRIN, M. 1998. Consensus statement of the Movement Disorder Society on Tremor. Ad Hoc Scientific Committee. *Mov Disord,* 13 Suppl 3**,** 2-23.

DIJKHUIZEN, T., VAN ESSEN, T., VAN DER VLIES, P., VERHEIJ, J.B., SIKKEMA-RADDATZ, B., VAN DER VEEN, A.Y., GERSSEN-SCHOORL, K.B., BUYS, C.H. & KOK, K. 2006. FISH and

array-CGH analysis of a complex chromosome 3 aberration suggests that loss of CNTN4 and CRBN contributes to mental retardation in 3pter deletions. *Am J Med Genet A,* 140**,** 2482-7.
DIMAURO, S., KULIKOVA, R., TANJI, K., BONILLA, E. & HIRANO, M. 1999. Mitochondrial genes for generalized epilepsies. *Adv Neurol,* 79**,** 411-9.
DIRECTOR, R.E.S. & COLUMBIA, J.G.H.P.P.U.B. 2005. *Human Malformations and Related Anomalies*, Oxford University Press, USA.
DUDEK, R.W. & FIX, J.D. 1998. *Embryology*, Williams & Wilkins.
DUNCAN, E., BROWN, M. & SHORE, E.M. 2014. The revolution in human monogenic disease mapping. *Genes (Basel),* 5**,** 792-803.
ELDER, J.H. & ALEXANDER, S. 1982. endo-beta-N-acetylglucosaminidase F: endoglycosidase from Flavobacterium meningosepticum that cleaves both high-mannose and complex glycoproteins. *Proc Natl Acad Sci U S A,* 79**,** 4540-4.
EMERSON, E. 2012. Deprivation, ethnicity and the prevalence of intellectual and developmental disabilities. *Journal of Epidemiology and Community Health,* 66**,** 218-224.
ETHAYATHULLA, A.S., YOUSEF, M.S., AMIN, A., LEBLANC, G., KABACK, H.R. & GUAN, L. 2014. Structure-based mechanism for Na(+)/melibiose symport by MelB. *Nat Commun,* 5**,** 3009.
FAHN, S., BRESSMAN, S.B. & MARSDEN, C.D. 1998. Classification of dystonia. *Adv Neurol,* 78**,** 1-10.
FELLERMANN, K., STANGE, D.E., SCHAEFFELER, E., SCHMALZL, H., WEHKAMP, J., BEVINS, C.L., REINISCH, W., TEML, A., SCHWAB, M., LICHTER, P., RADLWIMMER, B. & STANGE, E.F. 2006. A chromosome 8 gene-cluster polymorphism with low human beta-defensin 2 gene copy number predisposes to Crohn disease of the colon. *Am J Hum Genet,* 79**,** 439-48.
FENICHEL, G.M. 2005. *Clinical Pediatric Neurology: A Signs and Symptoms Approach,* Philadelphia, Elsevier/Saunders.
FIORIO, M., WEISE, D., ONAL-HARTMANN, C., ZELLER, D., TINAZZI, M. & CLASSEN, J. 2011. Impairment of the rubber hand illusion in focal hand dystonia. *Brain,* 134**,** 1428-37.
FLEMING, A., DIEKMANN, H. & GOLDSMITH, P. 2013. Functional characterisation of the maturation of the blood-brain barrier in larval zebrafish. *PLoS One,* 8**,** e77548.
FORSGREN, L., HOLMGREN, G., ALMAY, B.G. & DRUGGE, U. 1988. Autosomal dominant torsion dystonia in a Swedish family. *Adv Neurol,* 50**,** 83-92.
FOUST, A., POPOVIC, M., ZECEVIC, D. & MCCORMICK, D.A. 2010. Action potentials initiate in the axon initial segment and propagate through axon collaterals reliably in cerebellar Purkinje neurons. *J Neurosci,* 30**,** 6891-902.
FRAZIER, A.E., TAYLOR, R.D., MICK, D.U., WARSCHEID, B., STOEPEL, N., MEYER, H.E., RYAN, M.T., GUIARD, B. & REHLING, P. 2006. Mdm38 interacts with ribosomes and is a component of the mitochondrial protein export machinery. *J Cell Biol,* 172**,** 553-64.
FRINTS, S.G., MARYNEN, P., HARTMANN, D., FRYNS, J.P., STEYAERT, J., SCHACHNER, M., ROLF, B., CRAESSAERTS, K., SNELLINX, A., HOLLANDERS, K., D'HOOGE, R., DE DEYN, P.P. & FROYEN, G. 2003. CALL interrupted in a patient with non-specific mental retardation: gene dosage-dependent alteration of murine brain development and behavior. *Hum Mol Genet,* 12**,** 1463-74.
FUCHS, T., GAVARINI, S., SAUNDERS-PULLMAN, R., RAYMOND, D., EHRLICH, M.E., BRESSMAN, S.B. & OZELIUS, L.J. 2009. Mutations in the THAP1 gene are responsible for DYT6 primary torsion dystonia. *Nat Genet,* 41**,** 286-8.
FUCHS, T., SAUNDERS-PULLMAN, R., MASUHO, I., LUCIANO, M.S., RAYMOND, D., FACTOR, S., LANG, A.E., LIANG, T.W., TROSCH, R.M., WHITE, S., AINEHSAZAN, E., HERVE, D.,

SHARMA, N., EHRLICH, M.E., MARTEMYANOV, K.A., BRESSMAN, S.B. & OZELIUS, L.J. 2013. Mutations in GNAL cause primary torsion dystonia. *Nat Genet,* 45**,** 88-92.
GARDNER, R.J.M.K., SUTHERLAND, G.R. & SHAFFER, L.G. 2011. *Chromosome Abnormalities and Genetic Counseling*, Oxford University Press, USA.
GARTNER, J.C., ZITELLI, B.J. & JA, N. 1997. *Common and Chronic Symptoms in Pediatrics*, Mosby.
GESCHWIND, D.H. & RAKIC, P. 2013. Cortical evolution: judge the brain by its cover. *Neuron,* 80**,** 633-47.
GITTIS, A.H. & KREITZER, A.C. 2012. Striatal microcircuitry and movement disorders. *Trends Neurosci,* 35**,** 557-64.
GOMEZ-CURET, I., ROBINSON, K.G., FUNANAGE, V.L., CRAWFORD, T.O., SCAVINA, M. & WANG, W. 2007. Robust quantification of the SMN gene copy number by real-time TaqMan PCR. *Neurogenetics,* 8**,** 271-8.
GONZALEZ, C.H., SOMMER, A., MEISNER, L.F., ELEJALDE, B.R. & OPITZ, J.M. 1977. The trisomy 4p syndrome: case report and review. *Am J Med Genet,* 1**,** 137-56.
GOVERT, F. & DEUSCHL, G. 2015. Tremor entities and their classification: an update. *Curr Opin Neurol,* 28**,** 393-9.
GROSSMANN, V., MULLER, D., MULLER, W., FRESSER, F., ERDEL, M., JANECKE, A.R., ZSCHOCKE, J., UTERMANN, G. & KOTZOT, D. 2009. "Essentially" pure trisomy 3q27 -> qter: further delineation of the partial trisomy 3q phenotype. *Am J Med Genet A,* 149a**,** 2522-6.
GRUMMER-STRAWN, L.M., REINOLD, C. & KREBS, N.F. 2010. Use of World Health Organization and CDC growth charts for children aged 0-59 months in the United States. *MMWR Recomm Rep,* 59**,** 1-15.
GUEMEZ-GAMBOA, A., NGUYEN, L.N., YANG, H., ZAKI, M.S., KARA, M., BEN-OMRAN, T., AKIZU, N., ROSTI, R.O., ROSTI, B., SCOTT, E., SCHROTH, J., COPELAND, B., VAUX, K.K., CAZENAVE-GASSIOT, A., QUEK, D.Q., WONG, B.H., TAN, B.C., WENK, M.R., GUNEL, M., GABRIEL, S., CHI, N.C., SILVER, D.L. & GLEESON, J.G. 2015. Inactivating mutations in MFSD2A, required for omega-3 fatty acid transport in brain, cause a lethal microcephaly syndrome. *Nat Genet*.
HALLETT, M. 2011. Neurophysiology of dystonia: The role of inhibition. *Neurobiol Dis,* 42**,** 177-84.
HAMADA, M., STRIGARO, G., MURASE, N., SADNICKA, A., GALEA, J.M., EDWARDS, M.J. & ROTHWELL, J.C. 2012. Cerebellar modulation of human associative plasticity. *J Physiol,* 590**,** 2365-74.
HAN, D.H., CHANG, J.Y., LEE, W.I. & BAE, C.W. 2012. A case of partial trisomy 3p syndrome with rare clinical manifestations. *Korean J Pediatr,* 55**,** 107-10.
HARRIS, J.C. 2013. New terminology for mental retardation in DSM-5 and ICD-11. *Curr Opin Psychiatry,* 26**,** 260-2.
HARRIS, J.C. 2014. New classification for neurodevelopmental disorders in DSM-5. *Curr Opin Psychiatry,* 27**,** 95-7.
HEDERA, P., CIBULCIK, F. & DAVIS, T.L. 2013. Pharmacotherapy of essential tremor. *J Cent Nerv Syst Dis,* 5**,** 43-55.
HORROCKS, L.A. & YEO, Y.K. 1999. Health benefits of docosahexaenoic acid (DHA). *Pharmacol Res,* 40**,** 211-25.
IADECOLA, C. 2013. The pathobiology of vascular dementia. *Neuron,* 80**,** 844-66.
IAFRATE, A.J., FEUK, L., RIVERA, M.N., LISTEWNIK, M.L., DONAHOE, P.K., QI, Y., SCHERER, S.W. & LEE, C. 2004. Detection of large-scale variation in the human genome. *Nat Genet,* 36**,** 949-51.
INNIS, S.M. 2007. Dietary (n-3) fatty acids and brain development. *J Nutr,* 137**,** 855-9.

INOUE, H., LIN, L., LEE, X., SHAO, Z., MENDES, S., SNODGRASS-BELT, P., SWEIGARD, H., ENGBER, T., PEPINSKY, B., YANG, L., BEAL, M.F., MI, S. & ISACSON, O. 2007. Inhibition of the leucine-rich repeat protein LINGO-1 enhances survival, structure, and function of dopaminergic neurons in Parkinson's disease models. *Proc Natl Acad Sci U S A,* 104**,** 14430-5.

ITSARA, A., COOPER, G.M., BAKER, C., GIRIRAJAN, S., LI, J., ABSHER, D., KRAUSS, R.M., MYERS, R.M., RIDKER, P.M., CHASMAN, D.I., MEFFORD, H., YING, P., NICKERSON, D.A. & EICHLER, E.E. 2009. Population analysis of large copy number variants and hotspots of human genetic disease. *Am J Hum Genet,* 84**,** 148-61.

JAIN, S., LO, S.E. & LOUIS, E.D. 2006. Common misdiagnosis of a common neurological disorder: how are we misdiagnosing essential tremor? *Arch Neurol,* 63**,** 1100-4.

JEPSON, S., VOUGHT, B., GROSS, C.H., GAN, L., AUSTEN, D., FRANTZ, J.D., ZWAHLEN, J., LOWE, D., MARKLAND, W. & KRAUSS, R. 2012. LINGO-1, a transmembrane signaling protein, inhibits oligodendrocyte differentiation and myelination through intercellular self-interactions. *Journal of Biological Chemistry,* 287**,** 22184-22195.

JIANG, D., ZHAO, L. & CLAPHAM, D.E. 2009. Genome-wide RNAi screen identifies Letm1 as a mitochondrial Ca2+/H+ antiporter. *Science,* 326**,** 144-7.

KAAS, J.H. 2013. The Evolution of Brains from Early Mammals to Humans. *Wiley Interdiscip Rev Cogn Sci,* 4**,** 33-45.

KAINDL, A.M., PASSEMARD, S., KUMAR, P., KRAEMER, N., ISSA, L., ZWIRNER, A., GERARD, B., VERLOES, A., MANI, S. & GRESSENS, P. 2010. Many roads lead to primary autosomal recessive microcephaly. *Prog Neurobiol,* 90**,** 363-83.

KAMAL, N., BHAT, D.P. & CARRICK, E. 2006. Dopa-responsive dystonia (Segawa syndrome). *Indian Pediatr,* 43**,** 635-8.

KANOVSKY, P. 2002. Dystonia: a disorder of motor programming or motor execution? *Mov Disord,* 17**,** 1143-7.

KANOVSKY, P., BHATIA, K.P. & ROSALES, R.L. 2015. *Dystonia and Dystonic Syndromes*, Springer Vienna.

KANTHIMATHI, S., VIJAYA, M. & RAMESH, A. 2008. Genetic study of Dravidian castes of Tamil Nadu. *J Genet,* 87**,** 175-9.

KAUFMAN, L., AYUB, M. & VINCENT, J.B. 2010. The genetic basis of non-syndromic intellectual disability: a review. *J Neurodev Disord,* 2**,** 182-209.

KHOURY, G.A., BALIBAN, R.C. & FLOUDAS, C.A. 2011. Proteome-wide post-translational modification statistics: frequency analysis and curation of the swiss-prot database. *Sci Rep,* 1.

KIDD, P.M. 2007. Omega-3 DHA and EPA for cognition, behavior, and mood: clinical findings and structural-functional synergies with cell membrane phospholipids. *Altern Med Rev,* 12**,** 207-27.

KLEIN, C. 2014. Genetics in dystonia. *Parkinsonism Relat Disord,* 20 Suppl 1**,** S137-42.

KONG, A., FRIGGE, M.L., MASSON, G., BESENBACHER, S., SULEM, P., MAGNUSSON, G., GUDJONSSON, S.A., SIGURDSSON, A., JONASDOTTIR, A., JONASDOTTIR, A., WONG, W.S., SIGURDSSON, G., WALTERS, G.B., STEINBERG, S., HELGASON, H., THORLEIFSSON, G., GUDBJARTSSON, D.F., HELGASON, A., MAGNUSSON, O.T., THORSTEINSDOTTIR, U. & STEFANSSON, K. 2012. Rate of de novo mutations and the importance of father's age to disease risk. *Nature,* 488**,** 471-5.

KORBEL, J.O., URBAN, A.E., AFFOURTIT, J.P., GODWIN, B., GRUBERT, F., SIMONS, J.F., KIM, P.M., PALEJEV, D., CARRIERO, N.J., DU, L., TAILLON, B.E., CHEN, Z., TANZER, A., SAUNDERS, A.C., CHI, J., YANG, F., CARTER, N.P., HURLES, M.E., WEISSMAN, S.M., HARKINS, T.T., GERSTEIN, M.B., EGHOLM, M. & SNYDER, M. 2007. Paired-end mapping reveals extensive structural variation in the human genome. *Science,* 318**,** 420-6.

KOTZOT, D., KRUGER, C. & BRAUN-QUENTIN, C. 1996. De novo direct duplication 3 (p25-->pter): a previously undescribed chromosomal aberration. *Clin Genet,* 50**,** 96-8.
KRALIC, J.E., CRISWELL, H.E., OSTERMAN, J.L., O'BUCKLEY, T.K., WILKIE, M.E., MATTHEWS, D.B., HAMRE, K., BREESE, G.R., HOMANICS, G.E. & MORROW, A.L. 2005. Genetic essential tremor in gamma-aminobutyric acidA receptor alpha1 subunit knockout mice. *J Clin Invest,* 115**,** 774-9.
KRISHNAMOORTHY, S. & AUDINARAYANA, N. 2001. Trends in consanguinity in South India. *J Biosoc Sci,* 33**,** 185-97.
KUMAR, D. 2012. *Genetic Disorders of the Indian Subcontinent*, Springer Netherlands.
KUO, S.H., ERICKSON-DAVIS, C., GILLMAN, A., FAUST, P.L., VONSATTEL, J.P. & LOUIS, E.D. 2011. Increased number of heterotopic Purkinje cells in essential tremor. *J Neurol Neurosurg Psychiatry,* 82**,** 1038-40.
KUO, S.H., TANG, G., LOUIS, E.D., MA, K., BABJI, R., BALATBAT, M., CORTES, E., VONSATTEL, J.P., YAMAMOTO, A., SULZER, D. & FAUST, P.L. 2013. Lingo-1 expression is increased in essential tremor cerebellum and is present in the basket cell pinceau. *Acta Neuropathol,* 125**,** 879-89.
KWASNY, D., VEDARETHINAM, I., SHAH, P., DIMAKI, M., SILAHTAROGLU, A., TUMER, Z. & SVENDSEN, W.E. 2012. Advanced microtechnologies for detection of chromosome abnormalities by fluorescent in situ hybridization. *Biomed Microdevices,* 14**,** 453-60.
LAFOURCADE, M., LARRIEU, T., MATO, S., DUFFAUD, A., SEPERS, M., MATIAS, I., DE SMEDT-PEYRUSSE, V., LABROUSSE, V.F., BRETILLON, L., MATUTE, C., RODRIGUEZ-PUERTAS, R., LAYE, S. & MANZONI, O.J. 2011. Nutritional omega-3 deficiency abolishes endocannabinoid-mediated neuronal functions. *Nat Neurosci,* 14**,** 345-350.
LALLI, S. & ALBANESE, A. 2010. The diagnostic challenge of primary dystonia: evidence from misdiagnosis. *Mov Disord,* 25**,** 1619-26.
LAM, H.Y., MU, X.J., STUTZ, A.M., TANZER, A., CAYTING, P.D., SNYDER, M., KIM, P.M., KORBEL, J.O. & GERSTEIN, M.B. 2010. Nucleotide-resolution analysis of structural variants using BreakSeq and a breakpoint library. *Nat Biotechnol,* 28**,** 47-55.
LEE, X., YANG, Z., SHAO, Z., ROSENBERG, S.S., LEVESQUE, M., PEPINSKY, R.B., QIU, M., MILLER, R.H., CHAN, J.R. & MI, S. 2007. NGF regulates the expression of axonal LINGO-1 to inhibit oligodendrocyte differentiation and myelination. *J Neurosci,* 27**,** 220-5.
LEROY, J.G. & FRIAS, J.L. 2005. Nonsyndromic microcephaly: an overview. *Adv Pediatr,* 52**,** 261-93.
LEUBE, B., RUDNICKI, D., RATZLAFF, T., KESSLER, K.R., BENECKE, R. & AUBURGER, G. 1996. Idiopathic torsion dystonia: assignment of a gene to chromosome 18p in a German family with adult onset, autosomal dominant inheritance and purely focal distribution. *Hum Mol Genet,* 5**,** 1673-7.
LEVITON, A., HOLMES, L.B., ALLRED, E.N. & VARGAS, J. 2002. Methodologic issues in epidemiologic studies of congenital microcephaly. *Early Hum Dev,* 69**,** 91-105.
LLORENS, F., GIL, V. & DEL RIO, J.A. 2011. Emerging functions of myelin-associated proteins during development, neuronal plasticity, and neurodegeneration. *FASEB J,* 25**,** 463-75.
LLORENS, F., GIL, V., IRAOLA, S., CARIM-TODD, L., MARTI, E., ESTIVILL, X., SORIANO, E., DEL RIO, J.A. & SUMOY, L. 2008. Developmental analysis of Lingo-1/Lern1 protein expression in the mouse brain: interaction of its intracellular domain with Myt1l. *Dev Neurobiol,* 68**,** 521-41.
LOCKE, D.P., SEGRAVES, R., NICHOLLS, R.D., SCHWARTZ, S., PINKEL, D., ALBERTSON, D.G. & EICHLER, E.E. 2004. BAC microarray analysis of 15q11-q13 rearrangements and the impact of segmental duplications. *J Med Genet,* 41**,** 175-82.

LÖÖV, C., FERNQVIST, M., WALMSLEY, A., MARKLUND, N. & ERLANDSSON, A. 2012. Neutralization of LINGO-1 during in vitro differentiation of neural stem cells results in proliferation of immature neurons. *PloS one,* 7**,** e29771.

LOUIS, E.D. & FERREIRA, J.J. 2010. How common is the most common adult movement disorder? Update on the worldwide prevalence of essential tremor. *Mov Disord,* 25**,** 534-41.

LOUIS, E.D., HERNANDEZ, N., ALCALAY, R.N., TIRRI, D.J., OTTMAN, R. & CLARK, L.N. 2013. Prevalence and features of unreported dystonia in a family study of "pure" essential tremor. *Parkinsonism Relat Disord,* 19**,** 359-62.

LOUIS, E.D., HERNANDEZ, N. & MICHALEC, M. 2015. Prevalence and correlates of rest tremor in essential tremor: cross-sectional survey of 831 patients across four distinct cohorts. *Eur J Neurol*.

LOUIS, E.D., JIANG, W., PELLEGRINO, K.M., RIOS, E., FACTOR-LITVAK, P., HENCHCLIFFE, C. & ZHENG, W. 2008. Elevated blood harmane (1-methyl-9H-pyrido[3,4-b]indole) concentrations in essential tremor. *Neurotoxicology,* 29**,** 294-300.

LOUIS, E.D., OTTMAN, R. & CLARK, L.N. 2014. Clinical classification of borderline cases in the family study of essential tremor: an analysis of phenotypic features. *Tremor Other Hyperkinet Mov (N Y),* 4**,** 220.

MAJUMDER, P.P. 2010. The human genetic history of South Asia. *Curr Biol,* 20**,** R184-7.

MALMGREN, H., SAHLEN, S., WIDE, K., LUNDVALL, M. & BLENNOW, E. 2007. Distal 3p deletion syndrome: detailed molecular cytogenetic and clinical characterization of three small distal deletions and review. *Am J Med Genet A,* 143a**,** 2143-9.

MANDEMAKERS, W.J. & BARRES, B.A. 2005. Axon regeneration: it's getting crowded at the gates of TROY. *Curr Biol,* 15**,** R302-5.

MATHEWS, T.J., MENACKER, F. & MACDORMAN, M.F. 2003. Infant mortality statistics from the 2001 period linked birth/infant death data set. *Natl Vital Stat Rep,* 52**,** 1-28.

MATTOS, T.C., GIUGLIANI, R. & HAASE, H.B. 1987. Congenital malformations detected in 731 autopsies of children aged 0 to 14 years. *Teratology,* 35**,** 305-7.

MCCARROLL, S.A., KURUVILLA, F.G., KORN, J.M., CAWLEY, S., NEMESH, J., WYSOKER, A., SHAPERO, M.H., DE BAKKER, P.I., MALLER, J.B., KIRBY, A., ELLIOTT, A.L., PARKIN, M., HUBBELL, E., WEBSTER, T., MEI, R., VEITCH, J., COLLINS, P.J., HANDSAKER, R., LINCOLN, S., NIZZARI, M., BLUME, J., JONES, K.W., RAVA, R., DALY, M.J., GABRIEL, S.B. & ALTSHULER, D. 2008. Integrated detection and population-genetic analysis of SNPs and copy number variation. *Nat Genet,* 40**,** 1166-74.

MCELREAVEY, K. & QUINTANA-MURCI, L. 2002. Understanding inherited disease through human migrations: a south-west Asian perspective. *Community Genet,* 5**,** 153-6.

MCGEE, A.W. & STRITTMATTER, S.M. 2003. The Nogo-66 receptor: focusing myelin inhibition of axon regeneration. *Trends Neurosci,* 26**,** 193-8.

MEDVEDEV, P., STANCIU, M. & BRUDNO, M. 2009. Computational methods for discovering structural variation with next-generation sequencing. *Nat Methods,* 6**,** S13-20.

MEGRAW, T.L., SHARKEY, J.T. & NOWAKOWSKI, R.S. 2011. Cdk5rap2 exposes the centrosomal root of microcephaly syndromes. *Trends Cell Biol,* 21**,** 470-80.

MENKES, J.H., SARNAT, H.B. & MARIA, B.L. 2006. *Child Neurology*, Lippincott Williams & Wilkins.

METZKER, M.L. 2010. Sequencing technologies - the next generation. *Nat Rev Genet,* 11**,** 31-46.

MI, S., HU, B., HAHM, K., LUO, Y., KAM HUI, E.S., YUAN, Q., WONG, W.M., WANG, L., SU, H., CHU, T.H., GUO, J., ZHANG, W., SO, K.F., PEPINSKY, B., SHAO, Z., GRAFF, C., GARBER, E., JUNG, V., WU, E.X. & WU, W. 2007. LINGO-1 antagonist promotes spinal cord remyelination and axonal integrity in MOG-induced experimental autoimmune encephalomyelitis. *Nat Med,* 13**,** 1228-33.

MI, S., LEE, X., SHAO, Z., THILL, G., JI, B., RELTON, J., LEVESQUE, M., ALLAIRE, N., PERRIN, S., SANDS, B., CROWELL, T., CATE, R.L., MCCOY, J.M. & PEPINSKY, R.B. 2004. LINGO-1 is a component of the Nogo-66 receptor/p75 signaling complex. *Nat Neurosci,* 7**,** 221-8.

MI, S., SANDROCK, A. & MILLER, R.H. 2008. LINGO-1 and its role in CNS repair. *Int J Biochem Cell Biol,* 40**,** 1971-8.

MILLER, D.T., ADAM, M.P., ARADHYA, S., BIESECKER, L.G., BROTHMAN, A.R., CARTER, N.P., CHURCH, D.M., CROLLA, J.A., EICHLER, E.E., EPSTEIN, C.J., FAUCETT, W.A., FEUK, L., FRIEDMAN, J.M., HAMOSH, A., JACKSON, L., KAMINSKY, E.B., KOK, K., KRANTZ, I.D., KUHN, R.M., LEE, C., OSTELL, J.M., ROSENBERG, C., SCHERER, S.W., SPINNER, N.B., STAVROPOULOS, D.J., TEPPERBERG, J.H., THORLAND, E.C., VERMEESCH, J.R., WAGGONER, D.J., WATSON, M.S., MARTIN, C.L. & LEDBETTER, D.H. 2010. Consensus statement: chromosomal microarray is a first-tier clinical diagnostic test for individuals with developmental disabilities or congenital anomalies. *Am J Hum Genet,* 86**,** 749-64.

MILLER, R.H. & MI, S. 2007. Dissecting demyelination. *Nat Neurosci,* 10**,** 1351-4.

MILLS, R.E., WALTER, K., STEWART, C., HANDSAKER, R.E., CHEN, K., ALKAN, C., ABYZOV, A., YOON, S.C., YE, K., CHEETHAM, R.K., CHINWALLA, A., CONRAD, D.F., FU, Y., GRUBERT, F., HAJIRASOULIHA, I., HORMOZDIARI, F., IAKOUCHEVA, L.M., IQBAL, Z., KANG, S., KIDD, J.M., KONKEL, M.K., KORN, J., KHURANA, E., KURAL, D., LAM, H.Y., LENG, J., LI, R., LI, Y., LIN, C.Y., LUO, R., MU, X.J., NEMESH, J., PECKHAM, H.E., RAUSCH, T., SCALLY, A., SHI, X., STROMBERG, M.P., STUTZ, A.M., URBAN, A.E., WALKER, J.A., WU, J., ZHANG, Y., ZHANG, Z.D., BATZER, M.A., DING, L., MARTH, G.T., MCVEAN, G., SEBAT, J., SNYDER, M., WANG, J., YE, K., EICHLER, E.E., GERSTEIN, M.B., HURLES, M.E., LEE, C., MCCARROLL, S.A. & KORBEL, J.O. 2011. Mapping copy number variation by population-scale genome sequencing. *Nature,* 470**,** 59-65.

MINK, J.W. 2003. The Basal Ganglia and involuntary movements: impaired inhibition of competing motor patterns. *Arch Neurol,* 60**,** 1365-8.

MOCHIDA, G.H. & WALSH, C.A. 2001. Molecular genetics of human microcephaly. *Curr Opin Neurol,* 14**,** 151-6.

MOESCHLER, J.B. 2008. Genetic evaluation of intellectual disabilities. *Semin Pediatr Neurol,* 15**,** 2-9.

MOORE, K.L., PERSAUD, T.V.N. & TORCHIA, M.G. 2011. *Before We Are Born: Essentials of Embryology and Birth Defects*, Elsevier Health Sciences.

MORETTI, R., PANSIOT, J., BETTATI, D., STRAZIELLE, N., GHERSI-EGEA, J.F., DAMANTE, G., FLEISS, B., TITOMANLIO, L. & GRESSENS, P. 2015. Blood-brain barrier dysfunction in disorders of the developing brain. *Front Neurosci,* 9**,** 40.

MOSKOWITZ, M.A., LO, E.H. & IADECOLA, C. 2010. The science of stroke: mechanisms in search of treatments. *Neuron,* 67**,** 181-98.

MOZAFFARIAN, D. & WU, J.H. 2011. Omega-3 fatty acids and cardiovascular disease: effects on risk factors, molecular pathways, and clinical events. *J Am Coll Cardiol,* 58**,** 2047-67.

MUHURI, P.K., MACDORMAN, M.F. & EZZATI-RICE, T.M. 2004. Racial differences in leading causes of infant death in the United States. *Paediatr Perinat Epidemiol,* 18**,** 51-60.

MUNCHAU, A., SCHRAG, A., CHUANG, C., MACKINNON, C.D., BHATIA, K.P., QUINN, N.P. & ROTHWELL, J.C. 2001. Arm tremor in cervical dystonia differs from essential tremor and can be classified by onset age and spread of symptoms. *Brain,* 124**,** 1765-76.

NATALE, V. & RAJAGOPALAN, A. 2014. Worldwide variation in human growth and the World Health Organization growth standards: a systematic review. *BMJ Open,* 4**,** e003735.

NEHRU, J. 2004. *The Discovery of India*, Penguin Books.

NEYCHEV, V.K., FAN, X., MITEV, V.I., HESS, E.J. & JINNAH, H.A. 2008. The basal ganglia and cerebellum interact in the expression of dystonic movement. *Brain,* 131**,** 2499-509.
NEYCHEV, V.K., GROSS, R.E., LEHERICY, S., HESS, E.J. & JINNAH, H.A. 2011. The functional neuroanatomy of dystonia. *Neurobiol Dis,* 42**,** 185-201.
NG, S.B., BUCKINGHAM, K.J., LEE, C., BIGHAM, A.W., TABOR, H.K., DENT, K.M., HUFF, C.D., SHANNON, P.T., JABS, E.W., NICKERSON, D.A., SHENDURE, J. & BAMSHAD, M.J. 2010. Exome sequencing identifies the cause of a mendelian disorder. *Nat Genet,* 42**,** 30-5.
NG, S.B., TURNER, E.H., ROBERTSON, P.D., FLYGARE, S.D., BIGHAM, A.W., LEE, C., SHAFFER, T., WONG, M., BHATTACHARJEE, A., EICHLER, E.E., BAMSHAD, M., NICKERSON, D.A. & SHENDURE, J. 2009. Targeted capture and massively parallel sequencing of 12 human exomes. *Nature,* 461**,** 272-6.
NGUYEN, L.N., MA, D., SHUI, G., WONG, P., CAZENAVE-GASSIOT, A., ZHANG, X., WENK, M.R., GOH, E.L. & SILVER, D.L. 2014a. Mfsd2a is a transporter for the essential omega-3 fatty acid docosahexaenoic acid. *Nature,* 509**,** 503-6.
NGUYEN, L.N., MA, D., SHUI, G., WONG, P., CAZENAVE-GASSIOT, A., ZHANG, X., WENK, M.R., GOH, E.L.K. & SILVER, D.L. 2014b. Mfsd2a is a transporter for the essential omega-3 fatty acid docosahexaenoic acid. *Nature,* 509**,** 503-506.
NICHOLS, R. 2008. *A History of Pashtun Migration, 1775-2006*, Oxford University Press.
NIETHAMMER, M., CARBON, M., ARGYELAN, M. & EIDELBERG, D. 2011. Hereditary dystonia as a neurodevelopmental circuit disorder: Evidence from neuroimaging. *Neurobiol Dis,* 42**,** 202-9.
NIMURA, K., URA, K., SHIRATORI, H., IKAWA, M., OKABE, M., SCHWARTZ, R.J. & KANEDA, Y. 2009. A histone H3 lysine 36 trimethyltransferase links Nkx2-5 to Wolf-Hirschhorn syndrome. *Nature,* 460**,** 287-91.
NISTICO, R., PIRRITANO, D., NOVELLINO, F., SALSONE, M., MORELLI, M., VALENTINO, P., CONDINO, F., ARABIA, G. & QUATTRONE, A. 2012a. Blink reflex recovery cycle in patients with essential tremor associated with resting tremor. *Neurology,* 79**,** 1490-5.
NISTICO, R., PIRRITANO, D., SALSONE, M., VALENTINO, P., NOVELLINO, F., CONDINO, F., BONO, F. & QUATTRONE, A. 2012b. Blink reflex recovery cycle in patients with dystonic tremor: a cross-sectional study. *Neurology,* 78**,** 1363-5.
NORGREN, N., MATTSON, E., FORSGREN, L. & HOLMBERG, M. 2011. A high-penetrance form of late-onset torsion dystonia maps to a novel locus (DYT21) on chromosome 2q14.3-q21.3. *Neurogenetics,* 12**,** 137-43.
NOWIKOVSKY, K., FROSCHAUER, E.M., ZSURKA, G., SAMAJ, J., REIPERT, S., KOLISEK, M., WIESENBERGER, G. & SCHWEYEN, R.J. 2004. The LETM1/YOL027 gene family encodes a factor of the mitochondrial K+ homeostasis with a potential role in the Wolf-Hirschhorn syndrome. *J Biol Chem,* 279**,** 30307-15.
NUTT, J.G. & NYGAARD, T.G. 2001. Response to levodopa treatment in dopa-responsive dystonia. *Arch Neurol,* 58**,** 905-10.
OGAWA, Y. & RASBAND, M.N. 2008. The functional organization and assembly of the axon initial segment. *Curr Opin Neurobiol,* 18**,** 307-13.
OTT, J., WANG, J. & LEAL, S.M. 2015. Genetic linkage analysis in the age of whole-genome sequencing. *Nat Rev Genet,* 16**,** 275-84.
OZELIUS, L.J., HEWETT, J.W., PAGE, C.E., BRESSMAN, S.B., KRAMER, P.L., SHALISH, C., DE LEON, D., BRIN, M.F., RAYMOND, D., COREY, D.P., FAHN, S., RISCH, N.J., BUCKLER, A.J., GUSELLA, J.F. & BREAKEFIELD, X.O. 1997. The early-onset torsion dystonia gene (DYT1) encodes an ATP-binding protein. *Nat Genet,* 17**,** 40-8.
PACIORKOWSKI, A.R., KEPPLER-NOREUIL, K., ROBINSON, L., SULLIVAN, C., SAJAN, S., CHRISTIAN, S.L., BUKSHPUN, P., GABRIEL, S.B., GLEESON, J.G., SHERR, E.H. &

DOBYNS, W.B. 2013. Deletion 16p13.11 uncovers NDE1 mutations on the non-deleted homolog and extends the spectrum of severe microcephaly to include fetal brain disruption. *Am J Med Genet A,* 161A**,** 1523-30.

PANG, A.W., MACDONALD, J.R., PINTO, D., WEI, J., RAFIQ, M.A., CONRAD, D.F., PARK, H., HURLES, M.E., LEE, C., VENTER, J.C., KIRKNESS, E.F., LEVY, S., FEUK, L. & SCHERER, S.W. 2010. Towards a comprehensive structural variation map of an individual human genome. *Genome Biol,* 11**,** R52.

PARTINGTON, M.W., FAGAN, K., SOUBJAKI, V. & TURNER, G. 1997. Translocations involving 4p16.3 in three families: deletion causing the Pitt-Rogers-Danks syndrome and duplication resulting in a new overgrowth syndrome. *J Med Genet,* 34**,** 719-28.

PATEL, S.V., DAGNEW, H., PAREKH, A.J., KOENIG, E., CONTE, R.A., MACERA, M.J. & VERMA, R.S. 1995. Clinical manifestations of trisomy 4p syndrome. *Eur J Pediatr,* 154**,** 425-31.

PEIFFER, D.A., LE, J.M., STEEMERS, F.J., CHANG, W., JENNIGES, T., GARCIA, F., HADEN, K., LI, J., SHAW, C.A., BELMONT, J., CHEUNG, S.W., SHEN, R.M., BARKER, D.L. & GUNDERSON, K.L. 2006. High-resolution genomic profiling of chromosomal aberrations using Infinium whole-genome genotyping. *Genome Res,* 16**,** 1136-48.

PETRICZKO, E., BICZYSKO-MOKOSA, A., BOGDANOWICZ, J., CONSTANTINOU, M., ZDZIENNICKA, E., HORODNICKA-JOZWA, A., BARG, E., GAWLIK-ZAWISLAK, S., SULEK-PIATKOWSKA, A., DAWID, G., WALCZAK, M., PESZ, K., KEDZIA, A. & ZAJACZEK, S. 2012. Familial distal monosomy 3p26.3-pter with trisomy 4q32.2-qter, presenting with progressive ataxia, intellectual disability, and dysmorphic features. *Am J Med Genet A,* 158a**,** 1442-6.

PFAFFL, M.W. 2001. A new mathematical model for relative quantification in real-time RT-PCR. *Nucleic Acids Res,* 29**,** e45.

PINKEL, D., SEGRAVES, R., SUDAR, D., CLARK, S., POOLE, I., KOWBEL, D., COLLINS, C., KUO, W.L., CHEN, C., ZHAI, Y., DAIRKEE, S.H., LJUNG, B.M., GRAY, J.W. & ALBERTSON, D.G. 1998. High resolution analysis of DNA copy number variation using comparative genomic hybridization to microarrays. *Nat Genet,* 20**,** 207-11.

PITTOCK, S.J., JOYCE, C., O'KEANE, V., HUGLE, B., HARDIMAN, M.O., BRETT, F., GREEN, A.J., BARTON, D.E., KING, M.D. & WEBB, D.W. 2000. Rapid-onset dystonia-parkinsonism: a clinical and genetic analysis of a new kindred. *Neurology,* 55**,** 991-5.

PLANTE, E. 1998. Criteria for SLI: the Stark and Tallal legacy and beyond. *J Speech Lang Hear Res,* 41**,** 951-7.

POHJOLA, P., DE LEEUW, N., PENTTINEN, M. & KAARIAINEN, H. 2010. Terminal 3p deletions in two families--correlation between molecular karyotype and phenotype. *Am J Med Genet A,* 152A**,** 441-6.

PONTIOUS, A., KOWALCZYK, T., ENGLUND, C. & HEVNER, R.F. 2008. Role of intermediate progenitor cells in cerebral cortex development. *Dev Neurosci,* 30**,** 24-32.

POPA, T., VELAYUDHAN, B., HUBSCH, C., PRADEEP, S., ROZE, E., VIDAILHET, M., MEUNIER, S. & KISHORE, A. 2013. Cerebellar processing of sensory inputs primes motor cortex plasticity. *Cereb Cortex,* 23**,** 305-14.

PUFFENBERGER, E.G., JINKS, R.N., SOUGNEZ, C., CIBULSKIS, K., WILLERT, R.A., ACHILLY, N.P., CASSIDY, R.P., FIORENTINI, C.J., HEIKEN, K.F., LAWRENCE, J.J., MAHONEY, M.H., MILLER, C.J., NAIR, D.T., POLITI, K.A., WORCESTER, K.N., SETTON, R.A., DIPIAZZA, R., SHERMAN, E.A., EASTMAN, J.T., FRANCKLYN, C., ROBEY-BOND, S., RIDER, N.L., GABRIEL, S., MORTON, D.H. & STRAUSS, K.A. 2012. Genetic mapping and exome sequencing identify variants associated with five novel diseases. *PLoS One,* 7**,** e28936.

QAMAR, R., AYUB, Q., MOHYUDDIN, A., HELGASON, A., MAZHAR, K., MANSOOR, A., ZERJAL, T., TYLER-SMITH, C. & MEHDI, S.Q. 2002. Y-chromosomal DNA variation in Pakistan. *Am J Hum Genet,* 70**,** 1107-24.

QUINN, N.P., SCHNEIDER, S.A., SCHWINGENSCHUH, P. & BHATIA, K.P. 2011. Tremor--some controversial aspects. *Mov Disord,* 26**,** 18-23.

QUINTANA-MURCI, L., KRAUSZ, C., ZERJAL, T., SAYAR, S.H., HAMMER, M.F., MEHDI, S.Q., AYUB, Q., QAMAR, R., MOHYUDDIN, A., RADHAKRISHNA, U., JOBLING, M.A., TYLER-SMITH, C. & MCELREAVEY, K. 2001. Y-chromosome lineages trace diffusion of people and languages in southwestern Asia. *Am J Hum Genet,* 68**,** 537-42.

RADOVICA, I., INASHKINA, I., SMELTERE, L., VITOLS, E. & JANKEVICS, E. 2012. Screening of 10 SNPs of LINGO1 gene in patients with essential tremor in the Latvian population. *Parkinsonism Relat Disord,* 18**,** 93-5.

RAKIC, P. 1988. Specification of cerebral cortical areas. *Science,* 241**,** 170-6.

RAKIC, P. 2007. The radial edifice of cortical architecture: from neuronal silhouettes to genetic engineering. *Brain Res Rev,* 55**,** 204-19.

RAKIC, P. 2009. Evolution of the neocortex: a perspective from developmental biology. *Nat Rev Neurosci,* 10**,** 724-35.

RAUCH, A., WIECZOREK, D., GRAF, E., WIELAND, T., ENDELE, S., SCHWARZMAYR, T., ALBRECHT, B., BARTHOLDI, D., BEYGO, J., DI DONATO, N., DUFKE, A., CREMER, K., HEMPEL, M., HORN, D., HOYER, J., JOSET, P., ROPKE, A., MOOG, U., RIESS, A., THIEL, C.T., TZSCHACH, A., WIESENER, A., WOHLLEBER, E., ZWEIER, C., EKICI, A.B., ZINK, A.M., RUMP, A., MEISINGER, C., GRALLERT, H., STICHT, H., SCHENCK, A., ENGELS, H., RAPPOLD, G., SCHROCK, E., WIEACKER, P., RIESS, O., MEITINGER, T., REIS, A. & STROM, T.M. 2012. Range of genetic mutations associated with severe non-syndromic sporadic intellectual disability: an exome sequencing study. *Lancet,* 380**,** 1674-82.

REICH, D., THANGARAJ, K., PATTERSON, N., PRICE, A.L. & SINGH, L. 2009. Reconstructing Indian population history. *Nature,* 461**,** 489-94.

RICHARDSON, S. 1992. The child with “delayed speech.”. *Contemp Pediatr,* 9**,** 55.

RIOS, A. 1996. Microcephaly. *Pediatr Rev,* 17**,** 386-7.

RODRIGUEZ-REVENGA, L., MILA, M., ROSENBERG, C., LAMB, A. & LEE, C. 2007. Structural variation in the human genome: the impact of copy number variants on clinical diagnosis. *Genet Med,* 9**,** 600-6.

SALEM, N., JR., LITMAN, B., KIM, H.Y. & GAWRISCH, K. 2001. Mechanisms of action of docosahexaenoic acid in the nervous system. *Lipids,* 36**,** 945-59.

SALVADOR-CARULLA, L., REED, G.M., VAEZ-AZIZI, L.M., COOPER, S.A., MARTINEZ-LEAL, R., BERTELLI, M., ADNAMS, C., COORAY, S., DEB, S., AKOURY-DIRANI, L., GIRIMAJI, S.C., KATZ, G., KWOK, H., LUCKASSON, R., SIMEONSSON, R., WALSH, C., MUNIR, K. & SAXENA, S. 2011. Intellectual developmental disorders: towards a new name, definition and framework for "mental retardation/intellectual disability" in ICD-11. *World Psychiatry,* 10**,** 175-80.

SCHAEFFELER, E., SCHWAB, M., EICHELBAUM, M. & ZANGER, U.M. 2003. CYP2D6 genotyping strategy based on gene copy number determination by TaqMan real-time PCR. *Hum Mutat,* 22**,** 476-85.

SCHINZEL, A., HANSON, J.W., PAGON, R.A., HOEHN, H. & SMITH, D.W. 1978. Trisomy 3 (p23-pter) resulting from maternal translocation, t (3 ; 4)(p23 ; q35). *Ann Genet,* 21**,** 168-71.

SCHLICKUM, S., MOGHEKAR, A., SIMPSON, J.C., STEGLICH, C., O'BRIEN, R.J., WINTERPACHT, A. & ENDELE, S.U. 2004. LETM1, a gene deleted in Wolf-Hirschhorn syndrome, encodes an evolutionarily conserved mitochondrial protein. *Genomics,* 83**,** 254-61.

SCHONEWOLF-GREULICH, B., RAVN, K., HAMBORG-PETERSEN, B., BRONDUM-NIELSEN, K. & TUMER, Z. 2013. Segregation of a 4p16.3 duplication with a characteristic appearance, macrocephaly, speech delay and mild intellectual disability in a 3-generation family. *Am J Med Genet A,* 161**,** 2358-62.

SCHOUTEN, J.P., MCELGUNN, C.J., WAAIJER, R., ZWIJNENBURG, D., DIEPVENS, F. & PALS, G. 2002. Relative quantification of 40 nucleic acid sequences by multiplex ligation-dependent probe amplification. *Nucleic Acids Res,* 30**,** e57.

SCHRAG, A., MUNCHAU, A., BHATIA, K.P., QUINN, N.P. & MARSDEN, C.D. 2000. Essential tremor: an overdiagnosed condition? *J Neurol,* 247**,** 955-9.

SCHWAB, M.E. 2004. Nogo and axon regeneration. *Curr Opin Neurobiol,* 14**,** 118-24.

SEBAT, J., LAKSHMI, B., MALHOTRA, D., TROGE, J., LESE-MARTIN, C., WALSH, T., YAMROM, B., YOON, S., KRASNITZ, A., KENDALL, J., LEOTTA, A., PAI, D., ZHANG, R., LEE, Y.H., HICKS, J., SPENCE, S.J., LEE, A.T., PUURA, K., LEHTIMAKI, T., LEDBETTER, D., GREGERSEN, P.K., BREGMAN, J., SUTCLIFFE, J.S., JOBANPUTRA, V., CHUNG, W., WARBURTON, D., KING, M.C., SKUSE, D., GESCHWIND, D.H., GILLIAM, T.C., YE, K. & WIGLER, M. 2007. Strong association of de novo copy number mutations with autism. *Science,* 316**,** 445-9.

SEBAT, J., LAKSHMI, B., TROGE, J., ALEXANDER, J., YOUNG, J., LUNDIN, P., MANER, S., MASSA, H., WALKER, M., CHI, M., NAVIN, N., LUCITO, R., HEALY, J., HICKS, J., YE, K., REINER, A., GILLIAM, T.C., TRASK, B., PATTERSON, N., ZETTERBERG, A. & WIGLER, M. 2004. Large-scale copy number polymorphism in the human genome. *Science,* 305**,** 525-8.

SEGAWA, M. 2009. Autosomal dominant GTP cyclohydrolase I (AD GCH 1) deficiency (Segawa disease, dystonia 5; DYT 5). *Chang Gung Med J,* 32**,** 1-11.

SERENIUS, F., WINBO, I., DAHIQUIST, G. & KALLEN, B. 2001. Cause-specific stillbirth and neonatal death in Sweden: a catchment area-based analysis. *Acta Paediatr,* 90**,** 1054-61.

SHARP, A.J., HANSEN, S., SELZER, R.R., CHENG, Z., REGAN, R., HURST, J.A., STEWART, H., PRICE, S.M., BLAIR, E., HENNEKAM, R.C., FITZPATRICK, C.A., SEGRAVES, R., RICHMOND, T.A., GUIVER, C., ALBERTSON, D.G., PINKEL, D., EIS, P.S., SCHWARTZ, S., KNIGHT, S.J. & EICHLER, E.E. 2006. Discovery of previously unidentified genomic disorders from the duplication architecture of the human genome. *Nat Genet,* 38**,** 1038-42.

SHENDURE, J. & JI, H. 2008. Next-generation DNA sequencing. *Nat Biotechnol,* 26**,** 1135-45.

SHENDURE, J.A., PORRECA, G.J., CHURCH, G.M., GARDNER, A.F., HENDRICKSON, C.L., KIELECZAWA, J. & SLATKO, B.E. 2011. Overview of DNA sequencing strategies. *Curr Protoc Mol Biol,* Chapter 7**,** Unit7.1.

SHINDOU, H., HISHIKAWA, D., HARAYAMA, T., ETO, M. & SHIMIZU, T. 2013. Generation of membrane diversity by lysophospholipid acyltransferases. *J Biochem,* 154**,** 21-8.

SHRIMPTON, A.E., JENSEN, K.A. & HOO, J.J. 2006. Karyotype-phenotype analysis and molecular delineation of a 3p26 deletion/8q24.3 duplication case with a virtually normal phenotype and mild cognitive deficit. *Am J Med Genet A,* 140**,** 388-91.

SINGH, J.R., SINGH, A.R. & SINGH, A.R. 2010. Directory of Human Genetic Services in India-2007. *International Journal of Human Genetics10***,** 1-3.

SNIJDERS, A.M., NOWAK, N., SEGRAVES, R., BLACKWOOD, S., BROWN, N., CONROY, J., HAMILTON, G., HINDLE, A.K., HUEY, B., KIMURA, K., LAW, S., MYAMBO, K., PALMER, J., YLSTRA, B., YUE, J.P., GRAY, J.W., JAIN, A.N., PINKEL, D. & ALBERTSON, D.G. 2001. Assembly of microarrays for genome-wide measurement of DNA copy number. *Nat Genet,* 29**,** 263-4.

SOBEL, E., SENGUL, H. & WEEKS, D.E. 2001. Multipoint estimation of identity-by-descent probabilities at arbitrary positions among marker loci on general pedigrees. *Hum Hered,* 52**,** 121-31.
SOMOGYI, P. & HAMORI, J. 1976. A quantitative electron microscopic study of the Purkinje cell axon initial segment. *Neuroscience,* 1**,** 361-5.
SPALDING, K.L., BHARDWAJ, R.D., BUCHHOLZ, B.A., DRUID, H. & FRISEN, J. 2005. Retrospective birth dating of cells in humans. *Cell,* 122**,** 133-43.
STAMELOU, M., CHARLESWORTH, G., CORDIVARI, C., SCHNEIDER, S.A., KAGI, G., SHEERIN, U.M., RUBIO-AGUSTI, I., BATLA, A., HOULDEN, H., WOOD, N.W. & BHATIA, K.P. 2014. The phenotypic spectrum of DYT24 due to ANO3 mutations. *Mov Disord,* 29**,** 928-34.
STAMELOU, M., EDWARDS, M.J. & BHATIA, K.P. 2013. Late onset rest-tremor in DYT1 dystonia. *Parkinsonism Relat Disord,* 19**,** 136-7.
STANKIEWICZ, P. & LUPSKI, J.R. 2002. Genome architecture, rearrangements and genomic disorders. *Trends Genet,* 18**,** 74-82.
STEC, I., WRIGHT, T.J., VAN OMMEN, G.J., DE BOER, P.A., VAN HAERINGEN, A., MOORMAN, A.F., ALTHERR, M.R. & DEN DUNNEN, J.T. 1998. WHSC1, a 90 kb SET domain-containing gene, expressed in early development and homologous to a Drosophila dysmorphy gene maps in the Wolf-Hirschhorn syndrome critical region and is fused to IgH in t(4;14) multiple myeloma. *Hum Mol Genet,* 7**,** 1071-82.
STEFANSSON, H., STEINBERG, S., PETURSSON, H., GUSTAFSSON, O., GUDJONSDOTTIR, I.H., JONSDOTTIR, G.A., PALSSON, S.T., JONSSON, T., SAEMUNDSDOTTIR, J., BJORNSDOTTIR, G., BOTTCHER, Y., THORLACIUS, T., HAUBENBERGER, D., ZIMPRICH, A., AUFF, E., HOTZY, C., TESTA, C.M., MIYATAKE, L.A., ROSEN, A.R., KRISTLEIFSSON, K., RYE, D., ASMUS, F., SCHOLS, L., DICHGANS, M., JAKOBSSON, F., BENEDIKZ, J., THORSTEINSDOTTIR, U., GULCHER, J., KONG, A. & STEFANSSON, K. 2009. Variant in the sequence of the LINGO1 gene confers risk of essential tremor. *Nat Genet,* 41**,** 277-9.
STHANADAR, A.A., BITTLES, A.H. & ZAHID, M. 2015. INCREASING PREVALENCE OF CONSANGUINEOUS MARRIAGE CONFIRMED IN KHYBER PAKHTUNKHWA PROVINCE, PAKISTAN. *J Biosoc Sci***,** 1-3.
STOESSL, A.J., LEHERICY, S. & STRAFELLA, A.P. 2014. Imaging insights into basal ganglia function, Parkinson's disease, and dystonia. *Lancet,* 384**,** 532-44.
STOLL, C. 2001. Problems in the diagnosis of fragile X syndrome in young children are still present. *Am J Med Genet,* 100**,** 110-5.
STRACHAN, T. & READ, A. 2010. *Human Molecular Genetics*, Taylor & Francis Group.
SUGIMOTO, T., YASUHARA, A., NISHIDA, N., MURAKAMI, K., WOO, M. & KOBAYASHI, Y. 1993. MRI of the head in the evaluation of microcephaly. *Neuropediatrics,* 24**,** 4-7.
SUN, T. & HEVNER, R.F. 2014. Growth and folding of the mammalian cerebral cortex: from molecules to malformations. *Nat Rev Neurosci,* 15**,** 217-32.
SWAIMAN, K.F., ASHWAL, S. & FERRIERO, D.M. 2006. *Pediatric Neurology: Principles & Practice*, Mosby Elsevier.
TAMANG, R., SINGH, L. & THANGARAJ, K. 2012. Complex genetic origin of Indian populations and its implications. *J Biosci,* 37**,** 911-9.
TAN, E.K., TEO, Y.Y., PRAKASH, K.M., LI, R., LIM, H.Q., ANGELES, D., TAN, L.C., AU, W.L., YIH, Y. & ZHAO, Y. 2009. LINGO1 variant increases risk of familial essential tremor. *Neurology,* 73**,** 1161-2.
TAN, X. & SHI, S.H. 2013. Neocortical neurogenesis and neuronal migration. *Wiley Interdiscip Rev Dev Biol,* 2**,** 443-59.
TANNER, C.M. & GOLDMAN, S.M. 1996. Epidemiology of Parkinson's disease. *Neurol Clin,* 14**,** 317-35.

TATTINI, L., D'AURIZIO, R. & MAGI, A. 2015. Detection of Genomic Structural Variants from Next-Generation Sequencing Data. *Front Bioeng Biotechnol,* 3**,** 92.

THIER, S., LORENZ, D., NOTHNAGEL, M., STEVANIN, G., DURR, A., NEBEL, A., SCHREIBER, S., KUHLENBAUMER, G., DEUSCHL, G. & KLEBE, S. 2010. LINGO1 polymorphisms are associated with essential tremor in Europeans. *Mov Disord,* 25**,** 717-23.

THUNSTROM, S., SODERMARK, L., IVARSSON, L., SAMUELSSON, L. & STEFANOVA, M. 2015. UBE2A deficiency syndrome: a report of two unrelated cases with large Xq24 deletions encompassing UBE2A gene. *Am J Med Genet A,* 167A**,** 204-10.

TINAZZI, M., FASANO, A., DI MATTEO, A., CONTE, A., BOVE, F., BOVI, T., PERETTI, A., DEFAZIO, G., FIORIO, M. & BERARDELLI, A. 2013. Temporal discrimination in patients with dystonia and tremor and patients with essential tremor. *Neurology,* 80**,** 76-84.

TINAZZI, M., FIORIO, M., FIASCHI, A., ROTHWELL, J.C. & BHATIA, K.P. 2009. Sensory functions in dystonia: insights from behavioral studies. *Mov Disord,* 24**,** 1427-36.

TOYDEMIR, R.M., BRASSINGTON, A.E., BAYRAK-TOYDEMIR, P., KRAKOWIAK, P.A., JORDE, L.B., WHITBY, F.G., LONGO, N., VISKOCHIL, D.H., CAREY, J.C. & BAMSHAD, M.J. 2006. A novel mutation in FGFR3 causes camptodactyly, tall stature, and hearing loss (CATSHL) syndrome. *Am J Hum Genet,* 79**,** 935-41.

UITTI, R.J. & MARAGANORE, D.M. 1993. Adult onset familial cervical dystonia: report of a family including monozygotic twins. *Mov Disord,* 8**,** 489-94.

ULUG, A.M., VO, A., ARGYELAN, M., TANABE, L., SCHIFFER, W.K., DEWEY, S., DAUER, W.T. & EIDELBERG, D. 2011. Cerebellothalamocortical pathway abnormalities in torsinA DYT1 knock-in mice. *Proc Natl Acad Sci U S A,* 108**,** 6638-43.

VALENTE, E.M., BENTIVOGLIO, A.R., CASSETTA, E., DIXON, P.H., DAVIS, M.B., FERRARIS, A., IALONGO, T., FRONTALI, M., WOOD, N.W. & ALBANESE, A. 2001. DYT13, a novel primary torsion dystonia locus, maps to chromosome 1p36.13--36.32 in an Italian family with cranial-cervical or upper limb onset. *Ann Neurol,* 49**,** 362-6.

VAN KARNEBEEK, C.D., SCHEPER, F.Y., ABELING, N.G., ALDERS, M., BARTH, P.G., HOOVERS, J.M., KOEVOETS, C., WANDERS, R.J. & HENNEKAM, R.C. 2005. Etiology of mental retardation in children referred to a tertiary care center: a prospective study. *Am J Ment Retard,* 110**,** 253-67.

VERBRUGGE, J., CHOUDHARY, A.K. & LADDA, R. 2009. Tethered cord, corpus callosum abnormalities, and periventricular cysts in Wolf-Hirschhorn syndrome. Report of two cases and review of the literature. *Am J Med Genet A,* 149A**,** 2280-4.

VILARINO-GUELL, C., ROSS, O.A., WIDER, C., JASINSKA-MYGA, B., COBB, S.A., SOTO-ORTOLAZA, A.I., KACHERGUS, J.M., KEELING, B.H., DACHSEL, J.C., MELROSE, H.L., BEHROUZ, B., WSZOLEK, Z.K., UITTI, R.J., AASLY, J.O., RAJPUT, A. & FARRER, M.J. 2010a. LINGO1 rs9652490 is associated with essential tremor and Parkinson disease. *Parkinsonism Relat Disord,* 16**,** 109-11.

VILARINO-GUELL, C., WIDER, C., ROSS, O.A., JASINSKA-MYGA, B., KACHERGUS, J., COBB, S.A., SOTO-ORTOLAZA, A.I., BEHROUZ, B., HECKMAN, M.G., DIEHL, N.N., TESTA, C.M., WSZOLEK, Z.K., UITTI, R.J., JANKOVIC, J., LOUIS, E.D., CLARK, L.N., RAJPUT, A. & FARRER, M.J. 2010b. LINGO1 and LINGO2 variants are associated with essential tremor and Parkinson disease. *Neurogenetics,* 11**,** 401-8.

VOELKERDING, K.V., DAMES, S.A. & DURTSCHI, J.D. 2009. Next-generation sequencing: from basic research to diagnostics. *Clin Chem,* 55**,** 641-58.

VON DER HAGEN, M., PIVARCSI, M., LIEBE, J., VON BERNUTH, H., DIDONATO, N., HENNERMANN, J.B., BUHRER, C., WIECZOREK, D. & KAINDL, A.M. 2014. Diagnostic approach to microcephaly in childhood: a two-center study and review of the literature. *Dev Med Child Neurol,* 56**,** 732-41.

WANG, C.J., QU, C.Q., ZHANG, J., FU, P.C., GUO, S.G. & TANG, R.H. 2014. Lingo-1 inhibited by RNA interference promotes functional recovery of experimental autoimmune encephalomyelitis. *Anat Rec (Hoboken),* 297**,** 2356-63.

WANG, G.J., YANG, P. & XIE, H.G. 2006. Gene variants in noncoding regions and their possible consequences. *Pharmacogenomics,* 7**,** 203-9.

WARNER, T.T. & HAMMANS, S.R. 2008. *Practical guide to neurogenetics*, Elsevier Health Sciences.

WEKSBERG, R., HUGHES, S., MOLDOVAN, L., BASSETT, A.S., CHOW, E.W. & SQUIRE, J.A. 2005. A method for accurate detection of genomic microdeletions using real-time quantitative PCR. *BMC Genomics,* 6**,** 180.

WELLESLEY, D., BOYD, P., DOLK, H. & PATTENDEN, S. 2005. An aetiological classification of birth defects for epidemiological research. *J Med Genet,* 42**,** 54-7.

WINTER, P., KAMM, C., BISKUP, S., KOHLER, A., LEUBE, B., AUBURGER, G., GASSER, T., BENECKE, R. & MULLER, U. 2012. DYT7 gene locus for cervical dystonia on chromosome 18p is questionable. *Mov Disord,* 27**,** 1819-21.

WOODS, C.G. 2004. Human microcephaly. *Curr Opin Neurobiol,* 14**,** 112-7.

WOODS, C.G., BOND, J. & ENARD, W. 2005. Autosomal recessive primary microcephaly (MCPH): a review of clinical, molecular, and evolutionary findings. *Am J Hum Genet,* 76**,** 717-28.

WRIGHT, T.J., COSTA, J.L., NARANJO, C., FRANCIS-WEST, P. & ALTHERR, M.R. 1999. Comparative analysis of a novel gene from the Wolf-Hirschhorn/Pitt-Rogers-Danks syndrome critical region. *Genomics,* 59**,** 203-12.

WRIGHT, T.J., RICKE, D.O., DENISON, K., ABMAYR, S., COTTER, P.D., HIRSCHHORN, K., KEINANEN, M., MCDONALD-MCGINN, D., SOMER, M., SPINNER, N., YANG-FENG, T., ZACKAI, E. & ALTHERR, M.R. 1997. A transcript map of the newly defined 165 kb Wolf-Hirschhorn syndrome critical region. *Hum Mol Genet,* 6**,** 317-24.

WU, Y.W., PRAKASH, K.M., RONG, T.Y., LI, H.H., XIAO, Q., TAN, L.C., AU, W.L., DING, J.Q., CHEN, S.D. & TAN, E.K. 2011. Lingo2 variants associated with essential tremor and Parkinson's disease. *Hum Genet,* 129**,** 611-5.

XIAO, J., UITTI, R.J., ZHAO, Y., VEMULA, S.R., PERLMUTTER, J.S., WSZOLEK, Z.K., MARAGANORE, D.M., AUBURGER, G., LEUBE, B., LEHNHOFF, K. & LEDOUX, M.S. 2012. Mutations in CIZ1 cause adult onset primary cervical dystonia. *Ann Neurol,* 71**,** 458-69.

XIAO, J., ZHAO, Y., BASTIAN, R.W., PERLMUTTER, J.S., RACETTE, B.A., TABBAL, S.D., KARIMI, M., PANIELLO, R.C., WSZOLEK, Z.K., UITTI, R.J., VAN GERPEN, J.A., SIMON, D.K., TARSY, D., HEDERA, P., TRUONG, D.D., FREI, K.P., DEV BATISH, S., BLITZER, A., PFEIFFER, R.F., GONG, S. & LEDOUX, M.S. 2010. Novel THAP1 sequence variants in primary dystonia. *Neurology,* 74**,** 229-38.

XIE, G., HARRISON, J., CLAPCOTE, S.J., HUANG, Y., ZHANG, J.Y., WANG, L.Y. & RODER, J.C. 2010. A new Kv1.2 channelopathy underlying cerebellar ataxia. *J Biol Chem,* 285**,** 32160-73.

XING, H.Y., MENG, E.Y., XIA, Y.P. & PENG, H. 2015. Effect of retinoic acid on expression of LINGO-1 and neural regeneration after cerebral ischemia. *J Huazhong Univ Sci Technolog Med Sci,* 35**,** 54-7.

XIROMERISIOU, G., HOULDEN, H., SCARMEAS, N., STAMELOU, M., KARA, E., HARDY, J., LEES, A.J., KORLIPARA, P., LIMOUSIN, P., PAUDEL, R., HADJIGEORGIOU, G.M. & BHATIA, K.P. 2012. THAP1 mutations and dystonia phenotypes: genotype phenotype correlations. *Mov Disord,* 27**,** 1290-4.

YIU, G. & HE, Z. 2003. Signaling mechanisms of the myelin inhibitors of axon regeneration. *Curr Opin Neurobiol,* 13**,** 545-51.

YIU, G. & HE, Z. 2006. Glial inhibition of CNS axon regeneration. *Nat Rev Neurosci,* 7**,** 617-27.

ZHAO, Z. & XU, Y. 2010. An extremely simple method for extraction of lysophospholipids and phospholipids from blood samples. *J Lipid Res,* 51**,** 652-9.
ZHAO, Z. & ZLOKOVIC, B.V. 2014. Blood-brain barrier: a dual life of MFSD2A? *Neuron,* 82**,** 728-30.
ZHOU, Z.D., SATHIYAMOORTHY, S. & TAN, E.K. 2012. LINGO-1 and Neurodegeneration: Pathophysiologic Clues for Essential Tremor. *Tremor Other Hyperkinet Mov (N Y),* 2.
ZITELLI, B.J. & DAVIS, H.W. 2007. *Atlas of Pediatric Physical Diagnosis*, Mosby/Elsevier.
ZLOKOVIC, B.V. 2008. The blood-brain barrier in health and chronic neurodegenerative disorders. *Neuron,* 57**,** 178-201.
ZLOKOVIC, B.V. 2011. Neurovascular pathways to neurodegeneration in Alzheimer's disease and other disorders. *Nat Rev Neurosci,* 12**,** 723-38.
ZOLLINO, M., LECCE, R., FISCHETTO, R., MURDOLO, M., FARAVELLI, F., SELICORNI, A., BUTTE, C., MEMO, L., CAPOVILLA, G. & NERI, G. 2003. Mapping the Wolf-Hirschhorn syndrome phenotype outside the currently accepted WHS critical region and defining a new critical region, WHSCR-2. *Am J Hum Genet,* 72**,** 590-7.
ZOLLINO, M., LECCE, R., SELICORNI, A., MURDOLO, M., MANCUSO, I., MARANGI, G., ZAMPINO, G., GARAVELLI, L., FERRARINI, A., ROCCHI, M., OPITZ, J.M. & NERI, G. 2004. A double cryptic chromosome imbalance is an important factor to explain phenotypic variability in Wolf-Hirschhorn syndrome. *Eur J Hum Genet,* 12**,** 797-804.
ZOLLINO, M., MURDOLO, M., MARANGI, G., PECILE, V., GALASSO, C., MAZZANTI, L. & NERI, G. 2008. On the nosology and pathogenesis of Wolf-Hirschhorn syndrome: genotype-phenotype correlation analysis of 80 patients and literature review. *Am J Med Genet C Semin Med Genet,* 148C**,** 257-69.
ZOLLINO, M., ORTESCHI, D., RUITER, M., PFUNDT, R., STEINDL, K., CAFIERO, C., RICCIARDI, S., CONTALDO, I., CHIEFFO, D., RANALLI, D., ACQUAFONDATA, C., MURDOLO, M., MARANGI, G., ASARO, A. & BATTAGLIA, D. 2014. Unusual 4p16.3 deletions suggest an additional chromosome region for the Wolf-Hirschhorn syndrome-associated seizures disorder. *Epilepsia,* 55**,** 849-57.